FINAL TECHNICAL REPORT

Measurements of Acidic Gases and Aerosol Species Aboard the NASA DC-8 Aircraft During the Pacific Exploratory Mission in the Tropics (PEM-Tropics A)

NASA Research Grant NAG 1-1761

awarded to

Institute for the Study of Earth, Oceans, and Space
Morse Hall
University of New Hampshire
Durham, NH 03824

Robert W. Talbot
Jack E. Dibb

Principal Investigators

July 1999

Executive Summary:

We received funding to provide measurements of nitric acid (HNO_3), formic acid (HCOOH), acetic acid (CH_3COOH), and the chemical composition of aerosols aboard the NASA Ames DC-8 research aircraft during the PEM-Tropics A mission. These measurements were successfully completed and the final data resides in the electronic archive (ftp-gte.larc.nasa.gov) at NASA Langley Research Center.

For the PEM-Tropics A mission the University of New Hampshire group was first author of four different manuscripts. Three of these have now appeared in the *Journal of Geophysical Research-Atmospheres*, included in the two section sections on PEM-Tropics A. The fourth manuscript has just recently been submitted to this same journal as a stand alone paper. All four of these papers are included in this report.

The first paper by Talbot et al. (Influence of biomass combustion emissions on the distribution of acidic trace gases over the Southern Pacific basin during austral springtime) describes the large-scale distributions of HNO_3, HCOOH, and CH_3COOH. These gases exhibited an overall correlation with CH_3Cl, a biomass burning tracer, but not industrial tracers such as C_2Cl_4. Arguments were presented to show, particularly in the middle tropospheric region, that biomass burning emissions from South America and Africa were a major source of acidic gases over the South Pacific basin. The lowest mixing ratios of these gases were observed in the marine boundary layer, which was isolated somewhat from the polluted air above by the trade wind inversion. The C_2H_2/CO ratio had a median value of 0.6 in the boundary layer which indicates it was not directly influenced by biomass burning emissions.

The second paper by Dibb et al. (Aerosol chemical composition and distribution during the Pacific Exploratory Mission (PEM) Tropics) covers the aerosol aspects of our measurement package. Compared to acidic gases, O_3, and selected hydrocarbons, the aerosol chemistry showed little influence from biomass burning emissions. We seldom observed enhancements in ammonium, nitrate or sulfate within combustion plumes well defined, for example, by C_2H_2. These distributions lead us to postulate that the plumes must of been scavenged effectively by convection over South America and Africa before undergoing long-range transport over the Pacific basin. The data collected in the marine boundary layer showed a possible marine source of NH_3 to the troposphere in equatorial areas. This source had been speculated on previously, but our data was the first collected from an airborne platform to show its large-scale features.

The third paper by Dibb et al. (Constraints on the age and dilution of Pacific Exploratory Mission-Tropics biomass burning plumes from the natural radionuclide tracer ^{210}Pb) utilized the unexpectedly high concentrations of ^{210}Pb in the combustion plumes to estimate their ages and mixing along the transport route to the South Pacific basin. A model was used to reproduce the observed ^{210}Pb activities to about ±10%, and then the ratios of four nonmethane hydrocarbon species to ±20%. The results of these estimated travel distances and rates agreed well with independent air parcel trajectory analysis conducted by Fuelberg et al. (1999). The model results show that the plumes underwent varying degrees of dilution along the travel route, with most of them entraining large fractions of surrounding ambient air during transport.

The final paper in the group by Talbot et al. (Tropospheric reactive-odd nitrogen over the South Pacific in austral springtime) has just been submitted to the *Journal of Geophysical Research-Atmospheres*. This paper provides a summary of reactive nitrogen during PEM-Tropics A, with HNO_3 and PAN showing the most impact from combustion emissions. We further speculated that lightning over continental areas and stratospheric inputs can not be ruled out as a source of reactive nitrogen. Due to the long transport times involved, these inputs are not perceivable in NO_x ($NO + NO_2$), but could of contributed to the enhancements in HNO_3 and PAN which reached 600 pptv in the middle troposphere. The sum of reactive nitrogen species (NO_y sum) had a median value of 285 pptv within combustion plumes compared to 120 pptv outside them. In the marine boundary layer, the plume and non-plume air parcels both exhibited NO_y sum median mixing ratios near 50 pptv, again showing the isolated nature of this region from the pollution above. Finally, the PEM-Tropics A data show that methyl and ethyl nitrate comprise 20-80% of NO_y sum in equatorial and high latitude regions over the South Pacific. The natural marine source for this species was hypothesized previously, but the PEM-Tropics data is the first to show the large-scale picture of the alkyl nitrate distribution over the remote ocean.

In addition to these first authored papers, researchers from the University of New Hampshire are co-authors on numerous other companion papers in both special issues. We had a very successful field mission during PEM-Tropics A which lead to our results appearing in numerous mission-related publications.

JOURNAL OF GEOPHYSICAL RESEARCH, VOL. 104, NO. D5, PAGES 5623–5634, MARCH 20, 1999

Influence of biomass combustion emissions on the distribution of acidic trace gases over the southern Pacific basin during austral springtime

R. W. Talbot,[1] J. E. Dibb,[1] E. M. Scheuer,[1] D. R. Blake,[2] N. J. Blake,[2] G. L. Gregory,[3] G. W. Sachse,[3] J. D. Bradshaw,[4,5] S. T. Sandholm,[4] and H. B. Singh[6]

Abstract. This paper describes the large-scale distributions of HNO_3, HCOOH, and CH_3COOH over the central and South Pacific basins during the Pacific Exploratory Mission-Tropics (PEM-Tropics) in austral springtime. Because of the remoteness of this region from continental areas, low part per trillion by volume (pptv) mixing ratios of acidic gases were anticipated to be pervasive over the South Pacific basin. However, at altitudes of 2-12 km over the South Pacific, air parcels were encountered frequently with significantly enhanced mixing ratios (up to 1200 pptv) of acidic gases. Most of these air parcels were centered in the 3-7 km altitude range and occurred within the 15°-65°S latitudinal band. The acidic gases exhibited an overall general correlation with CH_3Cl, PAN, and O_3, suggestive of photochemical and biomass burning sources. There was no correlation or trend of acidic gases with common industrial tracer compounds (e.g., C_2Cl_4 or CH_3CCl_3). The combustion emissions sampled over the South Pacific basin were relatively aged exhibiting C_2H_2/CO ratios in the range of 0.2-2.2 pptv/ppbv. The relationships between acidic gases and this ratio were similar to what was observed in aged air parcels (i.e., >3-5 days since they were over a continental area) over the western North Pacific during the Pacific Exploratory Mission-West Phases A and B (PEM-West A and B). In the South Pacific marine boundary layer a median C_2H_2/CO ratio of 0.6 suggested that this region was generally not influenced by direct inputs of biomass combustion emissions. Here we observed the lowest mixing ratios of acidic gases, with median values of 14 pptv for HNO_3, 19 pptv for HCOOH, and 18 pptv for CH_3COOH. These values were coincident with low mixing ratios of NO_x (<10 pptv), CO (≈50 parts per billion by volume (ppbv)), O_3 (< 20 ppbv), and long-lived hydrocarbons (e.g., C_2H_6 <300 pptv). Overall, the PEM-Tropics data suggest an important influence of aged biomass combustion emissions on the distributions of acidic gases over the South Pacific basin in austral springtime.

1. Introduction

Acidic gases are important participants in tropospheric chemical processes. They are major end products of oxidative cycles, with wet and dry removal of HNO_3 and H_2SO_4 from the atmosphere principal sinks for tropospheric NO_x ($NO + NO_2$) and SO_2 [*Logan*, 1983; *Hales and Dana*, 1979]. In remote regions the monocarboxylic acids HCOOH and CH_3COOH are often the dominant acidic gases and acidity components of cloud water and precipitation [*Keene et al.*, 1983; *Andreae et al.*, 1988, 1990]. Formic acid is also a major sink for OH radicals in cloudwater [*Jacob*, 1986].

Formic acid may be produced by aqueous phase OH oxidation of hydrated formaldehyde ($H_2C(OH)_2$) in cloudwater and subsequently provides an important source of gas phase HCOOH in the remote troposphere [*Chameides and Davis*, 1983; *Jacob*, 1986]. Aqueous phase production mechanisms for CH_3COOH appear to be quite slow and probably are a negligible source of this species to the troposphere [*Jacob and Wofsy*, 1988]. The major sources of HCOOH and CH_3COOH to the global troposphere appear to be emissions from combustion [*Kawamura et al.*, 1985; *Talbot et al.*, 1988; *Helas et al.*, 1992; *Lefer et al.*, 1994], vegetation [*Keene and Galloway*, 1986; *Talbot et al.*, 1988, 1990], and possibly soils [*Sanhueza and Andreae*, 1991; *Talbot et al.*, 1995]. Permutation reactions of peroxy radicals have been proposed as potentially important sources of carboxylic acids [*Madronich and Calvert*, 1990; *Madronich et al.*, 1990], but recent measurements at a continental site indicate that this pathway may be relatively unimportant [*Talbot et al.*, 1995].

There are potentially numerous production mechanisms for HNO_3 in the troposphere including, NO_2 + OH, recycling of reactive nitrogen reservoir species, and evaporation of NO_3^- in aerosol and aqueous phases [*Roberts*, 1995]. Many of these processes are thought to very slow in the upper tropical troposphere due to low O_3 mixing ratios and cold temperatures retaining most of the reactive nitrogen in the form of NO during the daytime [*Folkins et al.*, 1995].

Measurements conducted in winter 1992 at 10-12 km altitude between Tahiti and California showed an abrupt decrease in the mixing ratios of O_3 and NO_y (i.e., the sum of reactive nitrogen species) at the southern edge of the Intertropical Convergence Zone

[1]Institute for the Study of Earth, Oceans, and Space, University of New Hampshire, Durham.
[2]Department of Chemistry, University of California, Irvine.
[3]NASA Langley Research Center, Hampton, Virginia.
[4]Department of Earth and Atmospheric Science, Georgia Institute of Technology, Atlanta.
[5]Deceased June 16, 1997.
[6]NASA Ames Research Center, Moffett Field, California.

Paper number 98JD00879.
0148-0227/99/98JD-00879$09.00

(ITCZ) [*Folkins et al.*, 1995]. Owing to the remoteness of the South Pacific basin from continental areas, the observed trend in O_3 and NO_y is not surprising. In fact, low mixing ratios would be expected to be pervasive over the South Pacific basin for most tropospheric trace species, including acidic gases.

In this paper we present the large-scale distributions of HNO_3, HCOOH, and CH_3COOH over the central and South Pacific basins during the NASA Global Tropospheric Experiment/Pacific Exploratory Mission-Tropics (GTE/PEM-Tropics) in September/October 1996. Objectives of PEM-Tropics included obtaining baseline data for important tropospheric gases, evaluating the oxidizing capacity of the troposphere and factors influencing it, and improving our understanding of the natural sulfur cycle over the South Pacific basin.

The first part of this paper focuses on the distributions of acidic gases in the 2-12 km altitude range which were apparently heavily impacted by aged biomass combustion emissions. Supporting evidence for this source is provided by coincident distributions of selected hydrocarbon compounds. The distribution of acidic gases is examined in the marine boundary layer and overlying transition region in the second part of this paper. Here there was little evidence for a direct influence of biomass combustion inputs on the chemistry, in stark contrast to the middle and upper troposphere. Overall, the PEM-Tropics measurements provide unique information of the chemistry of this extensive remote region during austral springtime.

2. Experimental Methods

2.1. Study Area

The PEM-Tropics airborne expedition was conducted using the NASA Ames DC-8 research aircraft. Transit and intensive site science missions composed 18 flights, averaging 8-10 hours in duration and covering the altitude range of 0.3 to 12.5 km. The base of operations for these missions progressed as follows: (1) Tahiti (three missions), (2) Easter Island (two missions), (3) Tahiti (one mission), (4) New Zealand (one mission), and (5) Fiji (three missions). The data used in this paper were obtained in the geographic grid approximately bounded by 60°N-75°S latitude and 165°E-105°W longitude. Data obtained on transit flights (eight missions) were also utilized in this paper. A geographic map of the study region is shown in several companion papers [e.g., *Gregory et al.*, this issue; *Hoell et al.*, this issue].

The overall scientific rationale and description of individual aircraft missions is described in the PEM-Tropics overview paper [*Hoell et al.*, this issue]. The features of the large-scale meteorological regime and associated air mass trajectory analyses for the September-October 1996 time period are presented by *Fuelberg et al.* [this issue].

2.2. Sampling and Analytical Methodology

Acidic gases were subsampled from a high-volume (500-1500 standard liters per minute (sLpm)) flow of ambient air using the mist chamber technique [*Talbot et al.*, 1988, 1990, 1997a]. The subsample flow rate was always <10% of the primary manifold total flow. Sample collection intervals were typically 4 min in the boundary layer, 6 min at 2-9 km altitude, and 8 min above 9 km altitude, reflecting decreased pumping rates in the middle and upper troposphere. The inlet manifold consisted of a 0.9 m length of 41 mm ID glass coated stainless steel pipe. The pipe extended from the DC-8 fuselage to provide a 90° orientation to the ambient air streamline flow. To facilitate pumping of the high-volume manifold flow, a diffuser was mounted over the end of the inlet pipe parallel to the DC-8 fuselage. This device provided a "shroud" effect, slowing the flow of ambient air through it slightly below the true air speed of the DC-8 and adding 50-100 hPa of pressurization to the sampling manifold. This effectively eliminated the reverse venturi effect (≈40 hPa) on the sampling manifold. An additional feature of the diffuse was a curved step around the manifold pipe which provided the streamline effects of a backward facing inlet. Its function was to facilitate exclusion of aerosol particles greater than ≈2 μm in diameter from the sampling manifold. Aerosols smaller than this were removed from the sampled air stream using a 1μm pore-sized Zefluor teflon filter that was readily changeable every 5-10 min to minimize aerosol loading on the filter and gas/aerosol phase partitioning from ambient conditions.

In addition to the features described above, the inlet manifold was equipped with the capability for conducting a standard addition of HNO_3 into the manifold ambient air stream. This spike was added ≈10 cm downstream inside the manifold pipe through a 6.5 mm OD glass coated stainless steel tube mounted perpendicular to the air flow. This tube was ≈20 mm long and maintained at 40°C to facilitate passing of calibration gas through it. Through a tee, this injection length of tubing was connected to about 1.5 m of heated tubing that was directly linked to the perm oven output. This design effectively tested the passing efficiency of the entire manifold system, which was indistinguishable from 100 ± 15%. The calibration system for HNO_3 consisted of a permeation oven held at 50°C and a dilution flow of ultra zero air (1.5 sLpm) which swept the oven outflow to either a nylon filter for output quantification or the sampling manifold for standard addition on ambient air. The heated tubing through which the HNO_3 stream passed was kept equilibrated by a flow design that allowed the calibration gas to constantly pass to near the point of injection into the manifold flow before being dumped to waste through a return line. The mixing ratio of HNO_3 in the 1.5 sLpm flow was typically 200 parts per billion by volume (ppbv). This spike was then diluted several hundred times by the high flow rate of ambient air in the sampling manifold, producing standard additions of 100-1200 pptv. Previously we have studied the passing efficiency of carboxylic acids through our inlet manifold, and found it to be ≥95% [*Talbot et al.*, 1992]. Thus we focused our attention on HNO_3 due to its importance to the reactive nitrogen cycle and tropospheric chemistry.

The permeation oven output of HNO_3 was monitored on the ground and in the air in near-real time. We fabricated a new calibration system for PEM-Tropics which maintained the permeation tube to 50.0 ± 0.1°C and 1850 ±1 hPa pressure at all altitudes. The permeation source was constant to ± 8.5% over the course of the expedition, with no equilibration time required at any altitude, even with rapid changes such as during spiral maneuvers. This new design utilized upstream pressure control (i.e., before the permeation tube) so that there were no fittings, valves, or flow/pressure controllers in-line between the tube and the injection point into our sampling manifold. The flow through the oven varied from 20-25 $cm^3\ min^{-1}$ depending on the ambient pressure and was diluted into the 1.5 sLpm flow described above. Standard additions were conducted with and without a teflon filter in-line to verify that the filter did not influence the passing efficiency of the sampling manifold.

Computer controlled syringe pumps were used to move sample solutions in and out of the mist chamber samplers and our sample containers. This essentially provided a closed system of liquid handling which greatly simplified contamination control. The concentrations of acidic gases in our samples were quantified using

a custom built dual ion chromatography system equipped with a computer interface for data acquisition. The system was composed primarily of Dionex components with the detectors and flow system thermostated to 40°C. Eluants were constantly purged with He gas. Nitric acid was measured using a fast anion column while the carboxylic acids were determined using an AS4 column. Concentrator columns and electronic suppression was used in both chromatography systems. Calibration curves generated on the ground and in the air agreed within ±2%. We thus were able to determine atmospheric mixing ratios of acidic gases in near-real time.

In addition to data for acidic gases, we present selected information on several important trace gases including ozone (O_3), carbon monoxide (CO), ethyne (C_2H_2), perchloroethylene (C_2Cl_4), and peroxyacetylnitrate (PAN). Aerosol NO_3^- was measured on bulk filter samples collected with a forward facing isokinectic probe housed in a shroud to ensure isoaxial flow [*Dibb et al.*, 1996a]. Ninety millimeter diameter 2 μm pore-sized Zefluor teflon filters were used as the collection substrate. Specific details regarding the measurement of various other species used in this paper are presented in companion papers [*Blake et al.*, this issue; *Dibb et al.*, this issue; *Gregory et al.*, this issue; *Vay et al.*, this issue]. The measurements of these species were averaged to provide mean values that corresponded directly to the acidic gas sampling times. This merged data product was generated at Harvard University, and it is used exclusively in this paper.

3. Results

In the data presented in this paper, obvious stratospherically impacted values have been removed based on coincident measurements of O_3, CO, dew point, and selected hydrocarbons and halocarbons. This amounted to removing a total of about 25 data points obtained on three different flights.

The large-scale latitudinal distribution of acidic gases over the central and South Pacific basins is presented in Figure 1. It is evident from these distributions that numerous air parcels were encountered between 15° and 60°S latitude which contained large mixing ratios of acidic gases. The northern border of the impacted Pacific troposphere appears to be controlled by the presence and location of the South Pacific Convergence Zone (SPCZ) [*Gregory et al.*, this issue]. Nitric acid mixing ratios, for example, typically decreased by a factor of 2-5 in crossing the SPCZ region from south to north. This trend was also apparent in other trace gases such as CO, C_2H_2, C_2H_6, O_3, and PAN [*Gregory et al.*, this issue]. Thus polluted air parcels appeared to be present south of the SPCZ with "clean" air north of it fed by an easterly flow regime along the southern edge of the ITCZ.

Mixing ratios of acidic gases over the South Pacific were generally less than 200 pptv but approached or exceeded 1000 pptv in some air parcels. These air parcels (i.e., plumes) were observed mainly between 2 and 7 km altitude (Figures 2a-2c). Because of the strong trade wind inversion over this region, the marine boundary layer exhibited very small mixing ratios of acidic gases. The inversion appeared to be a very effective barrier to downward mixing of acidic gases from aloft. Indeed, the most processed (i.e., aging and mixing influences) air parcels were sampled in the marine boundary layer. This feature of the data is illustrated using the ratio C_2H_2/CO which had a median value of 0.6 below 1 km altitude but showed significantly larger values in the rest of the tropospheric column (Figure 3). Values of this ratio less than 1.0 are typical of photochemically aged and well mixed (diluted) air parcels [*Smyth et al.*, 1998; *Talbot et al.*, 1997b].

As an example of the detailed vertical structure over the South Pacific selected data from a slow spiral (80 m min^{-1}) conducted east of Fiji is shown in Figure 4. An apparent combustion plume was sampled near 5 km, with corresponding large increases in HNO_3, C_2H_2, and C_2H_2/CO but not C_2Cl_4. Notice the very rapid vertical changes in the mixing ratios and generally good correspondence between HNO_3 and C_2H_2. While the plumes with large mixing ratios of many trace gases clearly stand out, the PEM-Tropics data in general support the idea that much of the tropospheric column from 2-10 km altitude was fumigated with varying degrees of combustion emissions. The smooth shape of the vertical distribution of C_2Cl_4 is typical of what was observed over the South Pacific (Figure 1), and it suggests minimal influence on the chemistry from industrial emissions. The distribution of CH_3CCl_3 and other halocarbons also supports this ascertain (N. Blake, personal communication, 1998).

To provide a detailed description of the distribution of acidic gases over the central and South Pacific basins, this information is presented in a regional summary format (Table 1) consistent with that used in companion papers [*Gregory et al.*, this issue; *Dibb et al.*, this issue]. Information on the distribution of many other trace gases can be found in these papers, so it is not duplicated here. The regional breakdown was developed to provide data summaries that correspond to logical latitudinal and longitudinal areas (e.g., the ITCZ, and the eastern, central, and western Pacific basins). In some regions the sampling was quite sparse, so interregional comparisons need to be conducted with caution. On the basis of the vertical measurement density of acidic gases, the data were broken into four altitude bins: (1) the marine boundary layer (<1 km), (2) the transition or cloud layer (1-2 km), (3) the middle (2-8 km), and (4) upper (8-12 km) troposphere.

As shown in the large-scale vertical distributions (Table 1 and Figure 2), the smallest mixing ratios of acidic gases were found in the marine boundary layer. Here median mixing ratios were 14 pptv for HNO_3, 19 pptv for HCOOH, and 18 pptv for CH_3COOH. The very small mixing ratios of HNO_3 are consistent with the observed NO_x values of only a few or sub (i.e, <1) pptv in the boundary layer (Georgia Institute of Technology NO_x data are available from the Distributed Active Archive Center (DAAC) at NASA Langley Research Center, Hampton, Virginia). There was no significant regional difference in the mixing ratio of HNO_3 in the marine boundary layer, but the carboxylic acids exhibited values 2-3 times larger in the central Pacific region. In the middle troposphere the mixing ratios of acidic gases showed the largest values in the western and central regions. This is consistent with the generally westerly flow of air at these altitudes over the South Pacific basin, implying that the least processed air parcels would be found in these regions [*Fuelberg et al.*, this issue]. Most of the plumes that we sampled were, in fact, encountered over the western and central Pacific areas. The eastern Pacific regions were dominated by relatively "clean" air parcels. This longitudinal difference seemingly reflects chemical and physical losses of acidic gases as air parcels transverse the Pacific basin in a westerly flow regime.

The mixing ratios of the carboxylic acids HCOOH and CH_3COOH are generally found to be highly correlated in the gas and liquid phases in the troposphere [*Keene and Galloway*, 1986]. Over continental areas the ratio HCOOH/CH_3COOH usually has a value near 2.0 with a correlation coefficient between these two species near 0.9 [*Keene and Galloway*, 1986; *Talbot et al.*, 1988]. Although we observed linear correlations between HCOOH and CH_3COOH over the Pacific basin (Figures 5a and 5b), they were less robust than what we observed during the Pacific Exploratory Mission-West Phases A and B (PEM-West A and B) [*Talbot et al.*,

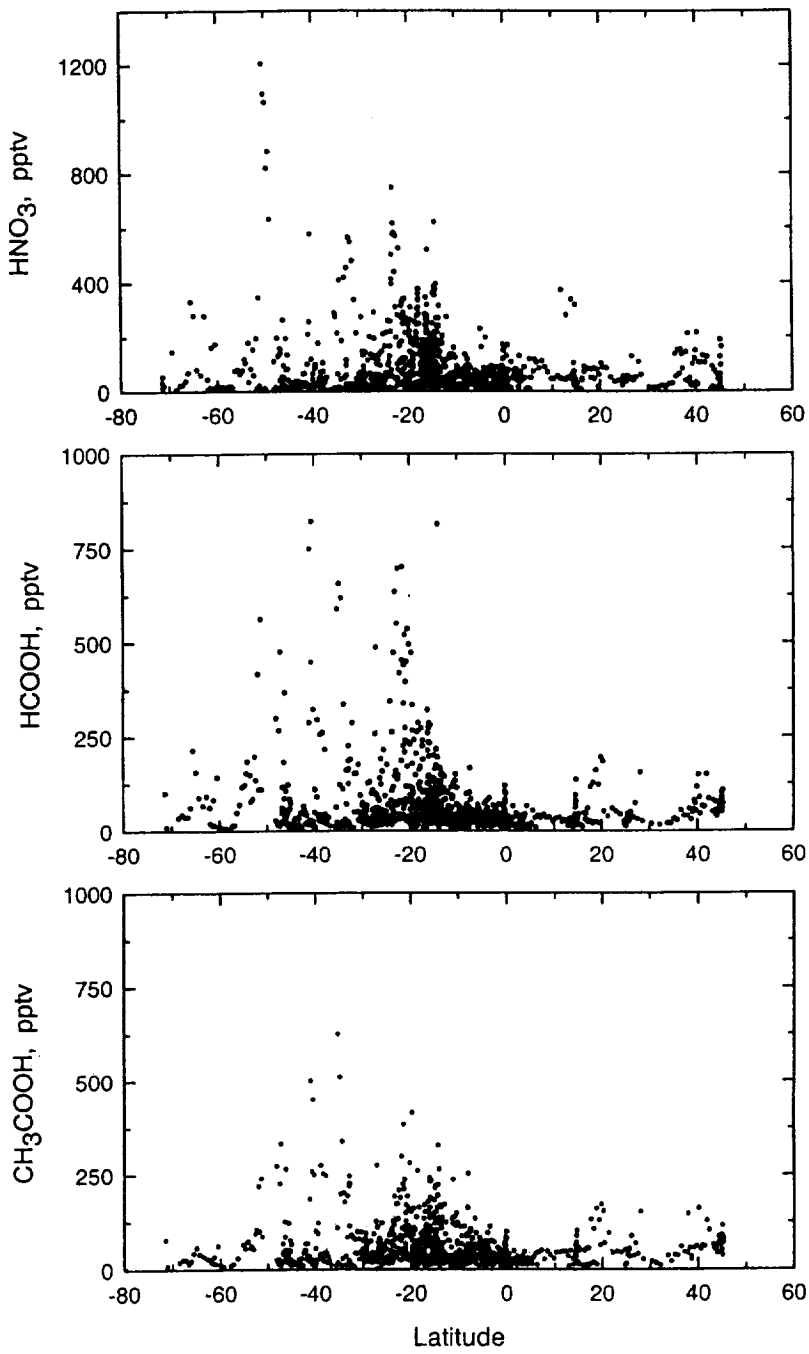

Figure 1. Latitudinal distribution of acidic gases at altitudes of 2-12 km over the central and southern Pacific basins.

1997a]. In some of the plumes, HCOOH was highly enhanced with regard to CH_3COOH, and the ratio $HCOOH/CH_3COOH$ had values as large as 5.0 (plume median equal to 1.6). This suggests the possibility of substantial photochemical production of HCOOH compared to CH_3COOH (or more efficient loss of CH_3COOH) in some of the plumes that we sampled over the South Pacific. This point is further explored in later sections of this paper.

4. Discussion

4.1. Altitude Range of 2-12 km

The large-scale impact of pollution over much of the western and central Pacific basins is a significant feature of the PEM-Tropics data set. Backward trajectories indicate that many of the air parcels we sampled had not been over continental areas for 10-20 days [*Fuelberg et al.*, this issue]. This is consistent with the chemical measurements which suggest that the air parcels were photochemically aged and physically processed for a week or two since the last injection of combustion emissions. Many of the trajectories follow a path that implies that the last continental areas that the air parcels passed over were Brazil and Africa. Since biomass burning occurs on both of these continental areas during austral spring [*Cahoon et al.*, 1992], this is likely to be a major source of combustion emissions over the Pacific basin at this time of year.

Methyl chloride is a reasonably good chemical tracer of biomass burning emissions [*Blake et al.*, 1996]. The relationship between

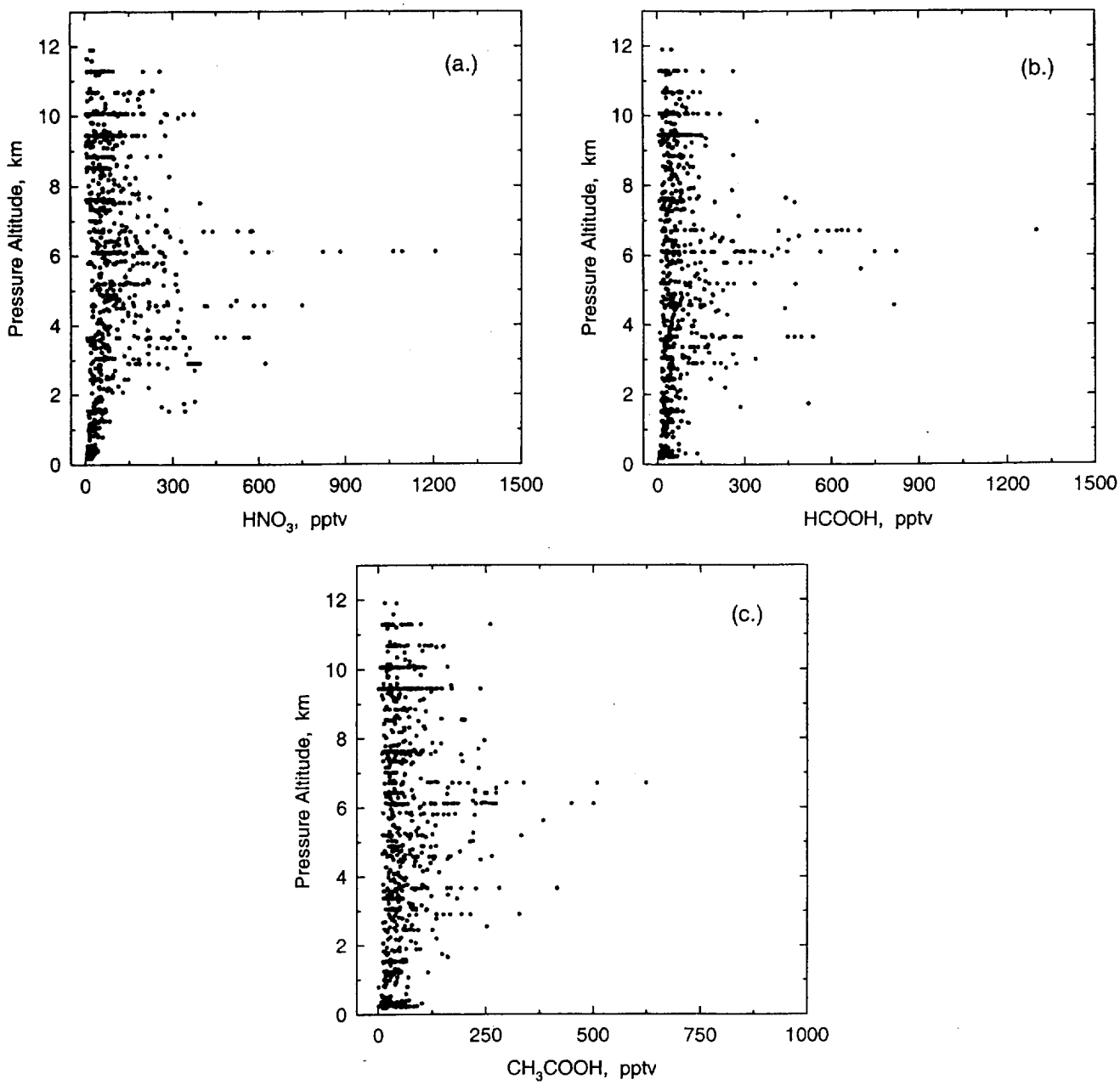

Figure 2. Vertical distribution of acidic gases over the central and southern Pacific basins. These distributions show that plume encounters with enhanced mixing ratios of acidic gases commonly occurred in the 3-7 km altitude region.

the mixing ratios of CH_3Cl and acidic gases is depicted in Figure 6. These plots indicate a general relationship between acidic gases and CH_3Cl ($r^2 = 0.4$). The enhancements of CH_3Cl in the plumes are small due to the significant dilution these well aged air parcels have undergone. Plots of C_2H_2 and C_2H_6 versus CH_3Cl (not shown) show similar relationships to those in Figure 6, again reflecting the substantial processing of the air parcels over the Indian and Pacific basins.

One feature of the plumes is the absence of enhancements in aerosol or aerosol associated species [*Dibb et al.*, this issue], even for ammonium which is released in large quantities from biomass combustion [*Lobert et al.*, 1991]. This indicates that the air parcels over the Pacific basin have been effectively scavenged by clouds and precipitation. It also suggests, since most acidic gases are highly water-soluble, that their large mixing ratios in some of the plumes may be due to photochemical production since the last scavenging event. Evidence for a photochemical source of acidic gases is provided in Figures 7 and 8, where the relationships between these species and O_3 and PAN are presented. As with CH_3Cl, the trends are only general (r^2 near 0.4) but suggestive of photochemical production of acidic gases. The break in the relationships at <5 pptv of PAN is presumably due to thermal decomposition of PAN to NO_x at lower altitudes [*Roberts*, 1995]. The data corresponding to <5 pptv PAN was obtained in the 2-4 km altitude band where air temperatures were typically 280-285°K.

Plotting an individual species as a function of the ratio C_2H_2/CO gives insight on the effect of air parcel processing on its mixing ratio. These relationships for acidic gases are shown in Figure 9. It is evident that the relationship is much tighter for the carboxylic acids compared to HNO_3, but it is unclear as to why this is the case.

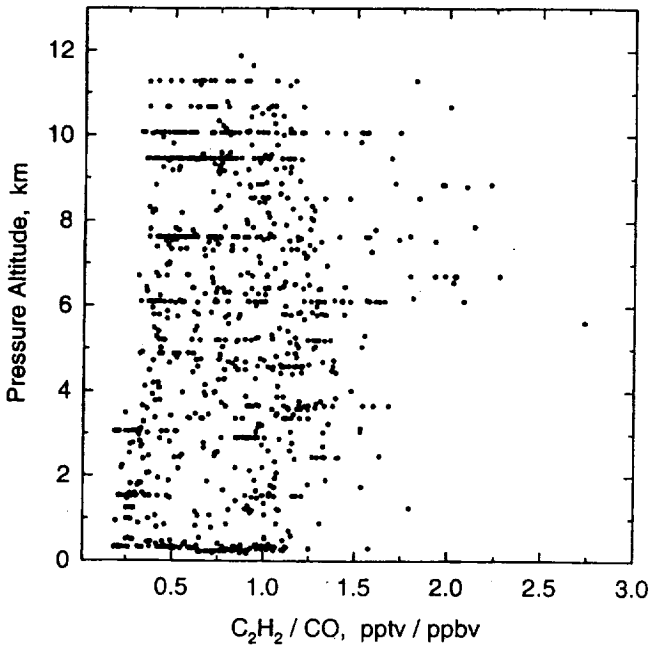

Figure 3. Vertical distribution of the ratio C_2H_2/CO over the central and southern Pacific basins.

Clearly, the largest mixing ratios of acidic gases were contained in the least processed air parcels (C_2H_2/CO >1). On the basis of the correlations shown in this paper, it follows that these same air parcels also contained the largest mixing ratios of CH_3Cl, O_3, and PAN. It appears that the chemical composition of these air parcels reflects photochemical activity of biomass burning emissions aged over a minimum of a one week time frame. This is based largely on the absence of reactive hydrocarbons (i.e., C_4 and higher) in these air parcels. It appears that mixing processes (i.e., dilution) are responsible for much of the variation in individual species mixing ratios and inter-relationships between various compounds. Thus, air parcels can be quite photochemically aged with significant mixing ratios of secondary species but still appear much younger (e.g., C_2H_2/CO >1) due to less mixing with background air.

To examine the potential combustion source of HNO_3, only mixing ratios greater than 100 pptv are plotted versus CO and C_2H_2 (Figure 10). Only in a few plumes does there appear to be a direct relationship between HNO_3 and CO or C_2H_2. The largest mixing ratios of HNO_3 occurred at relatively low values of CO and C_2H_2 and correspond to a C_2H_2/CO ratio near 1 (Figure 9). In general, there was very substantial amounts of HNO_3 in air parcels with CO of 50-100 ppbv and C_2H_2 <150 pptv. Together these results point to significant photochemical production of HNO_3 (since the last scavenging event) during long-range transport of air parcels over the South Pacific. Similar arguments can be made for photochemical generation of carboxylic acids in these air parcels, especially HCOOH. Previous measurements of the ratio HCOOH/CH_3COOH in biomass burning plumes transported long distances in the middle troposphere show values of 1.5-3 [*Helas et al.*, 1992; *Lefer et al.*, 1994; *Dibb et al.*, 1996b].

Additional modeling studies are needed to enhance our understanding of photochemical processes occurring within plumes over the South Pacific basin. Limited insight as to whether we observed loss of CH_3COOH in these plumes can be gleamed by examination of the CH_3COOH and CH_3OOH data. Plotting various subsets of these data obtained over the South Pacific (not shown) revealed no correspondence between the two species, as would be expected if CH_3COOH were a significant decomposition source of CH_3OOH

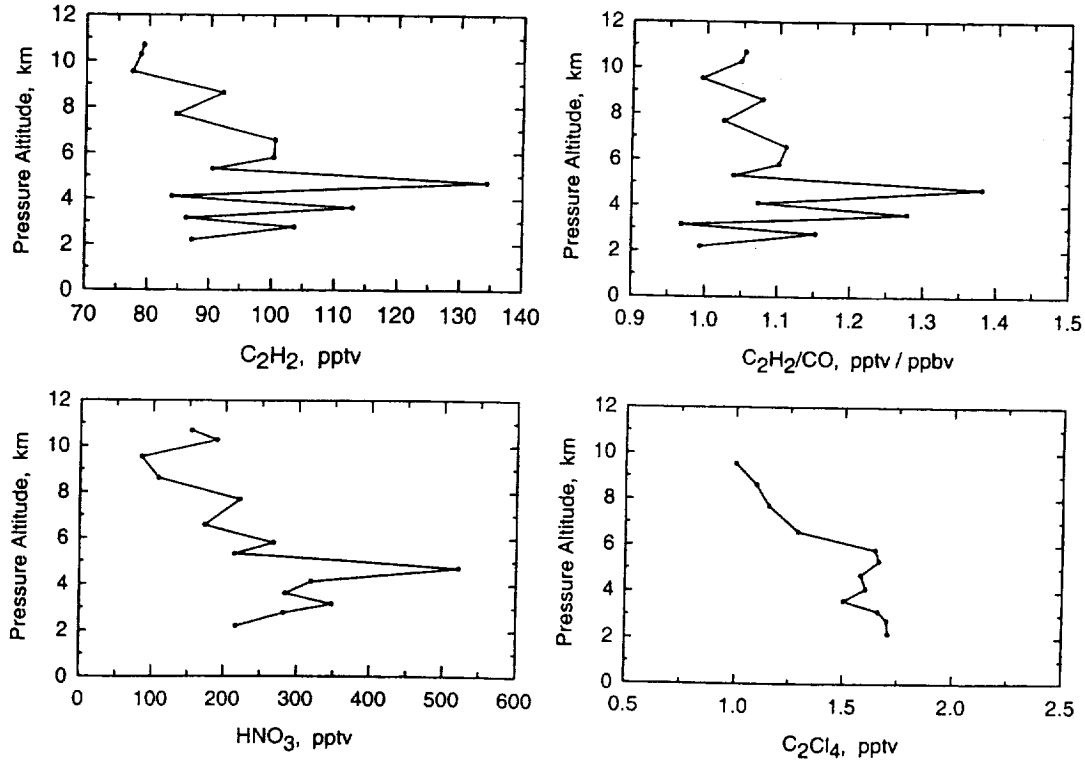

Figure 4. Vertical distribution of selected trace gases during a slow spiral conducted during mission 17 just east of Fiji.

Table 1. Regional Summary of Acidic Gases Over the Central and Pacific Basins

Altitude, km	HNO_3	HCOOH, pptv	CH_3COOH	N
		15°-45°N, 120°-170°W		
< 1	13 ± 8.5 (10)	45 ± 18 (50)	55 ± 23 (60)	17
1-2	46 ± 10 (50)	39 ± 30 (30)	44 ± 35 (36)	6
2-8	87 ± 43 (83)	72 ± 49 (55)	72 ± 45 (59)	42
8-12	63 ± 53 (42)	55 ± 26 (52)	54 ± 30 (55)	29
		0°-15°N, 120°-170°W		
< 1	20 ± 11 (15)	35 ± 30 (27)	34 ± 23 (20)	19
1-2	52 ± 14 (49)	33 ± 24 (18)	36 ± 26 (22)	10
2-8	67 ± 35 (51)	31 ± 14 (33)	33 ± 14 (35)	31
8-12	150 ± 107 (107)	27 ± 26 (14)	23 ± 19 (13)	16
		0°-35°S, 120°-170°W		
< 1	18 ± 10 (17)	66 ± 216 (23)	84 ± 293 (27)	40
1-2	32 ± 14 (30)	44 ± 20 (43)	43 ± 345 (39)	21
2-8	139 ± 145 (84)	124 ± 181 (49)	84 ± 81 (54)	192
8-12	63 ± 63 (37)	61 ± 54 (46)	56 ± 46 (41)	122
		0°-35°S, >170°W		
< 1	15 ± 7.7 (13)	18 ± 7.4 (17)	17 ± 8.1 (15)	12
1-2	40 ± 3.0 (40)	50 ± 5.0 (50)	46 ± 8.5 (46)	2
2-8	160 ± 124 (97)	71 ± 54 (47)	84 ± 70 (53)	46
8-12	100 ± 61 (81)	66 ± 32 (52)	92 ± 27 (94)	19
		0°-35°S, 80°-120°W		
< 1	13 ± 7.1 (14)	18 ± 5.9 (18)	16 ± 13 (18)	27
1-2	28 ± 8.2 (30)	33 ± 8.5 (32)	67 ± 47 (47)	5
2-8	43 ± 37 (31)	43 ± 28 (36)	52 ± 43 (36)	50
8-12	45 ± 30 (45)	54 ± 41 (39)	42 ± 26 (43)	28
		35°-72°S, >170°W		
< 1	14 ± 4.6 (14)	11 ± 4.1 (10)	13 ± 3.9 (12)	23
1-2	25 ± 9.9 (28)	38 ± 26 (33)	29 ± 16 (26)	13
2-8	180 ± 262 (80)	162 ± 176 (90)	114 ± 12 (57)	70
8-12	54 ± 71 (25)	54 ± 39 (40)	45 ± 25 (37)	23
		35°-72°S, 80°-120°W		
< 1	12 ± 2.3 (11)	16 ± 4.4 (18)	18 ± 4.6 (19)	7
1-2	31 ± NA (31)	22 ± NA (22)	20 ± NA (20)	1
2-8	26 ± 16 (23)	35 ± 19 (36)	33 ± 18 (26)	16
8-12	38 ± 60 (9.0)	18 ± 5.0 (19)	16 ± 4.8 (17)	5

Values are stated as mean ± one standard deviation (median). N represents the number of data in altitude bin. NA means not applicable.

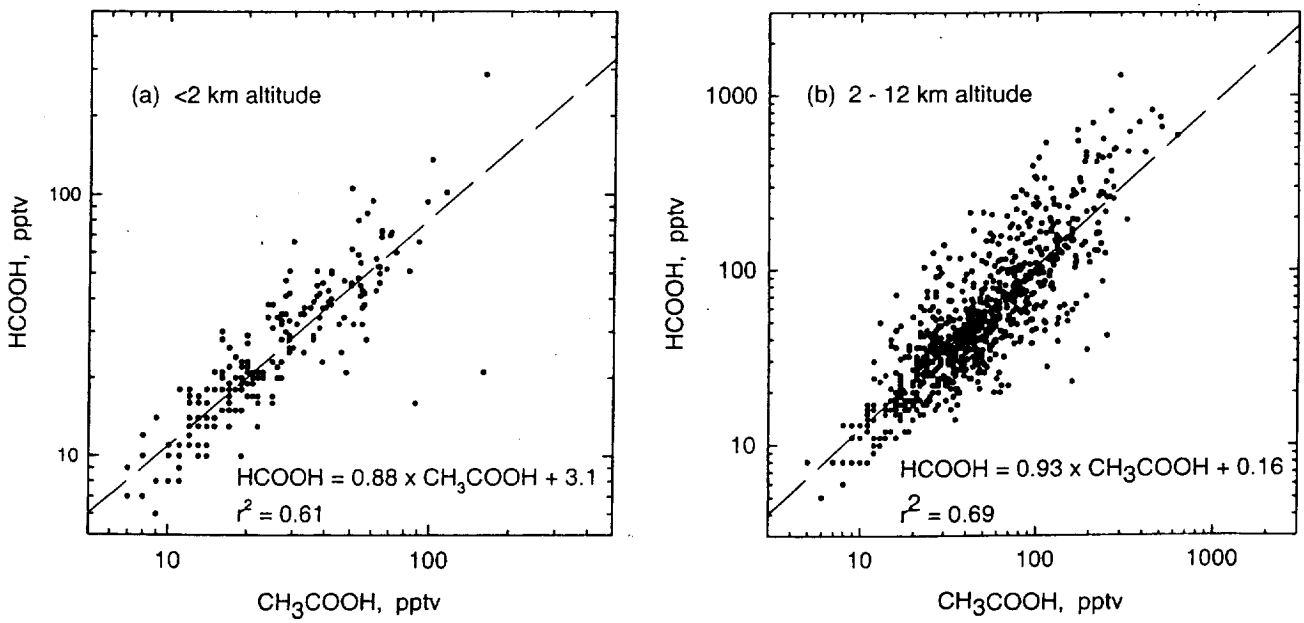

Figure 5. Relationship between mixing ratios of HCOOH and CH_3COOH over the central and southern Pacific basins; (a) <2 km and (b) 2-12 km altitude.

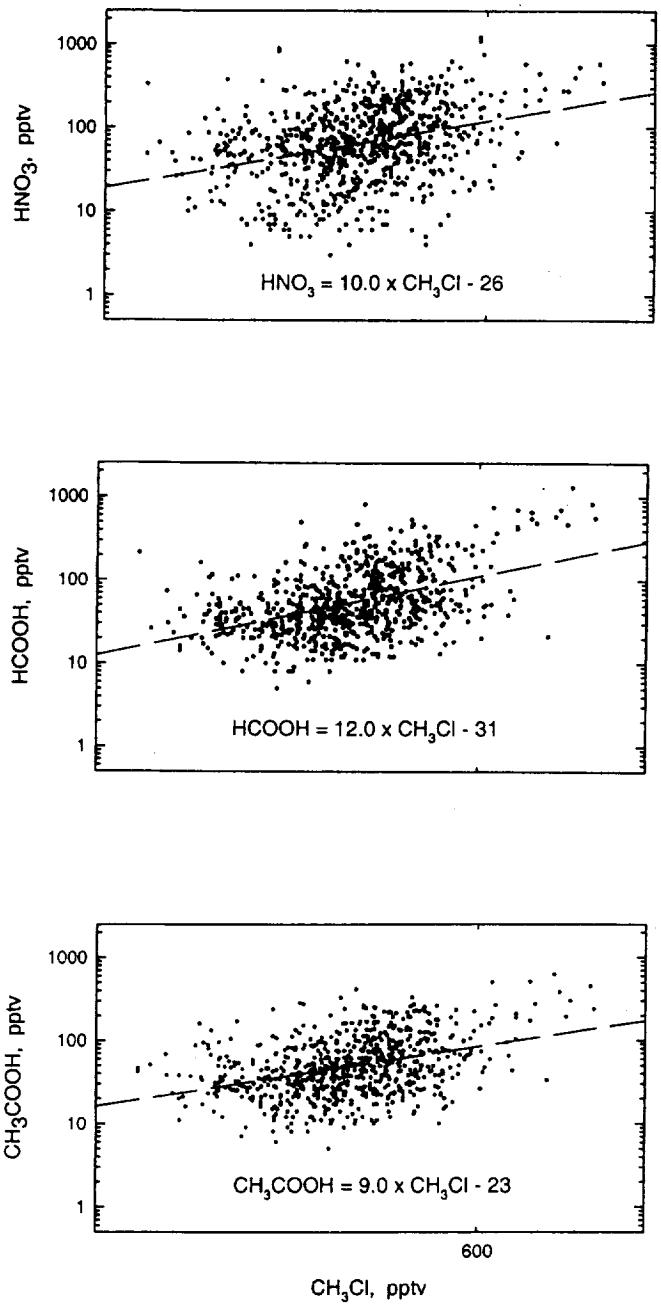

Figure 6. Relationships between mixing ratios of acidic gases and CH_3Cl in the altitude range 2-12 km. The r^2 values for these correlations were ≈0.35. Particularly for HCOOH and CH_3COOH, there is a general trend of enhanced mixing ratios at the largest values of CH_3Cl. These correlations potentially indicate an important biomass burning source for acidic gases over the South Pacific basin. Note that the abscissas are also a logarithmic scale, ranging from 500 to 650 pptv.

[*Madronich and Calvert*, 1990]. This result appears to support a significant photochemical source of HCOOH rather than a predominance of decomposition of CH_3COOH in aged biomass burning plumes over the South Pacific. We can not rule out, however, some photochemical production of CH_3COOH as well. Because of potentially complex (and unknown) chemistry in these biomass burning plumes, there is clearly much uncertainty surrounding the production and decomposition of carboxylic acids in such air parcels.

4.2 Altitude Range of 1-2 km

The altitude band <2 km was broken into the marine boundary layer (<1 km) and the transition or cloud layer from 1-2 km. The mixing ratio of acidic gases in these two layers are shown as a function of latitude in Figures 11a-11c. Nitric acid mixing ratios were smaller at <1 km compared to 1-2 km altitude, except for the most southerly data where they were about equal. There does not

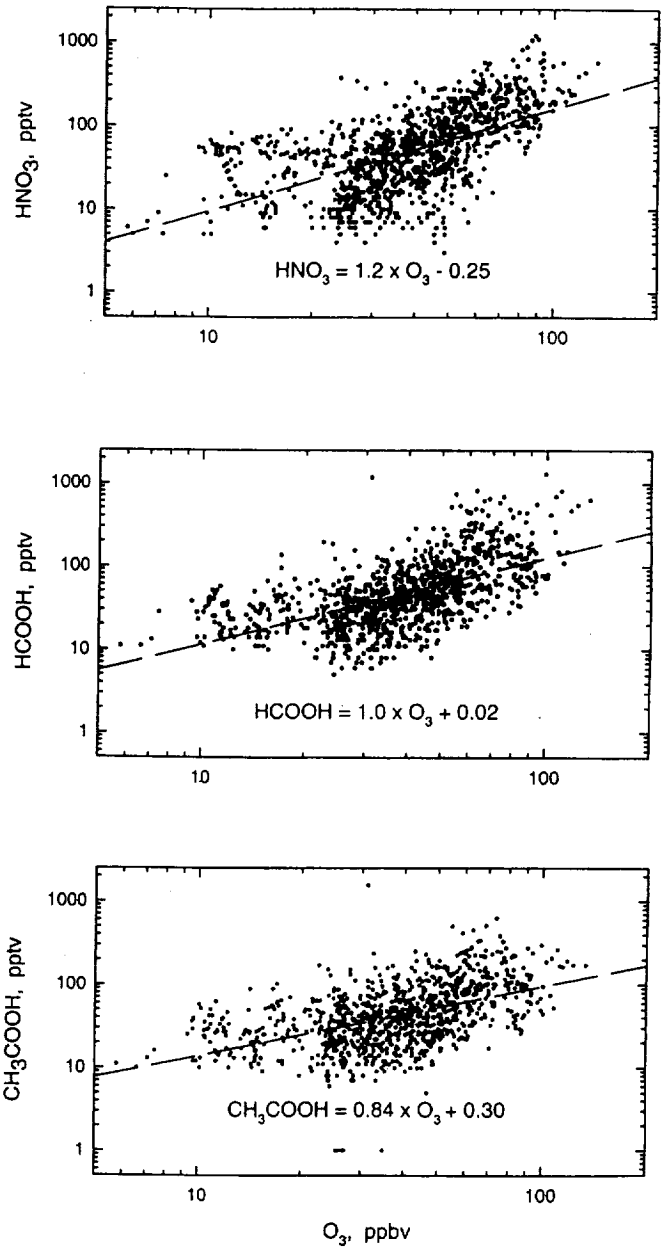

Figure 7. Relationships between mixing ratios of acidic gases and O_3 in the altitude range 2-12 km. The r^2 values for these correlations were ≈0.40. These general correlations potentially indicate a photochemical source for HCOOH and CH_3COOH.

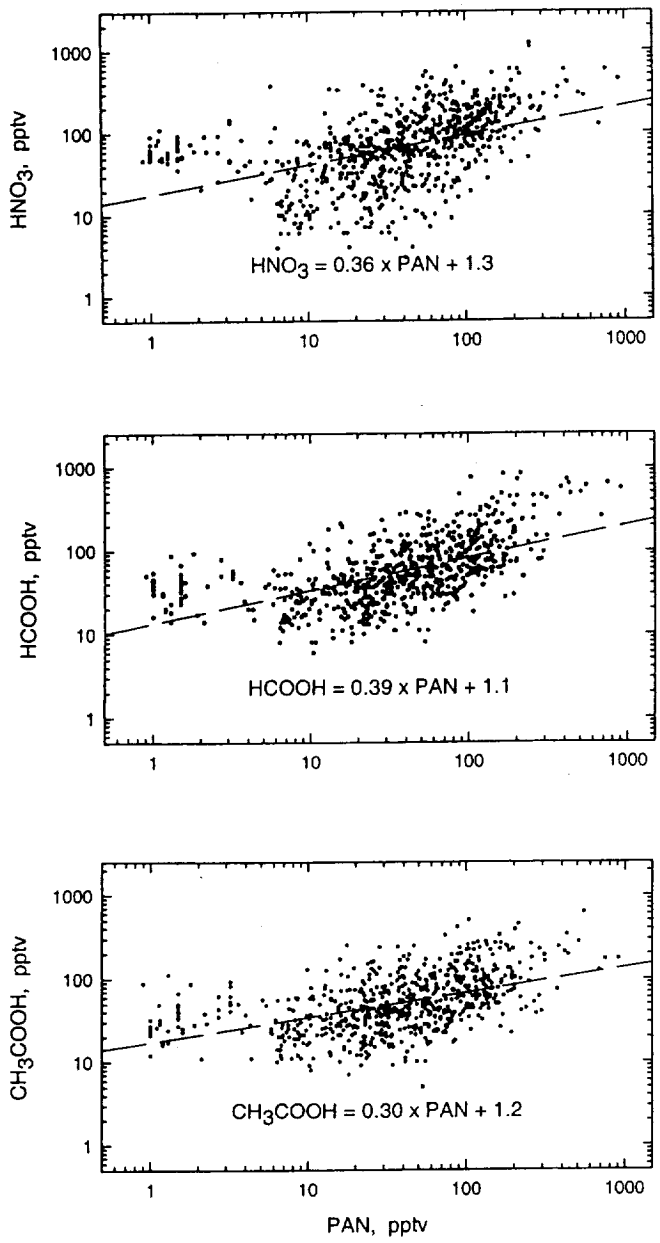

Figure 8. Relationships between mixing ratios of acidic gases and PAN in the altitude range 2-12 km. The r^2 values for these correlations were ≈0.40. These general correlations potentially indicate a photochemical source for HCOOH and CH_3COOH. Mixing ratios of PAN below ≈5 pptv were observed in the altitude range 2-4 km, where thermal decomposition of PAN was apparently significant.

appear to be any systematic variation of HNO_3 mixing ratios at <1 km altitude with latitude. Although the data are somewhat scattered, HNO_3 mixing ratios appear to increase in the transition layer going from south to north latitude. This apparent trend is driven to a large extent by the low values near 60°S. At midlatitudes and in the tropics there was 2-3 times more HNO_3 in the transition layer than at <1 km altitude. This observation could be related to evaporation of cloud droplets releasing HNO_3 to the gas phase in the transition layer. This process would be most active near the ITCZ, which is where the largest mixing ratios of HNO_3 were observed at this altitude. In both layers, aerosol NO_3^- mixing ratios were about a factor of 2 greater than those of HNO_3 [*Dibb et al.*, this issue], presumably due to uptake of HNO_3 onto sea-salt particles in the marine boundary layer [*Huebert*, 1980] and possibly production of aerosol-NO_3^- from cloud processing in the transition layer.

The mixing ratios of carboxylic acids in the marine boundary layer over the South Pacific were about an order of magnitude less than those previously determined from shipboard sampling in the central North Pacific region [*Arlander et al.*, 1990]. This probably is due to the remoteness of the South Pacific basin from continental areas and restricted downward mixing across the trade wind inversion. Formic and acetic acid did not exhibit a difference in their mixing ratios between the marine boundary and transition layers. In the marine boundary layer they had the largest mixing ratios north of the ITCZ. This may reflect the closer proximity of

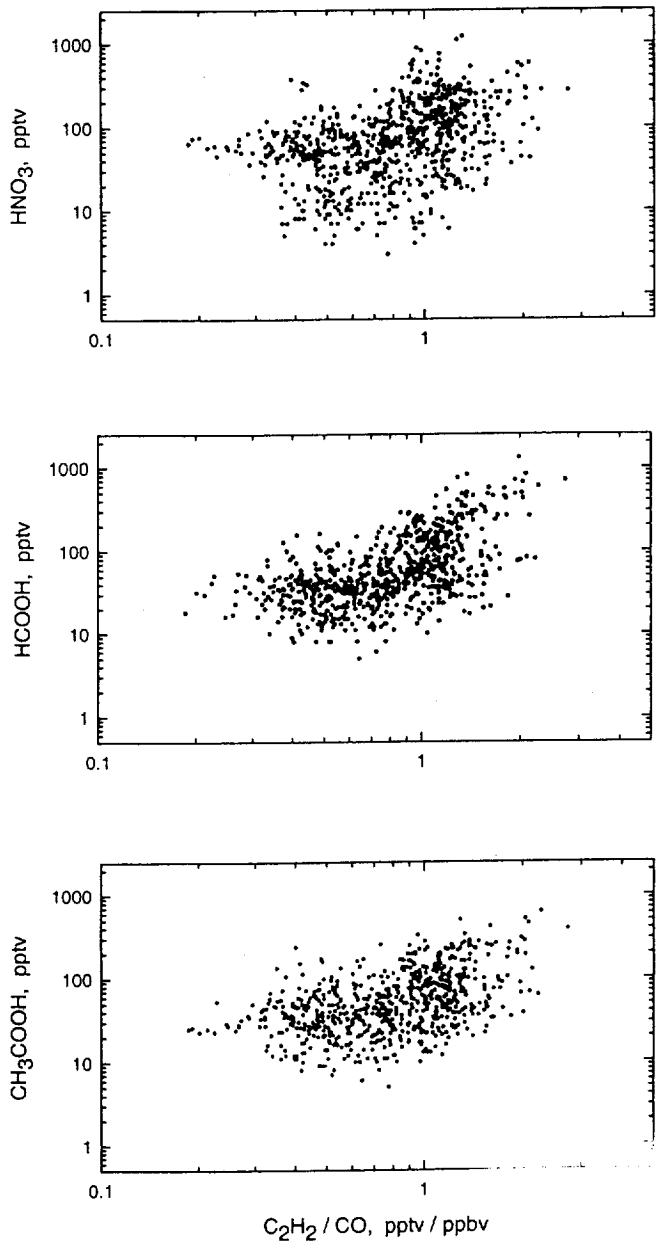

Figure 9. Distribution of the mixing ratios of acidic gases as a function of the ratio C_2H_2/CO.

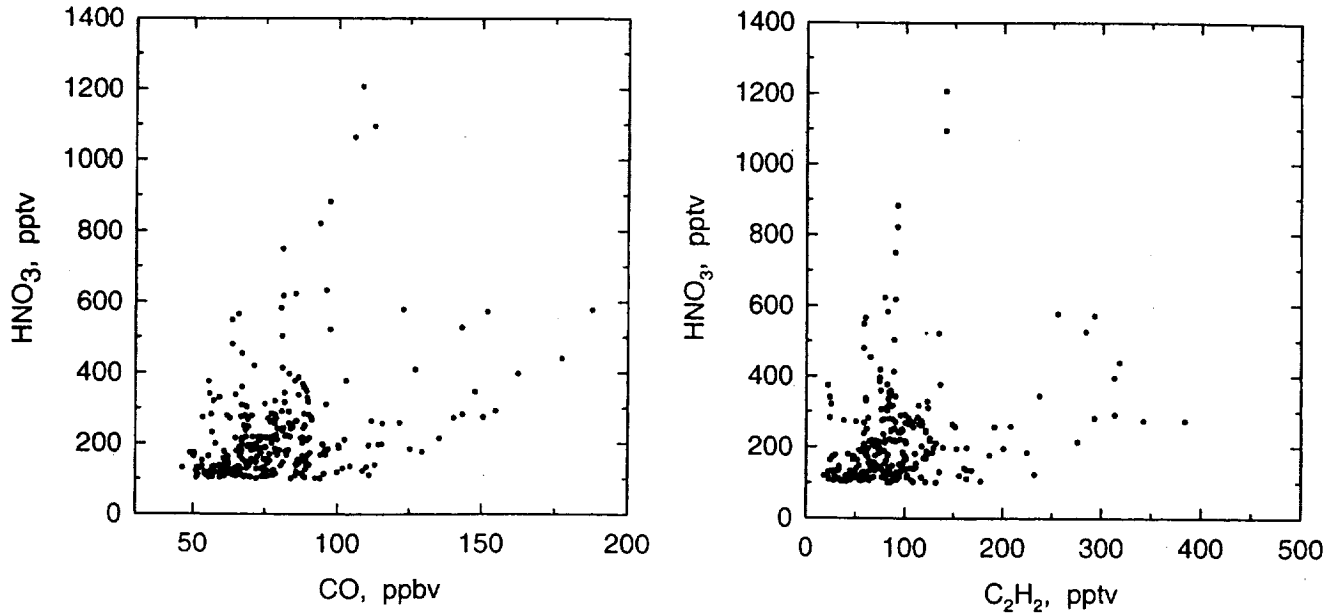

Figure 10. Mixing ratio of HNO_3 as a function of CO and C_2H_2 for HNO_3 >100 pptv.

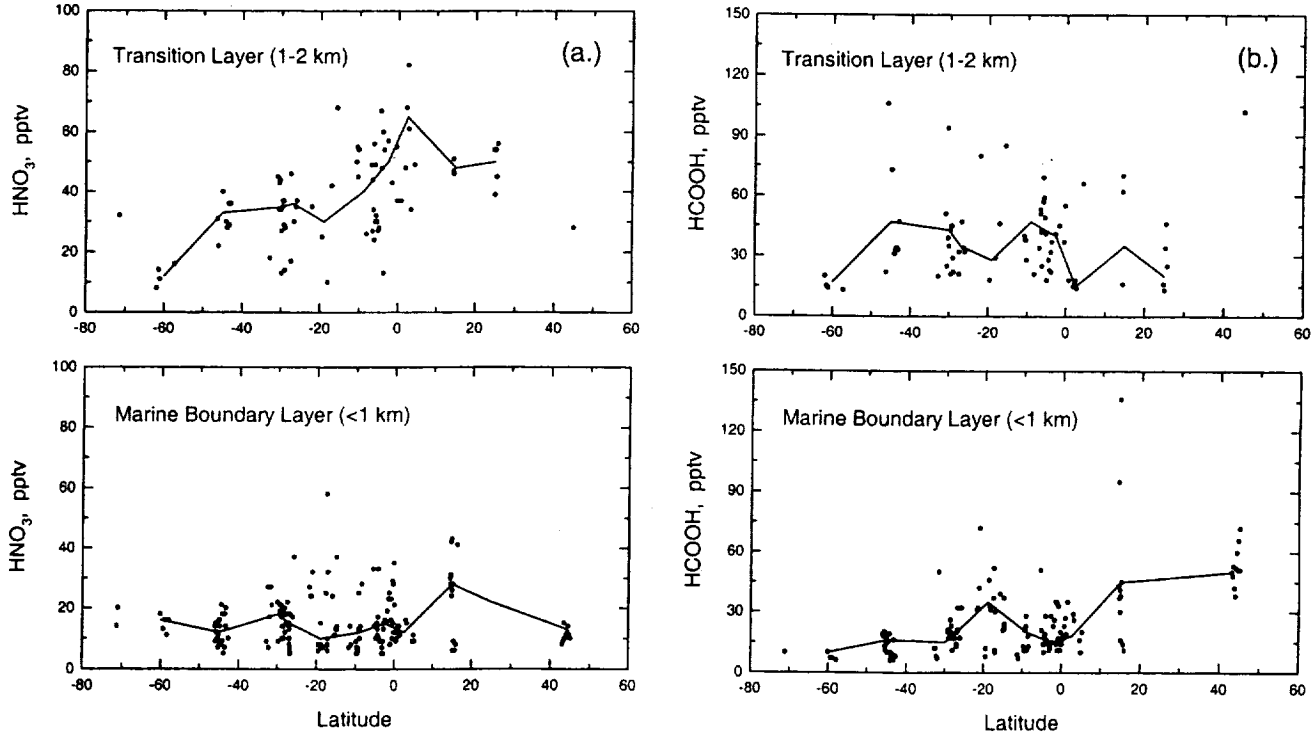

Figure 11. Latitudinal distribution of acidic gases in the marine boundary layer (<1 km) and the overlying transition layer (1-2 km). The solid lines represent a plot of the median mixing ratio value as a function of latitude.

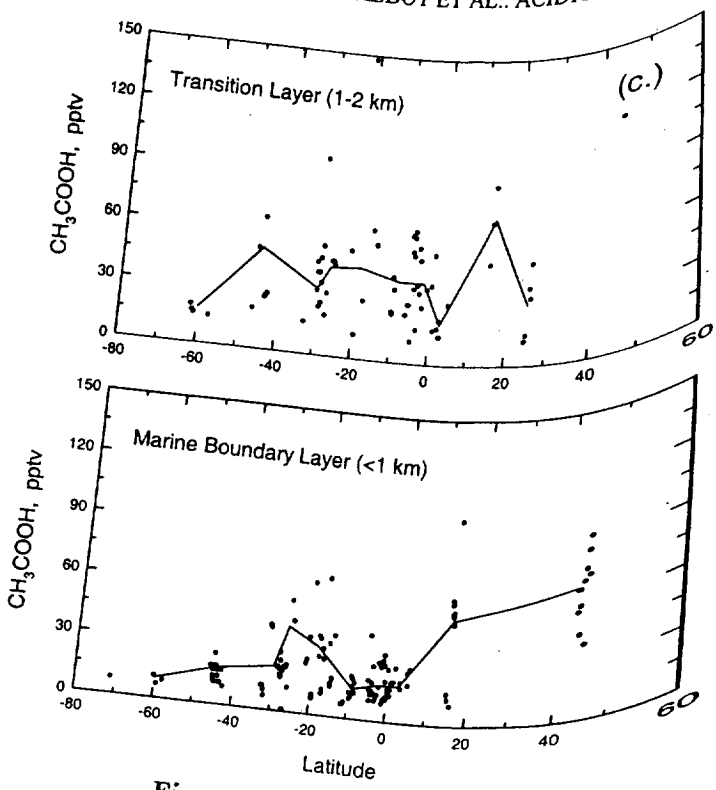

Figure 11. (continued)

continental areas to this region leading to enhanced primary or secondary production of these species. One difference between the vertical distribution of HNO_3 and the carboxylic acids in the two surface layers is the similarity of the mixing ratios of HCOOH and CH_3COOH in these two altitude bands but not those of HNO_3. This observation may be explained by more extensive uptake of HNO_3 onto sea salt aerosols compared to the carboxylic acids. Detailed gas phase, cloud droplet, and aerosol measurements over the remote oceans are needed to better understand this issue.

5. Conclusion

The distribution of acidic gases over the South Pacific basin in austral springtime appears to be strongly influenced by emissions from biomass burning, most likely occurring in Africa and Brazil. Owing to the generally westerly flow of air over this area in the middle and upper troposphere, elevated mixing ratios of acidic ases and the presence of pollution plumes were concentrated in the estern and central South Pacific. The eastern Pacific basin was latively "clean" presumably due to chemical and physical removal these species during the long transit across the South Pacific. The enhanced mixing ratios of acidic gases in pollution plumes e coincident with relatively low mixing ratios of the combustion ers CO and C_2H_2. This observation and their general correla- s with O_3 and PAN suggest that the mixing ratios of acidic gases have been sustained by photochemical production in the tion plumes. Most likely this generation of acidic gases red after the last scavenging event the air parcels encountered ther soluble species such as aerosols were not enhanced in same plumes. The PEM-Tropics data document the heric-scale pollution of the southern troposphere by biomass in austral springtime. The impact of these emissions on the try of the southern hemisphere troposphere appears to be reater than previously recognized.

Acknowledgments: We honor the outstanding unselfish contributions of our colleague and friend John Bradshaw (deceased) to the overall success and accomplishments of the GTE/PEM-Tropics airborne expedition. Excellent support was provided by the ground and flight crews of the NASA Ames DC-8 aircraft. This research was supported by the NASA Global Tropospheric Chemistry program.

References

Andreae, M. O., R. W. Talbot, T. W. Andreae, and R. C. Harriss, Formic and acetic acid over the central Amazon region, Brazil, 1, Dry season, *J. Geophys. Res.*, *93*, 1616-1624, 1988.

Andreae, M. O., R. W. Talbot, H. Berresheim, and K. C. Beecher, Precipitation chemistry in central Amazonia, *J. Geophys. Res.*, *95*, 16,987-16,999, 1990.

Arlander, D. W., D. R. Cronn, J. C. Farmer, F. A. Menzia, and H. H. Westberg, Gaseous oxygenated hydrocarbons in the remote marine troposphere, *J. Geophys. Res.*, *95*, 16,391-16,403, 1990.

Blake, N. J., D. R. Blake, B. C. Sive, T.-Y. Chen, and F. S. Rowland, Biomass burning emissions and vertical distribution of atmospheric methyl halides and other reduced carbon gases in the South Atlantic region, *J. Geophys. Res.*, *101*, 24,151-24,164, 1996.

Cahoon, D. R., Jr., B. J. Stocks, J. S. Levine, W. R. Cofer III, and K. P. O'Neill, Seasonal distribution of African savanna fires, *Nature*, *359*, 812-815, 1992.

Chameides, W. L., and D. D. Davis, Aqueous-phase source of formic acid in clouds, *Nature*, *304*, 427-429, 1983.

Dibb, J. E., R. W. Talbot, K. I. Klemm, G. L. Gregory, H. B. Singh, J. D. Bradshaw, and S. T. Sandholm, Asian influence over the western North Pacific during the fall season: Inferences from lead-210, soluble ionic species, and ozone, *J. Geophys. Res.*, *101*, 1779-1792, 1996a.

Dibb, J. E., R. W. Talbot, S. I. Whitlow, M. C. Shipham, J. Winterle, J. McConnell, and R. Bales, Biomass burning signatures in the atmosphere and snow at Summit, Greenland: An event on 5 August 1994, *Atmos. Environ.*, *30*, 553-561, 1996b.

Dibb, J. E., R. W. Talbot, E. M. Scheuer, D. R. Blake, N. J. Blake, G. L. Gregory, G. W. Sachse, and D. C. Thornton, Aerosol chemical characteristics and distribution during the Pacific Exploratory Mission, Tropics, *J. Geophys. Res.*, this issue.

Folkins, I. A., A. J. Weinheimer, B. A. Ridley, J. G. Walega, B. Anderson, J. E. Collins, G. Sachse, R. F. Pueschel, and D. R. Blake, O_3, NO_y, and NO_x/NO_y in the upper troposphere of the equatorial Pacific, *J. Geophys. Res.*, *100*, 20,913-20,926, 1995.

Fuelberg, H. E., R. E. Newell, S. Longmore, Y. Zhu, D. J. Westberg, E. V. Browell, D. R. Blake, G. R. Gregory, and G. W. Sachse, A meteorological overview of the PEM-Tropics experiment, *J. Geophys. Res.*, this issue.

Gregory, G. L., et al., Chemical characteristics of Pacific tropospheric air in the region of the ITCZ and SPCZ, *J. Geophys. Res.*, this issue.

Hales, J. M., and M. T. Dana, Wet removal of sulphur compounds from the atmosphere, *Atmos. Environ.*, *12*, 389-400, 1979.

Helas, G., H. Bingemer, and M. O. Andreae, Organic acids over equatorial Africa: Results from DECAFE 88, *J. Geophys. Res.*, *97*, 6187-6193, 1992.

Hoell, J. M., Jr, et al., Pacific Exploratory Mission in the tropical Pacific: PEM-Tropics A, August-September 1996, *J. Geophys. Res.*, this issue.

Huebert, B. J., Nitric acid and aerosol nitrate measurements in the equatorial Pacific region, *Geophys. Res. Lett.*, *7*, 325-328, 1980.

Jacob, D. J., Chemistry of OH in remote clouds and its role in the production of formic acid and peroxymonosulfate, *J. Geophys. Res.*, *91*, 9807-9826, 1986.

Jacob, D. J., and S. C. Wofsy, Photochemical production of carboxylic acids in a remote continental atmosphere, in *Acid Deposition Processes at High Elevation Sites*, edited by M. H. Unsworth, pp. 73-92, D. Reidel, Norwell, Mass., 1988.

Kawamura, K., L.-L. Ng, and I. R. Kaplan, Determination of organic acids (C_1-C_{10}) in the atmosphere, motor exhausts, and engine oils, *Envrion. Sci. Technol.*, *19*, 1082-1086, 1985.

Keene, W. C., and J. N. Galloway, Considerations regarding sources for formic and acetic acids in the troposphere, *J. Geophys. Res.*, *91*, 14,467-14,474, 1986.

Keene, W. C., J. N. Galloway, and J. D. Holden Jr., Measurements of weak organic acidity in precipitation from remote areas of the world, *J. Geophys. Res.*, *88*, 5122-5130, 1983.

Lefer, B. L., et al., Enhancement of acidic gases in biomass burning impacted air masses over Canada, *J. Geophys. Res.*, *99*, 1721-1737, 1994.

Lobert, J. M., D. H. Scharffe, W.-M. Hao, T. A. Kuhlbusch, R. Seuwen, P. Warneck, and P. J. Crutzen, Experimental evaluation of biomass burning emissions: Nitrogen and carbon containing compounds, in *Global Biomass Burning - Atmospheric, Climatic, and Biospheric Implications*, edited by J. S. Levine, 289-304, MIT Press, Cambridge, Mass., 1991.

Logan, J. A., Nitrogen oxides in the troposphere: Global and regional budgets, *J. Geophys. Res.*, *88*, 10,785-10,807, 1983.

Madronich, S., and J. G. Calvert, Permutation reactions of organic peroxy radicals in the troposphere, *J. Geophys. Res.*, *95*, 5697-5717, 1990.

Madronich, S., R. B. Chatfield, J. G. Calvert, G. K. Moortgat, B. Veyret, and R. Lesclaux, A photochemical origin of acetic acid in the troposphere, *Geophys. Res., Lett.*, *17*, 2361-2364, 1990.

Roberts, J. M., Reactive odd-nitrogen (NO_y) in the atmosphere, in *Composition, Chemistry, and Climate of the Atmosphere*, edited by H. B. Singh, pp. 176-215, Van Nostrand Reinhold, New York, 1995.

Sanhueza, E., and M. O. Andreae, Emission of formic and acetic acids from tropical savanna soils, *Geophys. Res. Lett.*, *18*, 1707-1710, 1991.

Smyth, S., et al., Comparison of the chemical signatures between air mass classes from the PEM experiments over the western Pacific, *J. Geophys. Res.*, in press, 1998.

Talbot, R. W., K. M. Beecher, R. C. Harriss, and W. R. Cofer, III, Atmospheric geochemistry of formic and acetic acids at a midlatitude temperate site, *J. Geophys. Res.*, *93*, 1638-1652, 1988.

Talbot, R. W., M. O. Andreae, H. Berresheim, D. J. Jacob, and K. M. Beecher, Sources and sinks of formic, acetic, and pyruvic acids over central Amazonia, 2, Wet season, *J. Geophys. Res.*, *95*, 16,799-16,811, 1990.

Talbot, R. W., B. W. Mosher, B. G. Heikes, D. J. Jacob, J. W. Munger, B. C. Daube, W. C. Keene, J. R. Maben, and R. S. Artz, Carboxylic acids in the rural continental atmosphere over the eastern United States during the Shenandoah Cloud and Photochemistry Experiment, *J. Geophys. Res.*, *100*, 9335-9343, 1995.

Talbot, R. W., et al., Large-scale distribution of tropospheric nitric, formic, and acetic acids over the western Pacific basin during wintertime, *J. Geophys. Res.*, 102, 28,303-28,313, 1997a.

Talbot, R. W., et al., Continental outflow over the western Pacific basin during February-March 1994: Results from PEM-West B, *J. Geophys. Res.*, *102*, 28,255-28,274, 1997b.

Vay, S. A., B. E. Anderson, T. J. Conway, S. W. Sachse, J. E. Collins, d. R. Blake, and D. J. Westberg, Airborne observations of the tropospheric CO_2 distribution and its controlling factors over the South Pacific basin, *J. Geophys. Res.*, this issue.

D. R. Blake and N. J. Blake, Department of Chemistry, University of California, Irvine, CA 92717.

J. E. Dibb, E. M. Scheuer, and R. W. Talbot, Institute for the Study of Earth, Oceans, and Space, University of New Hampshire, Durham, NH 03824. (e-mail: rwt@christa.unh.edu)

G. L. Gregory and G. W. Sachse, NASA Langley Research Center, Hampton, VA.

S. T. Sundholm, Georgia Institute of Technology, Atlanta, GA 30332.

H. B. Singh, NASA Ames Research Center, Moffett Field, CA 94035.

(Received October 10, 1997; revised March 2, 1998;
accepted March 10, 1998.)

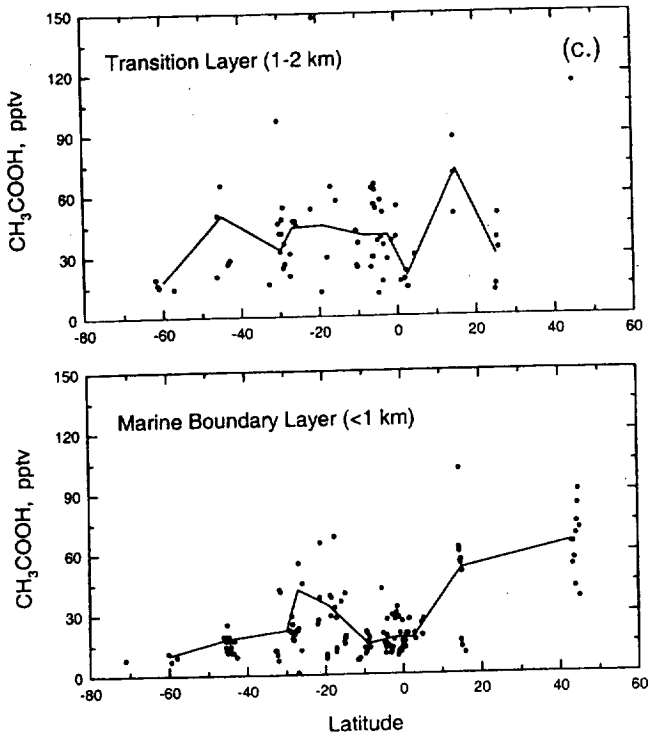

Figure 11. (continued)

continental areas to this region leading to enhanced primary or secondary production of these species. One difference between the vertical distribution of HNO_3 and the carboxylic acids in the two surface layers is the similarity of the mixing ratios of HCOOH and CH_3COOH in these two altitude bands but not those of HNO_3. This observation may be explained by more extensive uptake of HNO_3 onto sea salt aerosols compared to the carboxylic acids. Detailed gas phase, cloud droplet, and aerosol measurements over the remote oceans are needed to better understand this issue.

5. Conclusion

The distribution of acidic gases over the South Pacific basin in austral springtime appears to be strongly influenced by emissions from biomass burning, most likely occurring in Africa and Brazil. Owing to the generally westerly flow of air over this area in the middle and upper troposphere, elevated mixing ratios of acidic gases and the presence of pollution plumes were concentrated in the western and central South Pacific. The eastern Pacific basin was relatively "clean" presumably due to chemical and physical removal of these species during the long transit across the South Pacific.

The enhanced mixing ratios of acidic gases in pollution plumes were coincident with relatively low mixing ratios of the combustion tracers CO and C_2H_2. This observation and their general correlations with O_3 and PAN suggest that the mixing ratios of acidic gases may have been sustained by photochemical production in the pollution plumes. Most likely this generation of acidic gases occurred after the last scavenging event the air parcels encountered since other soluble species such as aerosols were not enhanced in these same plumes. The PEM-Tropics data document the hemispheric-scale pollution of the southern troposphere by biomass burning in austral springtime. The impact of these emissions on the chemistry of the southern hemisphere troposphere appears to be much greater than previously recognized.

Acknowledgments: We honor the outstanding unselfish contributions of our colleague and friend John Bradshaw (deceased) to the overall success and accomplishments of the GTE/PEM-Tropics airborne expedition. Excellent support was provided by the ground and flight crews of the NASA Ames DC-8 aircraft. This research was supported by the NASA Global Tropospheric Chemistry program.

References

Andreae, M. O., R. W. Talbot, T. W. Andreae, and R. C. Harriss, Formic and acetic acid over the central Amazon region, Brazil, 1, Dry season, *J. Geophys. Res.*, *93*, 1616-1624, 1988.

Andreae, M. O., R. W. Talbot, H. Berresheim, and K. C. Beecher, Precipitation chemistry in central Amazonia, *J. Geophys. Res.*, *95*, 16,987-16,999, 1990.

Arlander, D. W., D. R. Cronn, J. C. Farmer, F. A. Menzia, and H. H. Westberg, Gaseous oxygenated hydrocarbons in the remote marine troposphere, *J. Geophys. Res.*, *95*, 16,391-16,403, 1990.

Blake, N. J., D. R. Blake, B. C. Sive, T.-Y. Chen, and F. S. Rowland, Biomass burning emissions and vertical distribution of atmospheric methyl halides and other reduced carbon gases in the South Atlantic region, *J. Geophys. Res.*, *101*, 24,151-24,164, 1996.

Cahoon, D. R., Jr., B. J. Stocks, J. S. Levine, W. R. Cofer III, and K. P. O'Neill, Seasonal distribution of African savanna fires, *Nature*, *359*, 812-815, 1992.

Chameides, W. L., and D. D. Davis, Aqueous-phase source of formic acid in clouds, *Nature*, *304*, 427-429, 1983.

Dibb, J. E., R. W. Talbot, K. I. Klemm, G. L. Gregory, H. B. Singh, J. D. Bradshaw, and S. T. Sandholm, Asian influence over the western North Pacific during the fall season: Inferences from lead-210, soluble ionic species, and ozone, *J. Geophys. Res.*, *101*, 1779-1792, 1996a.

Dibb, J. E., R. W. Talbot, S. I. Whitlow, M. C. Shipham, J. Winterle, J. McConnell, and R. Bales, Biomass burning signatures in the atmosphere and snow at Summit, Greenland: An event on 5 August 1994, *Atmos. Environ.*, *30*, 553-561, 1996b.

Dibb, J. E., R. W. Talbot, E. M. Scheuer, D. R. Blake, N. J. Blake, G. L. Gregory, G. W. Sachse, and D. C. Thornton, Aerosol chemical characteristics and distribution during the Pacific Exploratory Mission, Tropics, *J. Geophys. Res.*, this issue.

Folkins, I. A., A. J. Weinheimer, B. A. Ridley, J. G. Walega, B. Anderson, J. E. Collins, G. Sachse, R. F. Pueschel, and D. R. Blake, O_3, NO_y, and NO_x/NO_y in the upper troposphere of the equatorial Pacific, *J. Geophys. Res.*, *100*, 20,913-20,926, 1995.

Fuelberg, H. E., R. E. Newell, S. Longmore, Y. Zhu, D. J. Westberg, E. V. Browell, D. R. Blake, G. R. Gregory, and G. W. Sachse, A meteorological overview of the PEM-Tropics experiment, *J. Geophys. Res.*, this issue.

Gregory, G. L., et al., Chemical characteristics of Pacific tropospheric air in the region of the ITCZ and SPCZ, *J. Geophys. Res.*, this issue.

Hales, J. M., and M. T. Dana, Wet removal of sulphur compounds from the atmosphere, *Atmos. Environ.*, *12*, 389-400, 1979.

Helas, G., H. Bingemer, and M. O. Andreae, Organic acids over equatorial Africa: Results from DECAFE 88, *J. Geophys. Res.*, *97*, 6187-6193, 1992.

Hoell, J. M., Jr, et al., Pacific Exploratory Mission in the tropical Pacific: PEM-Tropics A, August-September 1996, *J. Geophys. Res.*, this issue.

Huebert, B. J., Nitric acid and aerosol nitrate measurements in the equatorial Pacific region, *Geophys. Res. Lett.*, *7*, 325-328, 1980.

Jacob, D. J., Chemistry of OH in remote clouds and its role in the production of formic acid and peroxymonosulfate, *J. Geophys. Res.*, *91*, 9807-9826, 1986.

Jacob, D. J., and S. C. Wofsy, Photochemical production of carboxylic acids in a remote continental atmosphere, in *Acid Deposition Processes at High Elevation Sites*, edited by M. H. Unsworth, pp. 73-92, D. Reidel, Norwell, Mass., 1988.

Kawamura, K., L.-L. Ng, and I. R. Kaplan, Determination of organic acids (C_1-C_{10}) in the atmosphere, motor exhausts, and engine oils, *Envrion. Sci. Technol.*, *19*, 1082-1086, 1985.

Keene, W. C., and J. N. Galloway, Considerations regarding sources for formic and acetic acids in the troposphere, *J. Geophys. Res.*, *91*, 14,4[illegible] - 14,474, 1986.

Keene, W. C., J. N. Galloway, and J. D. Holden Jr., Measurements of weak organic acidity in precipitation from remote areas of the world, *J. Geophys. Res.*, *88*, 5122-5130, 1983.

Lefer, B. L., et al., Enhancement of acidic gases in biomass burning impacted air masses over Canada, *J. Geophys. Res.*, *99*, 1721-1737, 1994.

Lobert, J. M., D. H. Scharffe, W.-M. Hao, T. A. Kuhlbusch, R. Seuwen, P. Warneck, and P. J. Crutzen, Experimental evaluation of biomass burning emissions: Nitrogen and carbon containing compounds, in *Global Biomass Burning - Atmospheric, Climatic, and Biospheric Implications*, edited by J. S. Levine, 289-304, MIT Press, Cambridge, Mass., 1991.

Logan, J. A., Nitrogen oxides in the troposphere: Global and regional budgets, *J. Geophys. Res.*, *88*, 10,785-10,807, 1983.

Madronich, S., and J. G. Calvert, Permutation reactions of organic peroxy radicals in the troposphere, *J. Geophys. Res.*, *95*, 5697-5717, 1990.

Madronich, S., R. B. Chatfield, J. G. Calvert, G. K. Moortgat, B. Veyret, and R. Lesclaux, A photochemical origin of acetic acid in the troposphere, *Geophys. Res., Lett.*, *17*, 2361-2364, 1990.

Roberts, J. M., Reactive odd-nitrogen (NO_y) in the atmosphere, in *Composition, Chemistry, and Climate of the Atmosphere*, edited by H. B. Singh, pp. 176-215, Van Nostrand Reinhold, New York, 1995.

Sanhueza, E., and M. O. Andreae, Emission of formic and acetic acids from tropical savanna soils, *Geophys. Res. Lett.*, *18*, 1707-1710, 1991.

Smyth, S., et al., Comparison of the chemical signatures between air mass classes from the PEM experiments over the western Pacific, *J. Geophys. Res.*, in press, 1998.

Talbot, R. W., K. M. Beecher, R. C. Harriss, and W. R. Cofer, III, Atmospheric geochemistry of formic and acetic acids at a midlatitude temperate site, *J. Geophys. Res.*, *93*, 1638-1652, 1988.

Talbot, R. W., M. O. Andreae, H. Berresheim, D. J. Jacob, and K. M. Beecher, Sources and sinks of formic, acetic, and pyruvic acids over central Amazonia, 2, Wet season, *J. Geophys. Res.*, *95*, 16,799-16,811, 1990.

Talbot, R. W., B. W. Mosher, B. G. Heikes, D. J. Jacob, J. W. Munger, B. C. Daube, W. C. Keene, J. R. Maben, and R. S. Artz, Carboxylic acids in the rural continental atmosphere over the eastern United States during the Shenandoah Cloud and Photochemistry Experiment, *J. Geophys. Res.*, *100*, 9335-9343, 1995.

Talbot, R. W., et al., Large-scale distribution of tropospheric nitric, formic, and acetic acids over the western Pacific basin during wintertime, *J. Geophys. Res.*, 102, 28,303-28,313, 1997a.

Talbot, R. W., et al., Continental outflow over the western Pacific basin during February-March 1994: Results from PEM-West B, *J. Geophys. Res.*, *102*, 28,255-28,274, 1997b.

Vay, S. A., B. E. Anderson, T. J. Conway, S. W. Sachse, J. E. Collins, d. R. Blake, and D. J. Westberg, Airborne observations of the tropospheric CO_2 distribution and its controlling factors over the South Pacific basin, *J. Geophys. Res.*, this issue.

D. R. Blake and N. J. Blake, Department of Chemistry, University of California, Irvine, CA 92717.

J. E. Dibb, E. M. Scheuer, and R. W. Talbot, Institute for the Study of Earth, Oceans, and Space, University of New Hampshire, Durham, NH 03824. (e-mail: rwt@christa.unh.edu)

G. L. Gregory and G. W. Sachse, NASA Langley Research Center, Hampton, VA.

S. T. Sundholm, Georgia Institute of Technology, Atlanta, GA 30332.

H. B. Singh, NASA Ames Research Center, Moffett Field, CA 94035.

(Received October 10, 1997; revised March 2, 1998;
accepted March 10, 1998.)

JOURNAL OF GEOPHYSICAL RESEARCH, VOL. 104, NO. D5, PAGES 5785–5800, MARCH 20, 1999

Aerosol chemical composition and distribution during the Pacific Exploratory Mission (PEM) Tropics

J. E. Dibb,[1] R. W. Talbot,[1] E. M. Scheuer,[1] D. R. Blake,[2] N. J. Blake,[2] G. L. Gregory,[3] G. W. Sachse,[3] and D. C. Thornton[4]

Abstract. Distributions of aerosol-associated soluble ions over much of the South Pacific were determined by sampling from the NASA DC-8 as part of the Pacific Exploratory Mission (PEM) Tropics campaign. The mixing ratios of all ionic species were surprisingly low throughout the free troposphere (2-12 km), despite the pervasive influence from biomass burning plumes advecting over the South Pacific from the west during PEM-Tropics. At the same time, the specific activity of ^{7}Be frequently exceeded 1000 fCi m^{-3} through much of the depth of the troposphere. These distributions indicate that the plumes must have been efficiently scavenged by precipitation (removing the soluble ions), but that the scavenging must have occurred far upwind of the DC-8 sampling regions (otherwise ^{7}Be activities would also have been low). This inference is supported by large enhancements of HNO_3 and carboxylic acids in many of the plumes, as these soluble acidic gases would also be readily scavenged in any precipitation events. Decreasing mixing ratios of NH_4^+ with altitude in all South Pacific regions sampled provide support for recent suggestions that oceanic emissions of NH_3 constitute a significant source far from continents. Our sampling below 2 km reaffirms the latitudinal pattern in the methylsulfonate/non-sea-salt sulfate (MSA/nss $SO_4^=$) molar ratio established through surface-based and shipboard sampling, with values increasing from <0.05 in the tropics to nearly 0.6 at 70°S. However, we also found very high values of this ratio (0.2-0.5) at 10 km altitude above the intertropical convergence zone near 10°N. It appears that wet convective pumping of dimethylsulfide from the tropical marine boundary layer is responsible for the high values of the MSA/nss $SO_4^=$ ratio in the tropical upper troposphere. This finding complicates use of this ratio to infer the zonal origin of biogenic S transported long distances.

1. Introduction

In September/October 1996 the NASA Global Tropospheric Experiment (GTE) mounted a two-aircraft airborne sampling campaign over a large expanse of the South Pacific Ocean. The primary objectives of the Pacific Exploratory Mission-Tropics (PEM-Tropics) were to test current understanding of nitrogen oxide/ozone chemistry by extensive sampling in a region where the levels of NO_x and O_3 (and most other tropospheric trace gases) were expected to be quite low, and to further understanding of sulfur cycling in and between the marine boundary layer and the free troposphere over the South Pacific where anthropogenic influences on the sulfur cycle should be small.

Each of the aircraft (the Wallops P3-B and the Ames DC-8) carried an extensive suite of instrumentation to measure the mixing ratios of various trace gases central to O_3 photochemical cycling and the S cycle, as well as to characterize the physical and chemical characteristics of aerosols. The scientific payloads of the planes differed in some respects, reflecting the performance characteristics of the two platforms. The higher ceiling and greater range of the DC-8 make it better suited for surveys over large areas, while the low-altitude capabilities of the P3-B allow more detailed investigation of structure and processes within the marine boundary layer. The PEM-Tropics overview paper [*Hoell et al.*, this issue] provides details of the in situ and remote sensing instruments on both aircraft and describes the specific objectives of each mission flown during the deployment.

This paper is restricted to measurements made on the DC-8 and focuses on aerosol-associated soluble ionic species and the aerosol-associated cosmogenic radionuclide ^{7}Be. Comparisons are made with the distributions of several trace gases also measured on the DC-8, and with the distributions of aerosol-associated species over the North Pacific measured in the first two GTE Pacific Exploratory Missions, PEM-West A and B.

2. Methods

2.1. Sampling

Aerosol samples were collected from the NASA DC-8 on 17 flights over the Pacific Ocean as part of the GTE PEM-Tropics mission in September-October 1996. We employed the same inlet aerosol sampling system that was used on the GTE PEM-West missions [*Dibb et al.*, 1996, 1997]. One of the inlets was used to expose 2 μm pore size teflon (Gelman Zefluor) filters for the determination of the mixing ratios of soluble ionic species. The other inlet was generally used with glass fiber filters (Whatman GF/A) that were analyzed for the activities of the natural radionuclide tracers ^{7}Be

[1]Institute for the Study of Earth, Oceans, and Space, University of New Hampshire, Durham.
[2]Department of Chemistry, University of California, Irvine.
[3]NASA Langley Research Center, Hampton, Virginia.
[4]Department of Chemistry, Drexel University, Philadelphia, Pennsylvania.

Paper number 1998JD100001.
0148-0227/99/1998JD100001$09.00

and ^{210}Pb. When samples for determination of the radionuclides were collected, the integration intervals of both systems were identical, so that the mixing ratios of the ionic species and the radionuclides were determined in the same air masses. Sampling for the radionuclides was interrupted when the DC-8 crossed the Intertropical and South Pacific convergence zones (ITCZ and SPCZ) to allow collection of large-volume samples for elemental analyses (by instrumental neutron activation), primarily for halogen species such as I. The results of these analyses are not discussed herein, but it is important to note that this modification to our usual sampling protocol resulted in collection of 40 samples for determination of ionic species mixing ratios without the radionclide tracers.

Aerosol collection was restricted to flight legs at constant altitude. Exposure times in the mid and upper troposphere were usually in the 15-20 min range; below 2 km the integration interval was shortened to 10 min or less. A total of 322 samples was collected for ionic species analyses, with parallel samples for the radionuclide tracers in 282 of these intervals.

2.2 Analysis

Our analytical techniques were essentially unchanged from those used on the PEM-West campaigns [*Dibb et al.*, 1996, 1997]. However, we have slightly modified our handling of aerosol filters between exposure and analysis. On all GTE missions through PEM-West B our protocol involved placing exposed filters, still in the cassete, immediately into clean room bags and heat sealing them. Samples were then placed in a cooler with eutectic packs at -20°C for storage until extraction after the flight. Recognizing that the sealed bags contained a small amount of cabin air which could interact with the particles on the filter, we have begun including a purge of the bags with dry zero air. This procedure consists of sealing the clean bags with a tube delivering the zero air inside. A flow rate of about 2 L min^{-1} sweeps cabin air out of the bag and begins to inflate it. At this point the tube is withdrawn, and the bag is sealed again. Filters are then stored in a cooler. We have used this protocol for the Subsonic Assessment (SASS), Subsonic Aircraft Contrail and Cloud Effects Special Study (SUCCESS), and Subsonic Assessment Ozone and Nitrogen Oxide Experiment (SONEX) campaigns as well as during PEM-Tropics. The primary motivation for this change is to exclude any NH_3 in cabin air from contact with the exposed filters.

Concentrations of Cl^-, NO_3^-, $SO_4^{=}$, $C_2O_4^{=}$, $CH_3SO_3^-$, Na^+, NH_4^+, K^+, Mg^{2+}, and Ca^{2+} in aqueous extracts of the teflon filters were determined by ion chromatography. Extractions and quantitation of the anionic species were conducted in the field within 24 hours of each flight. Aliquots of extracts were preserved with chloroform and returned to our laboratory in New Hampshire for cation determinations; these were completed within 6 weeks of the final flight. Glass fiber filters were express-mailed to New Hampshire at intervals through the campaign so that ^7Be activities could be determined by gamma spectrometry as quickly as possible. However, the large number of relatively small volume samples collected created a backlog, so the final filters were not counted until 2 months after the last flight. Our ^{210}Pb technique (determination of the activity of the ^{210}Po daughter by alpha spectrometry) requires approximately 1 year for in-growth of the daughter before counting [*Dibb et al.*, 1996]. At the time of writing, these analyses were in progress, with samples from the first 12 flights (approximately 1/2 of the total) completed. As a result, the ^{210}Pb distribution during PEM-Tropics will be presented in a subsequent paper.

2.3. Data Binning

The DC-8 flights during PEM-Tropics extended over a very large region, covering over 100° of longitude (108°W-152°E) and extending from 55°N to 72°S (see overview paper by *Hoell et al.* [this issue]). In order to organize discussion of our results, the samples were binned into seven regions and three altitude ranges. The vertical bins roughly correspond to the marine boundary layer (<2 km), the lower to midtroposphere (2-8 km), and the upper troposphere (>8 km). The highest bin includes a few penetrations of the lower stratosphere in the higher-latitude spatial regions (>15°N and >35°S)

Selection of regional bins was based on a combination of large-scale features of atmospheric circulation convolved with the DC-8 flight tracks. In the northern hemisphere we defined two latitude bands (>15°N and 0°-15°N) on the basis of the position of the Intertropical Convergence Zone (ITCZ). Two latitude belts were defined in the southern hemisphere; a tropical and subtropical band (0°-35°S) and mid to high latitudes (>35°S). The operational bases of the DC-8 suggested three longitudinal zones, with flights out of Fiji and New Zealand defining the western region (west of 170°W), those out of Hawaii and Tahiti sampling the central zone (120°W to 170°W), and the Easter Island flights defining the eastern region (east of 120°W). See Figure 1 and its caption for a graphical representation of the regional bins.

The South Pacific Convergence Zone (SPCZ) represents another possible meteorological dividing line within our 0°-35°S latitude band. *Gregory et al.* [this issue] document and discuss the large spatial gradients in the mixing ratios of many species across the SPCZ. The aerosol-associated species that are the focus of this paper showed little difference on opposite sides of the SPCZ. We also considered dividing this bin at 15°S to reflect the oceanographic boundaries between the south equatorial current and the subtropical gyre. This division reveals nearly two-fold higher sea-salt concentrations in the boundary layer 15°-35°S compared to 0°-15°S in the western most region, a smaller boundary layer enhancement of sea-salt in the southerly portion of the central region, but no significant differences for the other species, or at higher altitudes. We therefore chose to maintain the 0°-35°S region as three bins rather than six with smaller numbers of samples in each.

In several sections of this paper we make comparisons between the aerosol composition and the mixing ratios of various trace gases measured by other experimenters on the DC-8. The sampling frequencies for analysis of these other species were all shorter than our integration intervals, but were not always the same for different gaseous species. We use a merged data file (generated at Harvard University) wherein the mixing ratios of all other parameters measured from the DC-8 were averaged over the aerosol sampling times to make these comparisons. This and several other merged products, as well as the original data reported from all instruments, are archived in the Langley Distributed Active Archive Center (DAAC).

3. Results

Aerosol composition in the 21 space-height bins described above is statistically summarized in Table 1. It should be noted that the mixing ratios of one or more of the species of interest were often below our detection limit. The detection limits are largely determined by variability in the concentrations of the analytes extracted from blank filters (which were generated at a rate of at least 2/flight by loading a filter into the sampling system, opening all valves to allow airflow for 15 s, and then removing the filter). We subtract the mission specific mean blank (nmol of analyte $filter^{-1}$) from each sample. Therefore the mixing ratios at detection limit vary inversely with the volume of air filtered for each sample. During PEM-Tropics our mean (standard deviation) blank values were 4.1 (2.8), 9.5 (7.5), 1.9 (1.8), 0.7 (1.9), 0.02 (0.08), 25.7 (16.2), 7.1 (4.5), 6.6 (5.2), 3.3 (1.3), and 1.2 (0.6) nmol $filter^{-1}$ of Cl^-, NO_3^-, $SO_4^{=}$, $C_2O_4^{=}$, $CH_3SO_3^-$, Na^+, NH_4^+, K^+, Ca^{2+}, and Mg^{2+}, respectively. Sample volumes ranged from 0.8 - 16.6 m^3 STP, with mean and median values of 4.2 and 3.8, respectively. For a

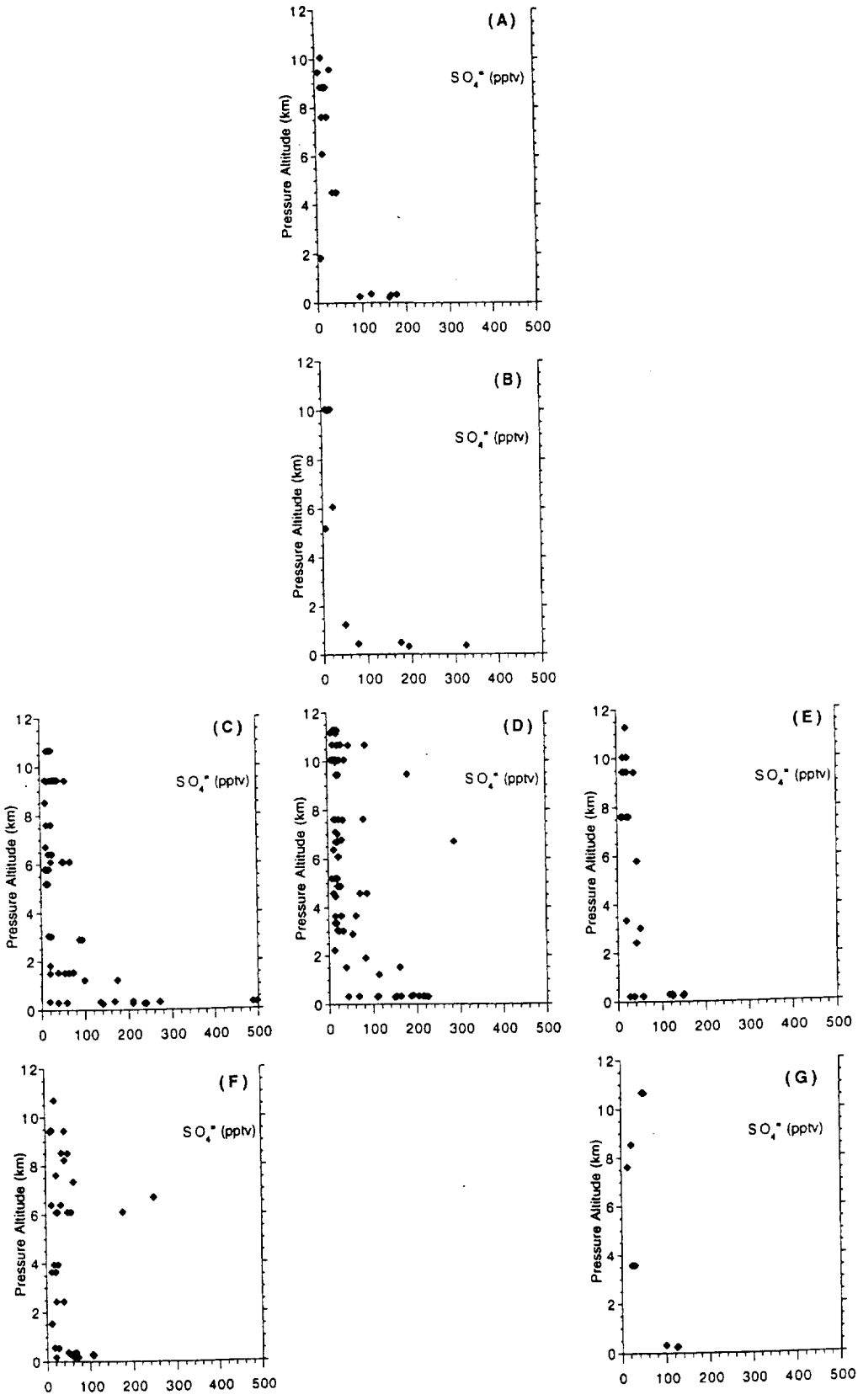

Figure 1. Altitude distribution of aerosol-associated $SO_4^=$ in the seven geographic regions sampled from the DC-8 during PEM-Tropics. The regions are the same as those defined in Table 1: (a) >15°N, 120°-170°W, (b) 0°-15°N, 120°-170°W, (c) 0°-35°S, West of 170°W, (d) 0°-35°S, 120°-170°W, (e) 0°-35°S, East of 120°W, (f) >35°S, West of 170°W, (g) >35°S, East of 120°W.

Table 1. Summary of Aerosol Composition, Binned by Region and Altitude

	Cl^-	NO_3^-	$SO_4^=$	$C_2O_4^=$	MSA	Na^+	NH_4^+	K^+	Ca^{2+}	Mg^{2+}	^7Be
			>15°N, 120°-170°W		*0-2 km*		*Six Samples[a] (6)*				
Mean	533	28	120	1.6	8.1	1025	122	73	40	119	382
s.d.	740	16	64	0.4	6.8	824	126	23	21	98	
Median	130	28	140	1.6	11.0	1316	82	73	52	152	
n	3	4	6	2	3	5	6	2	3	5	1
				2-8 km		*Seven Samples[a] (7)*					
Mean	25	67	26			30	62	10	21	7	245
s.d.	--	37	13			--	33	--	14	--	111
Median	25	67	25			30	64	10	21	7	243
n	1	2	5	0	0	1	6	1	2	1	6
				>8 km		*12 Samples[a] (12)*					
Mean		13	17				59				986
s.d.		5	8				19				1069
Median		15	17				59				530
n	0	3	7	0	0	0	5	0	0	0	9
			0°-15°N,120°-170°W		*0-2 km*		*Five Samples[a] (2)*				
Mean	1112	29	163	1.9	1.0	961	186	19	46	114	
s.d.	921	24	109	--	--	623	111	8	28	77	
Median	1064	24	174	1.9	1.0	1122	159	19	33	132	
n	5	5	5	1	1	5	5	2	3	5	0
				2-8 km		*Five Samples[a] (0)*					
Mean	89	19	14				22		20	7	
s.d.	71	17	12				--		--	--	
Median	89	16	14				22		20	7	
n	2	3	2	0	0	0	1	0	1	1	0
				>8 km		*Six Samples[a] (1)*					
Mean	23	68	13		3.5		69		17		
s.d.	4	23	5		1.4		34		4		
Median	23	68	13		3.7		62		17		
n	2	2	5	0	5	0	5	0	2	0	0
			0°-35°S,East of 120°W		*0-2 km*		*Eight Samples[a] (8)*				
Mean	996	46	97		2.3	993	123	43	31	113	
s.d.	763	23	50		1.0	706	46	24	7	81	
Median	1088	45	119		2.0	1094	129	35	35	134	
n	8	5	8	0	8	8	8	5	5	8	0
				2-8 km		*Twelve Samples[a] (12)*					
Mean	47	24	24		0.7	47	61	17		9	582
s.d.	21	20	15		--	55	25	--		--	270
Median	47	22	20		0.7	47	46	17		9	604
n	2	7	10	0	1	3	11	1	0	1	9
				>8 km		*10 Samples[a] (10)*					
Mean	33	35	21	3		84	43	20			539
s.d.	--	9	9	--		--	24	--			302
Median	33	35	20	3		84	40	20			439
n	1	2	7	1	0	1	8	1	0	0	8
			0°-35°S,120°-170°W		*0-2 km*		*18 Samples[a] (18)*				
Mean	1127	77	136	1.7	1.3	957	159	43	44	88	203
s.d.	731	102	64	--	0.8	718	78	20	39	61	76
Median	1116	47	150	1.7	1.2	885	163	45	34	69	179
n	18	17	18	1	14	16	17	9	13	17	12
				2-8 km		*46 Samples[a] (45)*					
Mean	116	61	33	6.2	0.3	183	73	42	19	53	363
s.d.	234	46	44	4.5	0.0	308	89	39	5	56	287
Median	47	44	21	6.8	0.3	75	53	22	20	21	277
n	14	22	42	4	3	9	33	9	3	5	36
				>8 km		*40 Samples[a] (40)*					
Mean	46	65	28	9.8	0.5	64	53	23	18	16	558
s.d.	19	76	34	9	0.0	--	57	10	2	--	439
Median	42	35	19	9.4	0.5	64	30	19	18	16	434
n	5	17	28	3	2	1	27	9	2	1	29
			0°-35°S,West of 170°W		*0-2 km*		*22 Samples[a] (12)*				
Mean	1111	62	154		1.4	1207	125	69	45	127	540
s.d.	991	42	138		1.1	856	78	32	24	95	0
Median	933	42	135		1	1133	102	68	47	112	540
n	19	11	21	0	16	19	22	12	12	18	2

Table 1. (continued)

	Cl^-	NO_3^-	$SO_4^=$	$C_2O_4^=$	MSA	Na^+	NH_4^+	K^+	Ca^{2+}	Mg^{2+}	^7Be
				2-8 km	*36 Samples[a] (31)*						
Mean	72	39	30		0.3	114	59	24	28	11	601
s.d.	92	30	25		0.1	88	30	10	14	6	467
Median	38	28	19		0.3	65	53	22	24	8	394
n	11	15	20	0	3	3	21	7	3	6	24
				>8 km	*32 Samples[a] (21)*						
Mean	41	41	26		0.8		112	19	23	8	775
s.d.	25	26	14		0.4		55	3	8	1	433
Median	27	35	25		1.0		81	19	23	8	686
n	7	6	14	0	3	0	8	3	2	2	13
			>35° S, East of 120° W		*0-2 km*	*Three Samples[a] (3)*					
Mean	1638	31	116		1.1	1705	114	46	41	195	134
s.d.	391	16	15		0.2	410	28	21	12	34	0
Median	1551	31	123		1.1	1659	129	38	48	208	134
n	3	2	3	0	3	3	3	3	3	3	2
				2-8 km	*Three Samples[a] (3)*						
Mean	51		21				99				467
s.d.	--		8				20				0
Median	51		22				105				467
n	1	0	3	0	0	0	3	0	0	0	2
				>8 km	*Four Samples[a] (4)*						
Mean		13	36				119				4081
s.d.		--	8				64				3172
Median		13	36				134				3450
n	0	1	4	0	0	0	4	0	0	0	4
			>35° S, West of 170° W		*0-2 km*	*15 Samples[a] (15)*					
Mean	947	68	54	3.3	1.5	724	69	63	28	83	172
s.d.	993	31	32	1.5	1.2	692	63	49	19	75	36
Median	502	51	57	3.3	0.9	425	47	49	23	49	172
n	14	7	12	2	11	13	8	8	5	11	7
				2-8 km	*23 Samples[a] (23)*						
Mean	42	54	54			95	136	98	26	7	669
s.d.	30	39	65			--	158	49	--	--	522
Median	29	41	28			95	60	98	26	7	485
n	3	10	16	0	0	1	10	2	1	1	21
				>8 km	*Nine Samples[a] (9)*						
Mean	65	30	29				51	16			1363
s.d.	47	4	17				24	--			1295
Median	65	30	29				41	16			688
n	2	2	8	0	0	0	4	1			9

Units are pptv for all species except ^7Be, which is reported as fCi m^{-3} STP; *n* is the number of samples above our detection limits for the given species in each bin; s.d., standard deviation. See text for discussion of the precautions which should be taken when comparing these data to results from other campaigns.

[a]The number of samples collected for determination of soluble ion mixing ratios (followed by the number for radionuclide analyses) in each geographic/altitude bin.

sample of mean volume the standard deviation of the blanks leads to an uncertainty in mixing ratio of 15, 40, 10, 10, 0.4, 86, 24, 28, 7, and 3 pptv for the ions (listed in same order as above). These uncertainties decrease (increase) proportionately as the volume of air sampled increases (decreases).

Deciding how to incorporate samples below detection limits when calculating descriptive statistics is problematic. Considering such samples to be zeros would depress mean and median values artificially. Similarly, inserting the detection limit, or some constant fraction of it, could significantly overestimate the true mixing ratio, especially for small volume samples. We have calculated the summary statistics in Table 1 on the basis of those samples that were above detection limits, thus the means and medians often represent upper limit values. We also report the total number of samples collected, and those above detection limits for each species, in each of the bins.

We were able to quantify $SO_4^=$, NH_4^+, and ^7Be in 76, 67, and 69%, respectively, of all samples collected (Table 1). All other species were below detection limits more often than not, with the percentage of samples above detection limits ranging from 4% ($C_2O_4^=$) to 44% (NO_3^-). Below 2 km we were able to determine mixing ratios of all species except $C_2O_4^=$ most of the time, with K^+ above detection least often (53% of samples) and $SO_4^=$ nearly always quantified (95% of samples) (Table 1).

3.1. Spatial Distributions

3.1.1. Free troposphere. We focus first on the distributions of $SO_4^=$, NH_4^+, and ^7Be, since our data set for these species allows examination of variations with height as well as between geographic regions. In most of the regional bins the mixing ratios of $SO_4^=$ and NH_4^+ tended to decrease rapidly with height, while ^7Be increased (Figures 1-3). Below 2 km the range of $SO_4^=$ and NH_4^+ mixing ratios in most regions was substantial.

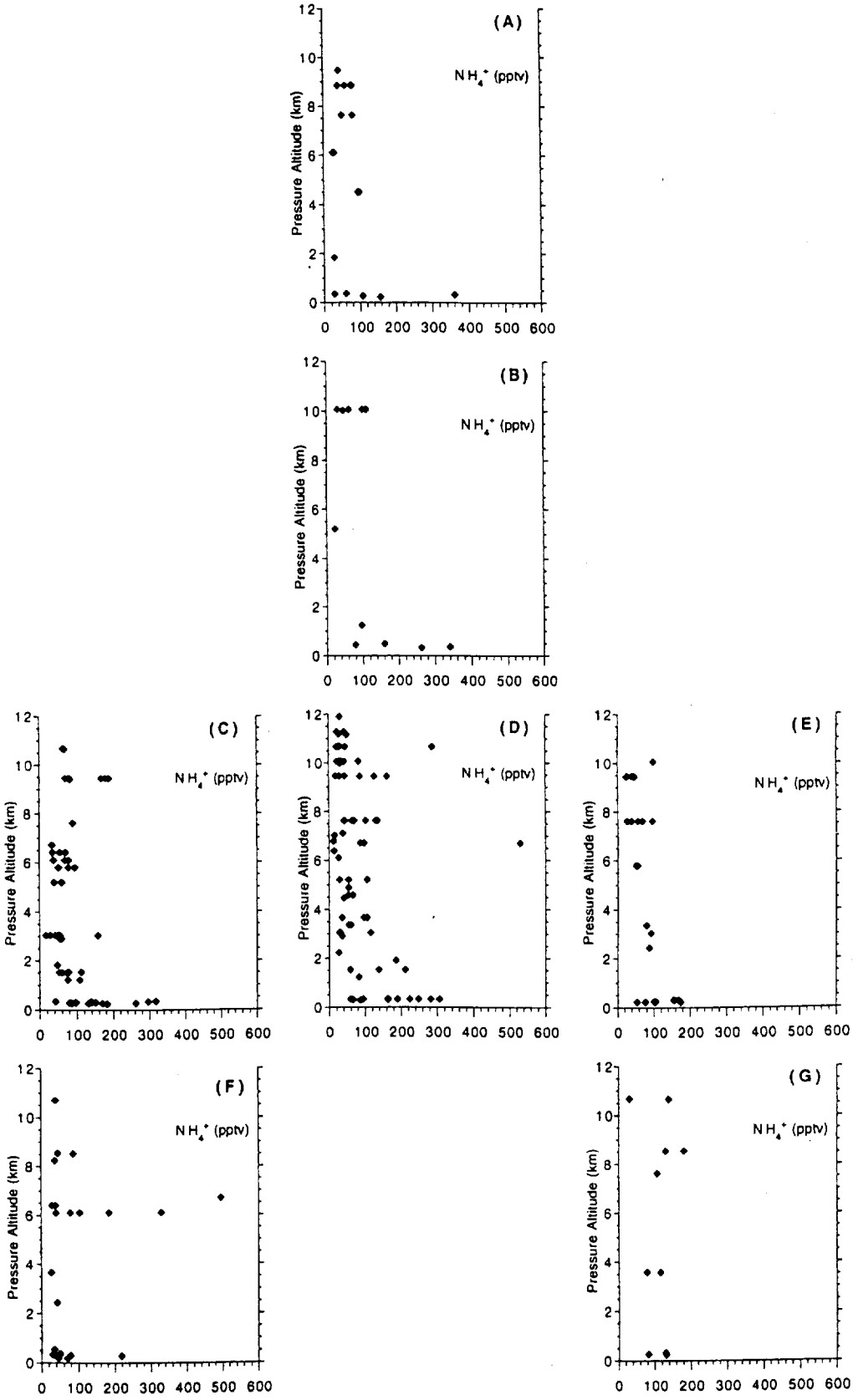

Figure 2. As in Figure 1, but for aerosol-associated NH_4^+.

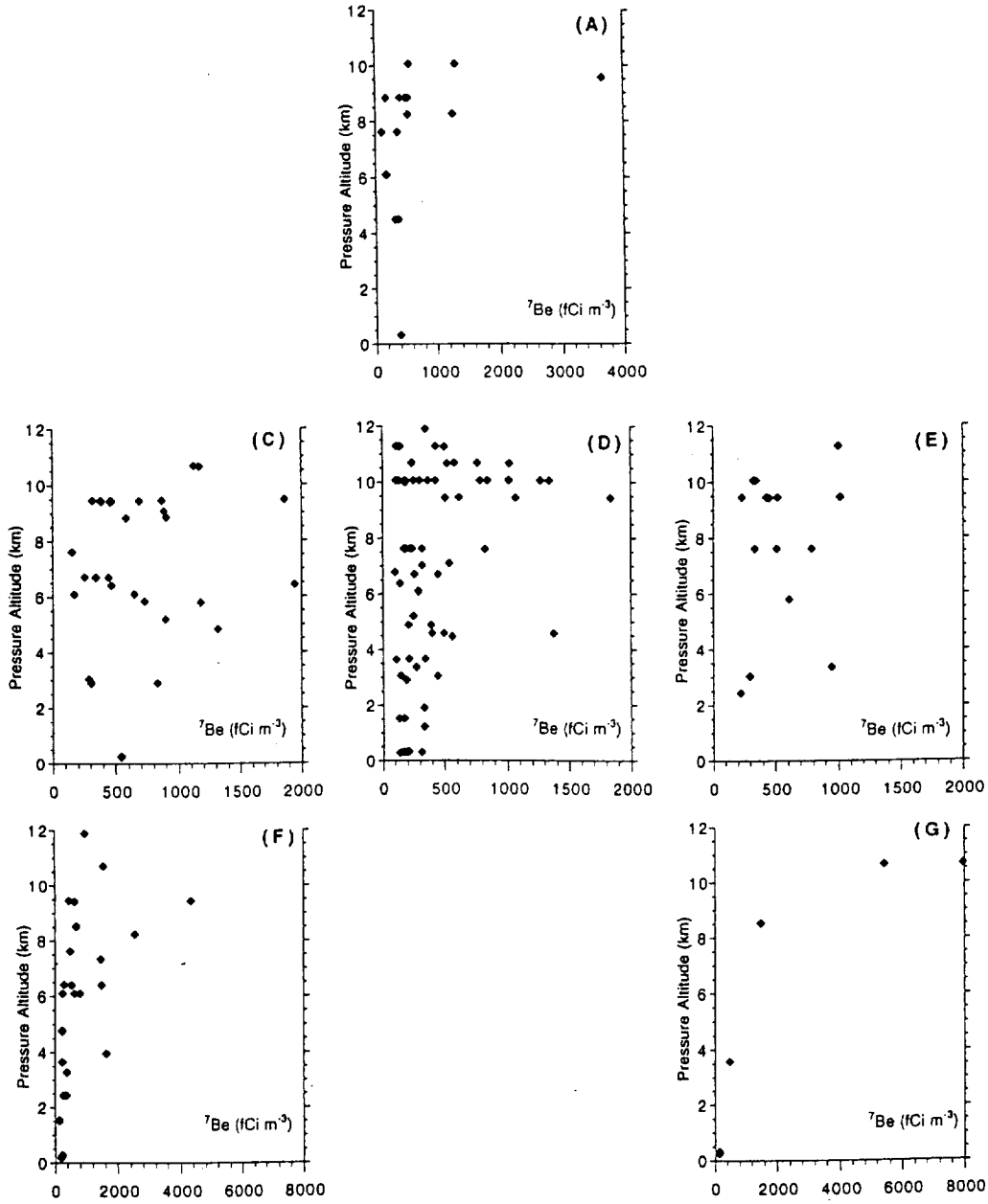

Figure 3. As in Figure 1, but for aerosol-associated ^{7}Be. Note that only three samples were collected for ^{7}Be determination in the region of Figure 1b, and they were all below detection limit. Also, note the changes in activity scale between the three latitude bands (greater range at higher latitudes).

There was a tendency for the greatest mixing ratios to occur at the lowest sampling altitude with substantially lower values often found only a few hundred meters higher (Figures 1 and 2). The small number of samples and large variability in the <2 km bins make differences between regions statistically insignificant, but the mean and median $SO_4^=$ and NH_4^+ mixing ratios were highest in the 0°-15°N region and lowest in the high southern latitude, western region (Table 1). In the middle troposphere (2-8 km) the situation was reversed, with the mixing ratios of both species quite low or below detection limits in the 0°-15°N bin and the highest mean concentrations found at latitudes greater than 35°S in the western Pacific (Table 1). However, the elevated mean $SO_4^=$ and NH_4^+ mixing ratios in this bin reflect several highly enriched samples (Figures 1 and 2). If medians are compared rather than means, the $SO_4^=$ enhancement in the >35°S, W bin was very modest, and the highest NH_4^+ value was found in the eastern high-latitude 2-8 km bin instead (Table 1). At the highest sampling altitudes the mean and median $SO_4^=$ mixing ratios were lowest north of the equator and highest south of 35°S, but nearly constant zonally within the two southern hemisphere latitude bands. In contrast, mean NH_4^+ mixing ratios increased from east to west in the 0°-35°S band, but were higher in the eastern, compared to western, bin south of 35°S (Table 1).

Beryllium 7 was often below detection limit in the <2 km altitude range, so comparison of means and medians between all regions are not very informative. Between 2 and 8 km, mean and median ^{7}Be activities increased considerably relative to boundary layer values in each region (bearing in mind that the high values reported for the lowest altitude in the 0°-15°N and 0°-35°S western regions represent only 1 or 2 samples with detectible ^{7}Be, while 5 times as many samples were below

detection limits in each region) (Table 1 and Figure 3). Concentrations of ^{7}Be in the middle troposphere averaged 1.3-2.7 times higher in the four eastern and western regions compared to the regions between 120° and 170°W. It should also be noted that the ^{7}Be activity in the 2-8 km altitude range varied widely. In all regions where >3 samples were collected the standard deviation exceeded 45% of the mean and was ≥78% of the mean in three of the five southern hemisphere regions (Table 1). Above 8 km, penetration of the lower stratosphere yielded high (>>1000 fCi m^{-3}) ^{7}Be activities in some samples from each of the high-latitude regions (Figure 3), causing average values to increase two- to eight-fold relative to the 2-8 km altitude range in these regions. Within the 0°-35°S latitude band, mean and median ^{7}Be activities showed little difference between the 2-8 and >8 km altitude ranges (Table 1 and Figure 3), with the largest increase (in the central region) about a factor of 1.5.

3.1.2. Boundary layer. Sea salt constitutes the overwhelmingly dominant fraction of aerosols in the <2 km range in all regions sampled. We found a wide range in mixing ratios of all species derived from sea salt (e.g., Na^+, Mg^{2+}, Ca^{2+}, and Cl^-) within each geographic bin (Table 1), but a large part of this variability is an artifact of our altitude binning. Steep gradients in the mixing ratios of sea-salt-derived species were often observed between the lowest sampling altitude of the DC-8 (approximately 0.3 km) and 2 km, similar to the vertical distributions of $SO_4^=$ and NH_4^+ shown in Figures 1 and 2. Furthermore, the abundance of sea-salt aerosol in the marine boundary layer varies rapidly in response to the wind field and as a result of precipitation scavenging. Since we have very little insight into the history of the marine boundary layer air masses in the hours to days before the DC-8 encountered them, our discussion of boundary layer aerosols will focus on spatial variations of species ratios rather than the abundance of individual species.

3.2. Comparison to Previous Measurements

Most measurements of aerosol composition in the South Pacific have been conducted at sea level sites, often on islands, or on board ship [e.g., *Ayers et al.*, 1986; *Raemdonck et al.*, 1986; *Saltzman et al.*, 1986a; *Bates et al.*, 1989, 1992a; *Pszenny et al.*, 1989; *Savoie and Prospero*, 1989; *Yamato et al.*, 1989; *Quinn et al.* 1990; *Clarke and Porter*, 1993; *Huebert et al.*, 1993]. Sampling has therefore focused on the bottom few tens of meters of the marine boundary layer, a region that is not accessible by the DC-8 platform. We suspect that agreement between our measurements of mixing ratios in a given region and previous results from surface-based sampling would be fortuitious for the reasons outlined above. Thus we will not make comparisons of absolute abundance of individual species, but in the following discussion we do examine our observed spatial variations in key ratios of species in the context of the patterns documented through surface-based campaigns.

Airborne sampling of aerosols presents a number of serious challenges related to the possible failure of the nozzle, inlet, and tubing to pass a representative sample of the ambient aerosol population to the actual sampling device (a filter in our case) [e.g., *Huebert et al.*, 1990; *Porter et al.*, 1992]. Our approach to meeting these challenges is outlined by *Dibb et al.* [1996]. Previous airborne sampling campaigns that characterized the distribution of aerosol-associated species over the South Pacific (e.g., Global Atmospheric Measurements Experiment on Tropospheric Aerosols and Gases (GAMETAG), First Aerosol Characterization Experiment (ACE 1)) used different sampling systems on platforms with operational characteristics unlike those of the DC-8. Similarly, the aerosol composition measurements made from the P-3B during PEM-Tropics [*Hoell et al.*, this issue], while showing general agreement with our results over large scales in the regions sampled by both aircraft (B. Heikes, personal communication, September 1997), may not be directly comparable in detail due to a combination of different sampling altitudes, spatial resolution, and the possibility that one or both systems suffer systematic sampling bias. In particular, we note that fast response instrumentation on both aircraft revealed large spatial gradients in CO, O_3, and aerosol number distributions within the marine boundary layer. Such gradients would have made rigorous intercomparison flights difficult to execute and suggest that there is little assurance that the DC-8 and P-3B actually sampled the same boundary layer air masses during the loosely coordinated flights that were conducted during PEM-Tropics. We recognize that the issue of sampling artifacts is a pressing concern for all groups collecting aerosol samples from airborne platforms and careful intercomparisons are needed. However, it is not possible to establish equivalence or discrepancies between our system and those on other platforms from data presently available. Therefore our focus will be solely on measurements that we have made from the DC-8 over the past 5 years.

The dual-inlet aerosol sampling system we fly on the DC-8, and the filter extraction and analytical procedures, have remained essentially unchanged through the three GTE Pacific Exploratory Missions (PEM-West A, PEM-West B, and PEM-Tropics) (as well as the Sub-sonic Assessment (SASS) SUCCESS mission over the central United States in spring 1996 and the SONEX mission over the North Atlantic in fall 1997). Comparison of the aerosol distributions we found on the three PEM campaigns should reflect real differences in the composition of the atmosphere over the North and South Pacific, though there may also be some influence of seasonal [*Dibb et al.*, 1997] and/or secular changes over the 5 year period between PEM-West A and PEM-Tropics.

PEM-West A was conducted in September-October 1991 [*Dibb et al.*, 1996], while PEM-West B occurred in February-March 1994 [*Dibb et al.*, 1997], in order to document the seasonal variation in the magnitude of Asian outflow over the North Pacific. In both campaigns, flights were conducted out of Hong Kong and Yakota, Japan (termed near Asia), and from Guam and Hawaii (termed remote Pacific) (Table 2). As expected, mixing ratios of species with strong anthropogenic sources like $SO_4^=$ and NH_4^+ (plus a host of trace gases) and tracers of continental dust (non-sea-salt Ca^{2+} in our data set) were higher near Asia during both missions and increased between fall and spring in response to the climatological increase in the strength and persistence of westerly winds blowing from Asia over the western North Pacific [see *Dibb et al.*, 1997, and references therein]. (Calcium is not included in Table 2, since the mixing ratios of Ca^{2+} in all PEM-Tropics samples were consistent with a sea-salt source.) However, the Asian outflow signal in aerosol-associated ionic species in both seasons was restricted to the lower troposphere, with upper tropospheric air generally quite "clean" (Table 2). The activity of ^{7}Be (an aerosol-associated tracer of upper tropospheric and stratospheric origin) was also much lower than anticipated in the upper troposphere over the North Pacific. In contrast, insoluble gaseous tracers of industrial activity were elevated throughout the troposphere over much of the North Pacific. We concluded that the low mixing ratios of aerosol-associated species were due to extensive wet scavenging in deep convection that pumped continental boundary layer air from Asia into the mid and upper troposphere where it could be advected over the Pacific [*Dibb et al.*, 1996, 1997].

Mean mixing ratios of $SO_4^=$ in the boundary layer near Asia during both PEM-West missions were more than two-fold (up to nine-fold) greater than in any of the 0-2 km bins sampled during

Table 2. Mean Mixing Ratios of Selected Aerosol-Associated Species in the North Pacific During the GTE PEM-West Missions

Altitude Range, km	$SO_4^=$, pptv	NH_4^+, pptv	Mg^{2+}, pptv	^7Be, fCi m^{-3}
	PEM-West A[a], Near Asia			
0.3-1.8	364	487	59	89
2-7	58	146	13	231
7-8.5	30	47	6	181
8.5-12.5	25	55	29	143
	PEM-West A[a], Remote Pacific			
0.3-1.8	233	335	68	69
2-7	25	28	12	137
7-8.5	31	35	22	74
8.5-12.5	18	36	--	176
	PEM-West B[b], Near Asia			
<1	500	646	69	158
1-6	242	394	69	277
6-9	47	129	24	372
>9	126	55	10	3207
	PEM-West B[b], Remote Pacific			
<1	174	239	22	125
1-6	51	79	16	66
6-9	12	22	17	125
>9	13	27	10	370

[a]The complete PEM-West A aerosol composition data set is presented by *Dibb et al.,[1996].*

[b]The complete PEM-West B aerosol composition data set is presented by *Dibb et al. [1997].*

PEM-Tropics (Tables 1 and 2). This enhancement near Asia extended up into the lower troposphere during PEM-West B (compare the near Asia 1-6 km, or the mean of the 1-6 and 6-9 km, bins (Table 2) to all 2-8 km bins from PEM-Tropics (Table 1)). The remote North Pacific $SO_4^=$ mixing ratios were comparable to those in the South Pacific. The slight enhancement in the northern low-altitude bins is probably mainly due to the shallower bins used for these missions (Tables 1 and 2). Elevated $SO_4^=$ mixing ratios above 9 km near Asia during PEM-West B reflect stratospheric air encountered in a tropopause fold [*Dibb et al.*, 1997]. If these samples are excluded, the mean $SO_4^=$ mixing ratios in all high-altitude bins during the three missions range from 13 to 36 parts per trillion by volume (pptv), with high and low values within this relatively narrow range occurring on both sides of the equator.

Comparing NH_4^+ mixing ratios between the North and South Pacific also reveals the continental influence on the boundary layer near Asia, where levels were again 2-9 times higher than the average in any <2 km bin during PEM-Tropics. The remote North Pacific boundary layer bins during both PEM-West campaigns also had higher NH_4^+ mixing ratios than any of the <2 km bins during PEM-Tropics including the two north of the equator (Tables 1 and 2). If, as we argue below, the ocean is a significant source of NH_3, part of this difference may be due to the 1 km top used for PEM-West boundary layer bins compared to 2 km for PEM-Tropics. In the low to middle troposphere the NH_4^+ comparisons are mixed, with PEM-Tropics means exceeding those in the remote North Pacific, but the highest means were found near Asia. At the highest altitudes (above 8 or 9 km) the differences in NH_4^+ mixing ratios are relatively small, except for the much higher averages in the PEM-Tropics western 0°-35°S and eastern high southern latitude regions (Tables 1 and 2). In the 0°-35°S bin this average is clearly an overestimate, since the NH_4^+ mixing ratio was below detection limit in 75% of the samples, but in the eastern zone above 35°S, NH_4^+ was quantified in all of the high-altitude samples.

Magnesium is included in Table 2 as an indicator of sea-salt aerosol, though a minor fraction of Mg^{2+} in the near Asia bins during both PEM-West missions was likely of continental dust origin. All low-altitude PEM-Tropics bins had higher Mg^{2+} mixing ratios than any of the PEM-West regions, implying more sea-salt aerosol in the marine boundary layer. In the free troposphere bins the reverse is generally true, the sole exception being the high Mg^{2+} mixing ratio in the central 0°-35°S region of PEM-Tropics (Tables 1 and 2).

Beryllium 7 was often below detection limits in the boundary layer bins of all three missions, so the means reported in Tables 1 and 2 should be viewed with caution. In the free troposphere the mean ^7Be activities were markedly higher in all of the PEM-Tropics regions. Perhaps of even greater relevance is the observation that below 8 km during both PEM-West missions the ^7Be activity never exceeded 500, and was only rarely above 300, fCi m^{-3} [*Dibb et al.*, 1996, 1997]. During PEM-Tropics ^7Be activities >1000 fCi m^{-3} were measured throughout the troposphere in all of the southern hemisphere regions (Figure 3). In the highest-altitude range the high mean ^7Be activities at latitudes above 15°N or 35°S during PEM-Tropics, and in the PEM-West B near Asia bin, reflect penetration of the stratosphere in several of the sample collection intervals. For those regions where the high-altitude bin was entirely within the troposphere, ^7Be activities were also greater during PEM-Tropics by factors ranging from 1.5 to 5.5 (Tables 1 and 2).

4. Discussion

4.1. Tropospheric Distributions

4.1.1. Biomass burning plumes. During PEM-Tropics the troposphere in western and central regions of the South Pacific was heavily impacted by emissions from biomass burning. These emissions were manifested as huge "plumes" up to several kilometers thick with elevated mixing ratios of O_3, CO, PAN, nitric, and carboxylic acids, and a suite of nonmethane hydrocarbons [e.g., *Talbot et al.*, this issue]. These plumes were all advected into the DC-8 sampling region from the west and had been over the South

Pacific for at least several days, and usually much longer, before we intercepted them [*Fuelberg et al.*, this issue].

Biomass burning plumes from boreal and tropical fires have been characterized in many previous investigations (e.g., the GTE Atmospheric Boundary Layer Experiment (ABLE 2), ABLE 3, and Transport and Atmospheric Chemistry Near the Equatorial Atlantic (TRACE A) campaigns, and Dynamique et Chimie Atmosphèrique en Foret Equatoriale (DECAFE)). Such plumes generally contain large enhancements in aerosol-associated species, most often including elemental C, NH_4^+, and K^+, though some have also had enhanced NO_3^- and $SO_4^=$. In this light, the low mixing ratios of aerosol-associated soluble ions measured throughout the PEM-Tropics study area are noteworthy.

In the central and western South Pacific regions, biomass burning plumes were encountered on every flight, and nearly all of these were in the 2-8 km altitude range. We noted earlier that the mean mixing ratios of $SO_4^=$ and NH_4^+ were slightly higher in the western high-latitude midtroposphere than any other bin; but that these averages were pulled up by two samples with very high mixing ratios. Closer examination of Figures 1 and 2 reveals that the mixing ratios of $SO_4^=$ and NH_4^+ in the 2-8 km range in the three southern hemisphere regions west of 120°W were below 100 and 200 pptv, respectively, in all except three samples (one in the central region and two in the high-latitude western zone). These three samples were all collected on the transit flight from Tahiti to New Zealand (flight 12).

Two separate plumes were encountered on flight 12 (Figure 4). The first plume, just before 2200 UTC, is representative of nearly all plumes encountered during PEM-Tropics. Large enhancements of CO and O_3 were accompanied by no enhancement in aerosol-associated ionic species. The second plume on flight 12 was first sampled at about 0045 at an altitude near 6.5 km (Figure 4). The large increase of the CO mixing ratio in this case was accompanied by a relatively small O_3 increase, but the mixing ratio of NH_4^+ in our first sample (529 pptv) was the highest measured at any time during PEM-Tropics. The $SO_4^=$ mixing ratio in this sample (287 pptv) was also the highest free tropospheric value that we measured (Figures 1, 2, and 4). The second sample collected during this leg showed small decreases in the mixing ratios of CO, $SO_4^=$, and NH_4^+, but the levels of the aerosol-associated species were still greatly enhanced compared to the bulk of our free troposphere samples. We ascended above the plume for about 40 min, then reentered it at ≈0200. Our first sample interval during the 6 km level leg again revealed elevated mixing ratios of CO, $SO_4^=$, and NH_4^+, with only a small enhancement in O_3. The mixing ratios of the ionic species in this second plume encounter were only about 65% of those seen earlier, but were still more than 1.5-fold higher than any other samples collected between 2 and 8 km during PEM-Tropics (Figures 1, 2, and 4). During the second sample of this level flight leg the DC-8 passed out of the plume.

The anomalous plume in the 30°-40°S latitude band on flight 12 was the only case when any of the aerosol-associated ionic species

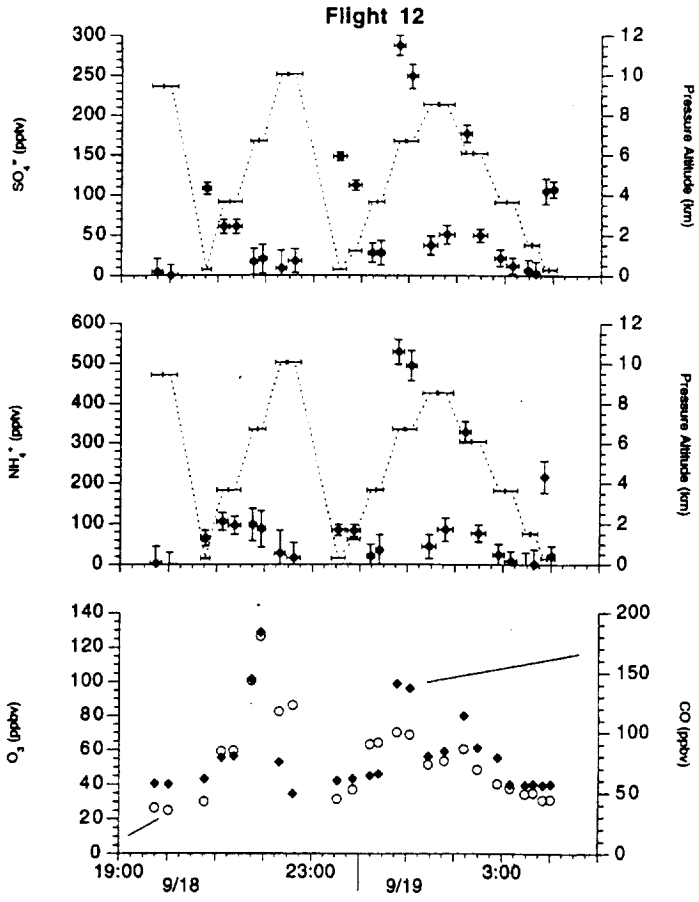

Figure 4. Time series of the mixing ratios of aerosol-associated $SO_4^=$ and NH_4^+ (solid diamonds), with average mixing ratios of O_3 (solid diamonds) and CO (open circles) for each aerosol collection interval, during the transit from Tahiti to New Zealand (flight 12). The dotted lines in the panels with aerosol composition indicate the altitude profile flown. Horizontal error bars define the integration period for each filter sample, and the vertical bars reflect uncertainty in the mixing ratios of the aerosol-associated ions.

increased with the gaseous tracers of combustion. The elevated mixing ratios of $SO_4^=$ and NH_4^+ in this singular plume suggest that large quantities of soluble aerosols and their precursors were removed from all of the other plumes at some point during transport to the South Pacific. Scavenging by precipitation seems the most likely process, with several lines of evidence suggesting that removal of primary aerosols and gaseous precursors of soluble aerosols occurred far upwind of the PEM-Tropics study region, perhaps in deep wet convective systems that lofted the fire emissions into the free troposphere. We cannot rule out precipitation scavenging at later times during transport on the basis of the depressed mixing ratios of aerosol-associated species alone, but the very high mixing ratios of nitric and carboxylic acids in many of the plumes [*Talbot et al.*, this issue] require at least several days between any cleansing by scavenging and interception by the DC-8. Similarly, the elevated ^{7}Be activities throughout the free troposphere over the South Pacific (Figure 3) would not have survived recent or frequent scavenging by rain, as we observed during the PEM-West campaigns [*Dibb et al.*, 1996, 1997]. Furthermore, every plume-impacted aerosol sample that we have analyzed for ^{210}Pb so far contained ^{210}Pb activities that were 2 to 4 times higher than other free troposphere samples on the same flights. This is similar to our findings during the PEM-West missions, where vertical pumping of ^{222}Rn in deep wet convection (that scavenged soluble aerosols and gases) resulted in ^{210}Pb being the only aerosol-associated species that was enhanced in free tropospheric air concurrent with elevated concentrations of insoluble anthropogenic trace gases from the boundary layer [*Dibb et al.*, 1996, 1997].

4.1.2. Sulfur cycle. Emission of S gases (principally dimethylsulfide [e.g., *Bates et al.*, 1992a; *Spiro et al.*, 1992]) from the ocean and their conversion into the S-bearing aerosol species non-sea-salt (nss) $SO_4^=$ and methylsulfonate (MSA) are topics of great current interest due to the possible importance of direct and indirect radiative effects of new particles formed in remote oceanic regions [e.g. *Charlson et al.*, 1987]. *Davis et al.* [this issue] and *Clarke et al.* [1997] discuss the results of several flights by the P-3B during PEM-Tropics that were designed to investigate the sulfur budget and extent of new particle production in the equatorial South Pacific. Our sampling from the DC-8 was in more of a survey mode, covering large distances but not allowing much insight into processes, especially those occurring in the marine boundary layer. However, the distributions of nss $SO_4^=$ and MSA in the free troposphere over the Pacific that we obtained appear to be unique.

The vertical profiles of MSA and nss $SO_4^=$ (calculated with Mg^{2+} as the sea-salt indicator) show decreasing trends with altitude up to about 10 km (Figure 5), consistent with surface emissions of DMS as a major source of both species. The three samples with elevated nss $SO_4^=$ are from the anomalous plume on flight 12 discussed above. On the other hand, DMS is the only known source of MSA, so the elevated MSA mixing ratios above 10 km must reflect pumping of MSA, or, as we will show is more likely, DMS from the marine boundary layer into the upper troposphere. Mixing ratios of nss $SO_4^=$ increased little, if at all, above 10 km, so the molar ratio MSA/nss $SO_4^=$ (R) also increased dramatically above 10 km (Figure 5).

Examining these data as a function of latitude provides important insight into the large-scale distribution of biogenic sulfur aerosols over the Pacific (Figure 6). Below 2 km the MSA mixing ratio near 45°N was 3-4 times higher than in all other regions, but the nss $SO_4^=$ mixing ratios in these samples were also relatively high, yielding values for R near 0.1 (Figure 6a). Between roughly 20°N and 35°S the mixing ratios of MSA and nss $SO_4^=$ varied considerably, but most values of R were < 0.05. The mixing ratios and variability of both species tended to decrease south of 35°S, with nss $SO_4^=$ mixing ratios dropping more and faster than those of MSA. As a result, R increased with latitude (Figure 6a). (Our data

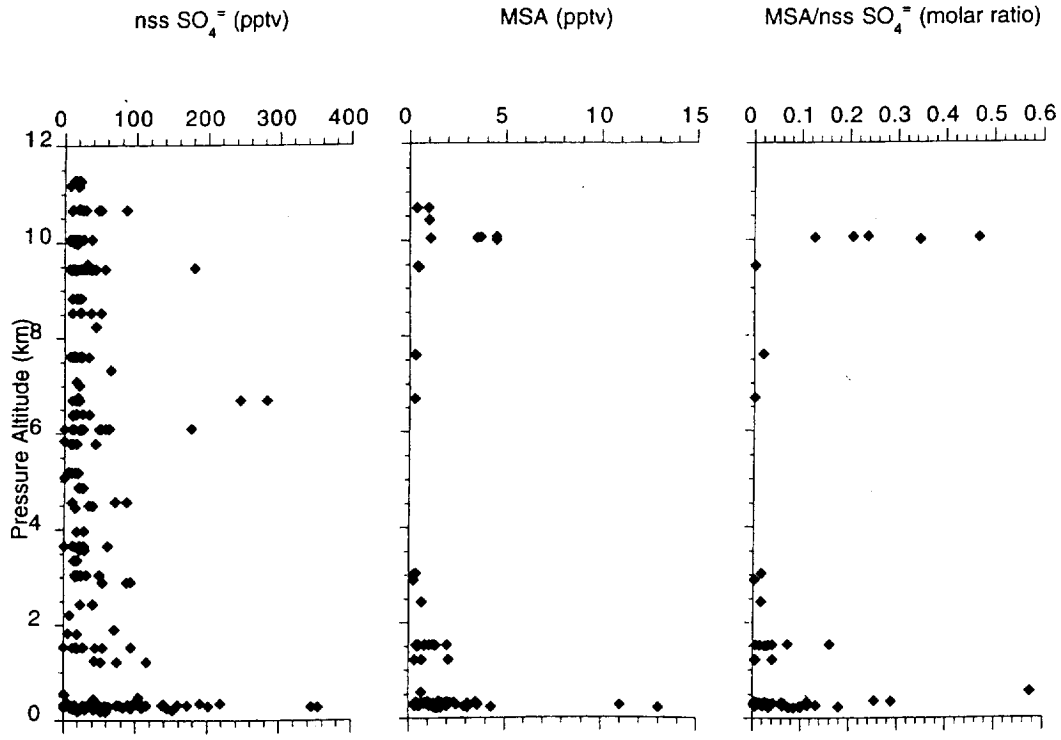

Figure 5. Altitude distributions of nss $SO_4^=$ (calculated using Mg^{2+} as the sea-salt indicator), aerosol-associated MSA, and their molar ratio. Samples from all regions are combined.

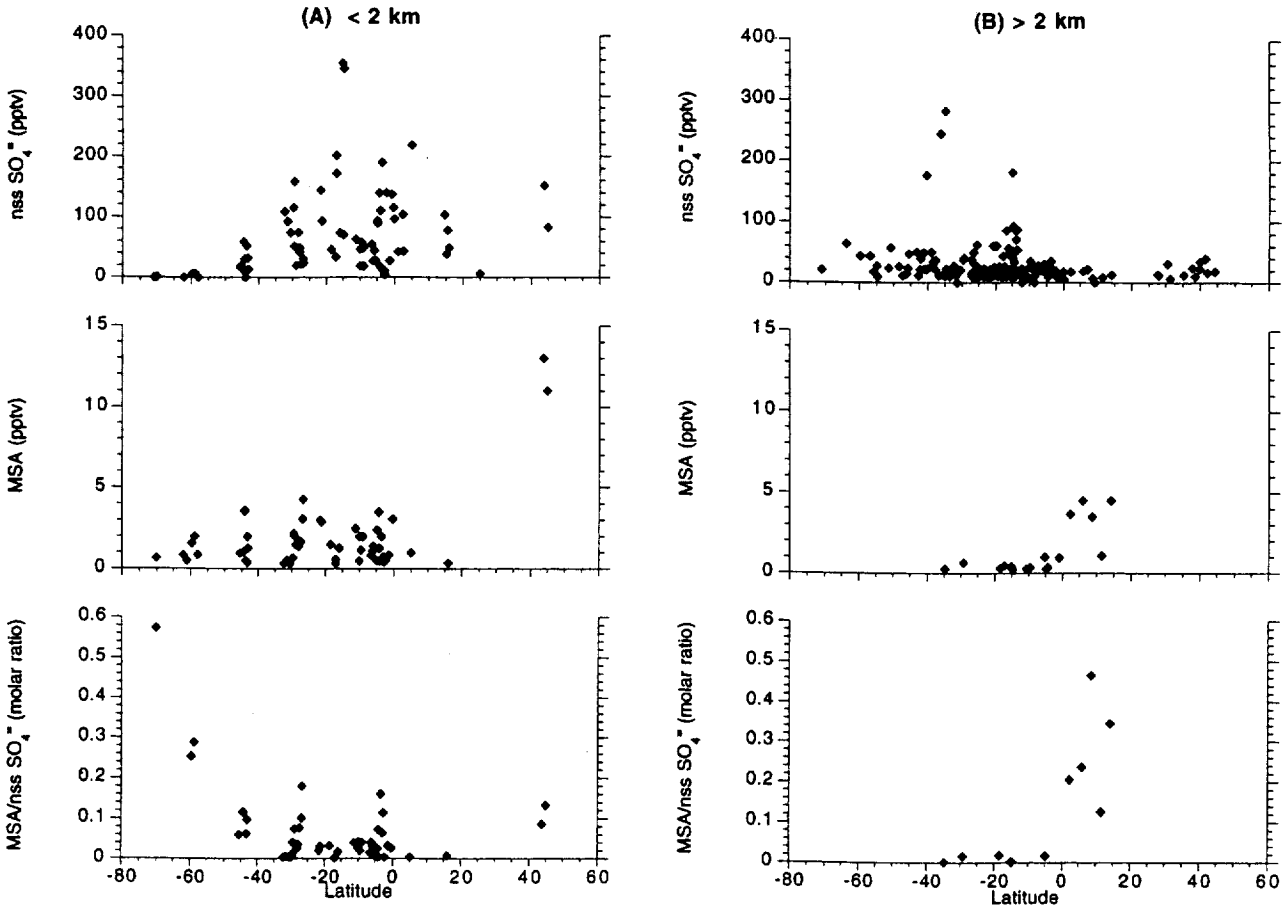

Figure 6. Distributions of nss $SO_4^=$, MSA, and their molar ratio as a function of latitude during PEM-Tropics. Data are separated into two altitude bins; (a) the marine boundary layer below 2 km and (b) the free troposphere above 2 km, but samples from all geographic regions are combined.

set provides only a hint of an increase in R with increasing latitude north of the equator due to the small number of samples, but the mid to high-latitude samples in the southern hemisphere reveal a steady increase from about 0.1 at 45°S to nearly 0.6 at 70°S.) The increasing trend of R with latitude in the PEM-Tropics data set is similar to a profile measured by *Bates et al.* [1992a] on a cruise in the eastern Pacific (between 105° and 110°W and 20°N to 60°S) in February and March 1989. Boundary layer values of R in the submicron fraction of the aerosol on this cruise were less than 0.01 between 10°N and 10°S, increased to 0.05 from 10°-30°S, and then rapidly increased to 0.18 near 40°S and 0.32 at 58°S (compare to the lower panel of Figure 6a). These authors suggested that the relative increase of MSA at higher latitudes was consistent with laboratory studies [*Hynes et al.*, 1986; *Yin et al.*, 1990] that found MSA to be favored over SO_2 as the product of DMS oxidation as both temperature and light intensity decreased. In fact, high values of R found in low-altitude aerosol samples from the high latitudes of both hemispheres have been tentatively ascribed mainly to the temperature dependence of the DMS branching ratio [e.g., *Berresheim*, 1987; *Pszenny et al.*, 1989; *Burgermeister and Georgii*, 1991; *Bates et al.*, 1992a; *Li et al.*, 1993; *Berresheim et al.*, 1995].

It must be noted that several investigations have found large variations in R as a function of particle size. The presence of a much more pronounced supermicron mode for MSA than for nss $SO_4^=$ results in higher values of R in the larger fractions of the aerosol population. This effect has been observed most frequently in the tropical Pacific: Quinn et al. [1993] found R to increase from 0.01 in the submicron fraction to 0.02 when all stages of an impactor sample (0-4 micron range) collected at 22°N were composited, *Huebert et al.* [1993] found a similar increase (R = 0.04 for Dp <1 μm compared to 0.07 in bulk (maximum diameter 10 μm)) during the equatorial Soviet-American Gas and Aerosol (SAGA) 3 cruise, while *Huebert et al.* [1996] reported an even larger increase between submicron and bulk values of R (0.016 to 0.053) during their 1994 sampling campaign on Christmas Island (2°N). In the tropical Atlantic the limited data do not provide a clear picture. *Andreae et al.* [1995] found R to increase from 0.049 to 0.066 when comparing submicron to bulk, while *Putaud et al.* [1993] did not see a significant supermicron mode of MSA, hence R varied little with particle size. In extratropical regions (but also closer to landmasses) any variations of R as a function of particle size have been quite small [*Saltzman et al.*, 1983, 1986a, b; *Pszenny et al.*, 1989].

The preceeding suggests that comparison between our bulk aerosol samples and surface-based results must consider the size range collected in previous studies and whether our system is biased against the larger particles. In the tropics where the dependence of R on particle size is expected to be largest, our 20 boundary layer samples (Figure 6a) have a mean R of 0.043. The low (<0.01) values reported by *Bates et al.* [1992a] are for fine (<0.6 μm) particles, and we can estimate that the bulk value might be 2 to 3 times higher. *Quinn et al.* [1990] measured an average R of about 0.03 between 9°N and 7°S for fine

samples (1 μm cut), and bulk values would presumably be higher but probably by no more than a factor of 2. Our mean value is 75% of the average bulk value (0.053) reported by *Huebert et al.* [1996] from Christmas Island and 2.7 times higher than the submicron average (0.016) for these same samples. These comparisons suggest that our sampling system is efficiently passing a high fraction of the large aerosol particles present in the marine boundary layer (more precisely, it appears that any inlet losses we do experience are nearly proportionately impacting both fine and coarse fractions, and we assume that the passing efficiency for the submicron particles is high). Of course, such comparisons are based on short periods of observation at different times and places, so they cannot be considered a rigorous test of our inlet design and performance.

The obvious benefit of airborne sampling as a complement to surface-based campaigns is that distributions in the free troposphere can only be determined from an airborne platform. For the case of the biogenic S aerosols, the free troposphere is quite different than the marine boundary layer. The samples with high MSA and R values above 10 km (Figure 5) were all clustered near the ITCZ, which was centered near 10°N when the DC-8 crossed it in early September and then again in early October (Figure 6b). Convection in the ITCZ would appear to be the mechanism lofting marine boundary layer air into the upper troposphere. We hypothesize that when DMS is pumped into the upper troposphere, the cold temperatures favor production of MSA over SO_2, leading to increased values of R. The lifetime of DMS in the tropical marine boundary layer is not very well constrained, but is likely to be of the order of several hours to no more than a few days [*Huebert et al.*, 1993, and references therein]. Given such short lifetimes of DMS in the boundary layer, finding significant mixing ratios of DMS in the free troposphere implies very frequent vertical transport events [e.g., *Chatfield and Crutzen*, 1984]. Mixing ratios of DMS above 6 km near 10°N ranged from 17-45 pptv (when averaged to aerosol sample integration times), compared to a 30-60 pptv range in the boundary layer in the same region (data not shown). The R values in the upper troposphere near the ITCZ are so high relative to those in the tropical boundary layer (in fact, compared to all boundary layer values between 20°N and 45°S), and the mixing ratios of nss $SO_4^=$ are so low (Figures 5 and 6), that it is likely that very little boundary layer aerosol is transported along with the DMS. We therefore suggest that wet convective events which efficiently scavenge the aerosols present in the marine boundary are the most important agents of vertical uplift transporting DMS into the tropical free troposphere.

It should also be noted that the biogenic S aerosols in the upper troposphere are more likely to be transported long distances than those that remain within the marine boundary layer. Our data thus suggest that interpreting R values measured in polar ice cores as a straightforward indication of the latitude from which an air mass carried water vapor and biogenic S to high latitudes [e.g., *Legrand and Feniet-Saigne*, 1991; *Legrand et al.*, 1991; *Whung et al.*, 1994] may be misleading. The well established latitudinal trend in R at low altitudes would suggest high-latitude origins for all of the upper troposphere samples between 0° and 20°N (Figure 6), yet it is quite clear that the biogenic S in these samples originated in the tropical or subtropical marine boundary layer.

4.2. Boundary Layer Distributions

4.2.1. Marine source of ammonia. The decreasing mixing ratios of NH_4^+ with increasing altitude in all regions sampled during PEM-Tropics (Figure 2) are consistent with a surface source. *Quinn et al.* [1990] and *Clarke and Porter* [1993] have presented evidence from recent cruises that significant amounts of NH_3 are emitted from the Pacific Ocean, particularly in equatorial regions. Our NH_4^+ data appear to reinforce these findings.

Mixing ratios of NH_4^+ in the marine boundary layer (<2 km) samples varied over a wide range in most latitude bands, though nearly all samples with elevated mixing ratios (>200 pptv) were collected within 20° of the equator (Figure 7). The tropical regions are also characterized by a more pronounced enhancement of boundary layer NH_4^+ mixing ratios relative to the overlying free troposphere. Similar trends were found in CH_3I, and to a lesser extent DMS, two trace gases known to be dominated by emission from the surface ocean [e.g., *Singh et al.*, 1983; *Bates et al.*, 1992b].

4.2.2. Coupling of the N and S cycles in the Pacific marine boundary layer. It has been suggested that most of the submicron sulfate aerosol in the Pacific boundary layer far from continental sources of NH_3 is present as H_2SO_4 [*Yamato et al.*, 1989; *Yamato and Tanaka*, 1994]. On the other hand, *Quinn et al.* [1990] reported NH_4^+/nss $SO_4^=$ molar ratios in the range of 0.8 to 1.9 in tropical regions of the Pacific where they inferred significant emissions of NH_3. Similarly, *Clarke and Porter* [1993] based their estimation of NH_3 fluxes from the equatorial Pacific on observations of decreased volatility of submicron aerosols due to neutralization of H_2SO_4 droplets to form NH_4HSO_4 and $(NH_4)_2SO_4$. Our results during PEM-Tropics indicate that H_2SO_4 did not constitute a major fraction of the boundary layer aerosol mass in any of the regions we sampled.

Scatterplots of NH_4^+ versus nss $SO_4^=$ reveal that only a few of our bulk aerosol samples were more acidic than would be consistent with NH_4HSO_4 as the dominant form of sulfate (Figure 8). In fact, more than 40% of all samples collected in the southern hemisphere, and all of those from east of 120°W, had more NH_4^+ than would be required to completely neutralize $SO_4^=$ to $(NH_4)_2SO_4$. If we assume that all measured aerosol NO_3^- reacted with NH_4^+ to form NH_4NO_3 after nss $SO_4^=$ was depleted, we are still left with "excess" NH_4^+ in more than 25% of the southern hemisphere samples and 9/11 samples collected east of 120°W. This is an unexpected result that is not readily explained, so we must consider whether it is real or an artifact caused by some aspect of our sampling, chemical analysis,

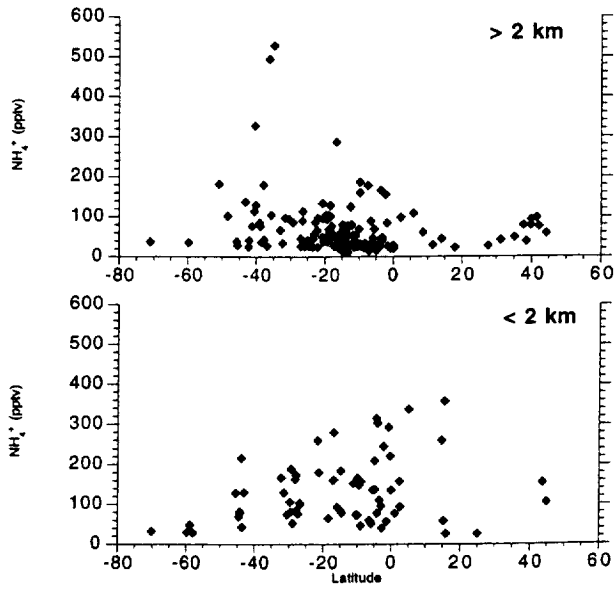

Figure 7. Mixing ratios of NH_4^+ as a function of latitude. The upper panel includes all samples collected above 2 km pressure altitude, and the lower panel includes those collected below 2 km.

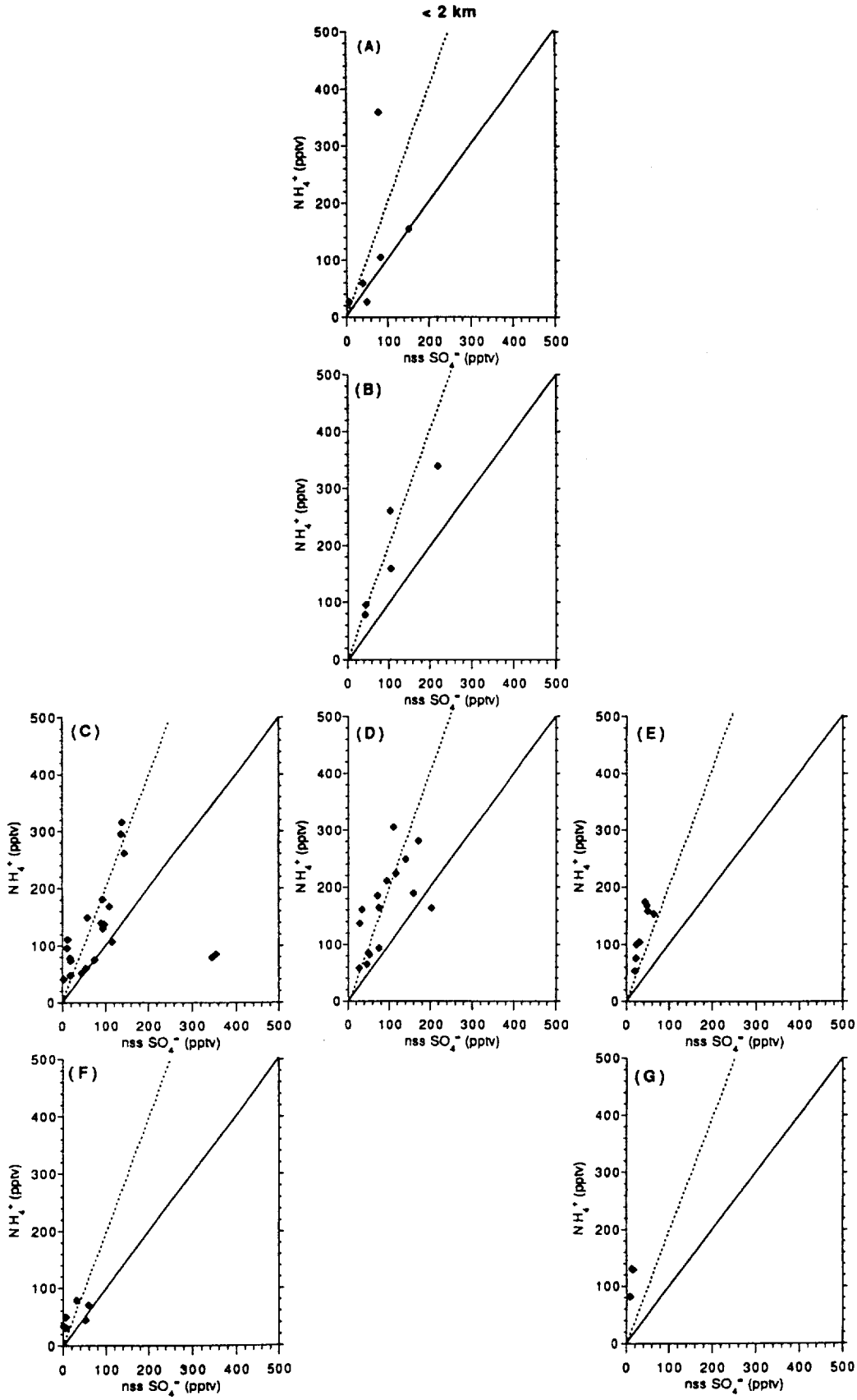

Figure 8. Scatterplots of NH_4^+ against nss $SO_4^=$. The solid line in each panel is the 1:1 ratio corresponding to NH_4HSO_4, and the dotted line is the 2:1 ratio corresponding to $(NH_4)_2SO_4$. Panels reflect the same geographic regions as in Figures 1-3.

or data reduction. It should be noted that, although we have flown numerous GTE missions over the oceans, PEM-Tropics is the first case where our aerosol NH_4^+ measurements have suggested a dominant marine source of NH_3.

It is possible that, despite our efforts to minimize exposure of collected aerosols to air inside the DC-8 cabin, some fraction of the measured NH_4^+ is an artifact of NH_3 reacting with acidic aerosols on the filters [e.g., *Hayes et al.*, 1980]. However, the samples collected in the marine boundary are so heavily loaded with sea salt that there is not likely to be much free acidity on the filters to drive such postcollection acid/base reactions. Furthermore, this type of artifact would not seem capable of pushing the NH_4^+/nss $SO_4^=$ ratio above the complete neutralization value of 2. It is also possible that the samples picked up NH_3 diffusing through the walls of the polyethylene bottles during transit back to our laboratory, but the NH_4^+ concentrations in PEM-Tropics blanks were not elevated compared to any other field program in which we have participated.

The magnitude of the excess NH_4^+ in most of the samples that have "too much" NH_4^+ is well above our analytical uncertainty. Sample volumes in the boundary layer were generally two- to three-fold greater than the mission mean of 4.2 m^{-3} STP, reducing uncertainty from blank subtraction to levels of the order of 5 pptv total $SO_4^=$ and 10 pptv NH_4^+. Similarly, while it is possible that our sampling system is oversampling large particles in the boundary layer, which would lead to overestimation of the sea-salt fraction of $SO_4^=$ and increase the NH_4^+/nss $SO_4^=$ ratio, our successful reproduction of the latitudinal profile of MSA/nss $SO_4^=$ suggests little or no such bias. (Note that losses of large particles in the inlet would be more likely than oversampling.) We could also be overestimating sea-salt $SO_4^=$ by adopting the standard assumption that there is no fractionation between Mg^{2+} and $SO_4^=$ during formation of sea-salt aerosols. This assumption has been shown to be invalid for aerosols and snow in coastal regions of Antarctica where the standard calculation yields substantially negative estimates of nss $SO_4^=$ during winter (i.e., a modified sea-salt aerosol that has much less $SO_4^=$ than expected from seawater composition is prevalent in this region) [*Wagenbach et al.*, 1988; *Gjessing*, 1989; *Mulvaney et al.*, 1992; *Minikin et al.*, 1994]. However, we are not aware of similar findings at lower latitudes. In any case, even if we make the extreme assumption that all of the measured $SO_4^=$ is nss $SO_4^=$ available to react with NH_3, we still find that NH_4^+ is present in excess in 10/66 southern hemisphere samples, with most of these from the western (five samples) and central (three samples) 0°-35°S bins.

In summary, it appears that the presence of excess NH_4^+ was a real characteristic of some of the regions sampled during PEM-Tropics, though the frequency of such aerosols may be less than suggested by the number of points above the 2:1 lines in Figure 8. We speculate that dissolution of NH_3 into hydrated sea-salt aerosols could account for the excess NH_4^+. In this case the solubility of NH_3 in the aqueous phase, rather than the presence of an acidic counter anion, would determine the final concentration of NH_4^+ in the extract of the filter. It is not possible to confirm this hypothesis from the PEM-Tropics data set, nor can we be certain that the excess NH_4^+ goes into the aerosol phase in the ambient marine boundary layer rather than on the filters during (or after) sample collection. It should be possible to test this hypothesis through chemical characterization of size-fractionated aerosol samples from the South Pacific boundary layer, since NH_3 dissolving into wet sea-salt aerosols would be found in the large particle mode (though it would still be difficult to discriminate between NH_3 uptake in the ambient aerosol versus artifact uptake by aerosols concentrated onto a filter during sampling). We note that *Quinn et al.* [1993] and *Andreae et al.* [1995] found no evidence for supermicron NH_4^+ in samples collected in the North Pacific and South Atlantic, respectively, but the NH_4^+/nss $SO_4^=$ ratios in these regions were generally $\leq$1.0, hence excess NH_3 was probably not available.

5. Conclusions

The extensive influence of biomass burning plumes in the free troposphere over the South Pacific was an unexpected highlight of the PEM-Tropics airborne sampling campaign. With only a single exception, these plumes did not carry enhanced levels of soluble aerosols into the region, as might have been expected based on previous characterizations of such plumes around the world. Precipitation scavenging apparently depressed the concentrations of soluble ions and their gaseous precursors. High ^7Be activities throughout the South Pacific troposphere imply that this cleansing must have occurred early in the plumes' history rather than shortly before they were intercepted by the DC-8. Elevated mixing ratios of nitric and carboxylic acids in most of the plumes [*Talbot et al.*, this issue] support the inference based on ^7Be, as these gases would also have been scavenged in recent precipitation events.

Mixing ratios of DMS up to 45 pptv, aerosol-associated MSA near 5 pptv, and values of the MSA/nss $SO_4^=$ molar ratio in the range of 0.2-0.5 near 10 km altitude between the equator and 10°N must reflect frequent and deep vertical mixing by wet convection in the ITCZ. The high values of the MSA/nss $SO_4^=$ ratio in this region are particularly noteworthy, as the latitudinal profile developed through surface-based sampling displays a tropical minimum ($\leq$0.05) and increases toward higher latitudes. The values we measured at altitude in the tropics would not be expected in surface air until latitudes greater than about 60° were reached.

Decreasing mixing ratios of NH_4^+ with increasing altitude throughout the PEM-Tropics study area suggest that emission of NH_3 from the ocean is an important source for remote marine air. The latitude distribution of NH_4^+ in the boundary layer (<2 km) shows that the highest mixing ratios were found in the tropics, consistent with recent shipboard sampling campaigns that suggested relatively strong emissions of NH_3 from the equatorial Pacific [*Quinn et al.*, 1990; *Clarke and Porter*, 1993].

Our observation of excess NH_4^+ in many PEM-Tropics boundary layer samples is somewhat problematic. We cannot entirely rule out the possibility that these data are artifacts of sampling and/or data processing, but feel that they are indicating a real feature of the boundary layer aerosol in some regions of the South Pacific. If so, the details of incorporation of NH_3 into the aerosol phase in the marine boundary layer merit additional attention.

Acknowledgments. The efforts of the Ames DC-8 flight and ground crews that made PEM-Tropics a success are greatly appreciated. We would also like to thank the two anonymous reviewers for their insightful comments that greatly improved the clarity of this paper. This research was supported by the NASA Global Tropospheric Chemistry Program.

References

Andreae, M. O., W. Elbert, and S. J. de Mora, Biogenic sulfur emissions and aerosols over the tropical South Atlantic, 3, Atmospheric dimethylsulfide, aerosols, and cloud condensation nuclei, *J. Geophys. Res.*, *100*, 11,335-11,356, 1995.

Ayers, G. P., J. P. Ivey, and H. S. Goodman, Sulfate methanesulfonate at Cape Grim, Tasmania, *J. Atmos. Chem.*, *4*, 173-185, 1986.

Bates, T. S., A. D. Clarke, V. N. Kapustin, J. E. Johnson, and R. J. Charlson, Oceanic dimethylsulfide and marine aerosol: Difficulties

associated with assessing their covariance, *Global Biogeochem. Cycles, 3*, 299-304, 1989.

Bates, T. S., J. A. Calhoun, and P. K. Quinn, Variations in the methanesulfonate to sulfate molar ratio in submicrometer marine aerosol particles over the South Pacific Ocean, *J. Geophys. Res., 97*, 9859-9865, 1992a.

Bates, T. S., B. K. Lamb, A. Guenther, J. Dignon, and R. E. Stoiber, Sulfur emission to the atmosphere from natural sources, *J. Atmos. Chem., 14*, 315-337, 1992b.

Berresheim, H., Biogenic sulfur emissions from the subantarctic and Antarctic oceans, *J. Geophys. Res., 92*, 13,245-13,262, 1987.

Berresheim, H., P. H. Wine, and D. D. Davis, Sulfur in the atmosphere, in *Composition, Chemistry, and Climate of the Atmosphere*, edited by H. B. Singh, 251-307, Van Nostrand Reinhold, New York, 1995.

Burgermeister, S., and H. W. Georgii, Distribution of methanesulfonate, nss sulfate and dimethylsulfide over the Atlantic and the North Sea, *Atmos. Environ., Part A, 25*, 587-595, 1991.

Charlson, R. J., J. E. Lovelock, M. O. Andreae, and S. G. Warren, Oceanic phytoplankton, atmospheric sulphur, cloud albedo and climate: A geophysical feedback, *Nature, 326*, 655-661, 1987.

Chatfield, R. B., and P. J. Crutzen, Sulfur dioxide in remote oceanic air: Cloud transport of reactive precursors, *J. Geophys. Res., 89*, 7111-7132, 1984.

Clarke, A. D., and J. N. Porter, Pacific marine aerosol, 2, Equatorial gradients in chlorophyll, ammonium, and excess sulfate during SAGA 3, *J. Geophys. Res., 98*, 16,997-17,010, 1993.

Clarke, A. D., K. G. Moore, Z. L. Varner, and F. Eisle, Three regimes for new particle production in the Pacific troposphere: Cumulus outflow, aged pollution, and the equatorial boundary layer (abstract), *Eos Trans. AGU, 78(46)*, F98, 1997.

Davis, D. D., et al., DMS oxidation in the equatorial Pacific: Comparison of model simulations with field observations for DMS, SO_2, H_2SO_4(g), MSA(g), MS, and NSS, *J. Geophys. Res.*, this issue.

Dibb, J. E., R. W. Talbot, K. I. Klemm, G. L. Gregory, H. B. Singh, J. D. Bradshaw, and S. T. Sandholm, Asian influence over the western North Pacific during the fall season: Inferences from lead 210, soluble ionic species, and ozone, *J. Geophys. Res., 101*, 1779-1792, 1996.

Dibb, J. E., R. W. Talbot, B. L. Lefer, E. Scheuer, G. L. Gregory, E. V. Browell, J. D. Bradshaw, S. T. Sandholm, and H. B. Singh, Distributions of beryllium-7, lead-210, and soluble aerosol-associated ionic species over the western Pacific: PEM-West B, February-March, 1994, *J. Geophys. Res., 102*, 28,287-28,302, 1997.

Fuelberg, H., et al., A meteorological overview of the PEM-Tropics period, *J. Geophys. Res.*, this issue.

Gjessing, Y. T., Excess and deficit of sulfate in polar snow, *Atmos. Environ., 18*, 825-830, 1989.

Gregory, G. L., et al., Chemical characteristics of Pacific tropospheric air in the region of the ITCZ and SPCZ, *J. Geophys. Res.*, this issue.

Hayes, D., K. Snetsinger, G. Ferry, V. Overbeck, and N. Farlow, Reactivity of stratospheric aerosol to small amounts of ammonia in the laboratory environment, *Geophys. Res. Lett., 7*, 974-976, 1980.

Hoell, J. M., Jr., et al., Pacific Exploratory Mission in the tropical Pacific: PEM-Tropics A, August-September 1996, *J. Geophys. Res.*, this issue.

Huebert, B. J., G. Lee, and W. L. Warren, Airborne aerosol inlet passing efficiency measurement, *J. Geophys. Res., 95*, 16,369-16,381, 1990.

Huebert, B. J., S. Howell, P. Laj, J. E. Johnson, T. S. Bates, P. K. Quinn, V. Yegorov, A. D. Clarke, and J. N. Porter, Observations of the atmospheric sulfur cycle on SAGA 3, *J. Geophys. Res., 98*, 16,985-16,995, 1993.

Huebert, B. J., D. J. Wylie, L. Zhuang, and J. A. Heath, Production and loss of methanesulfonate and non-sea-salt sulfate in the equatorial Pacific marine boundary layer, *Geophys. Res. Lett., 23*, 737-740, 1996.

Hynes, A. J., P. H. Wine, and D. H. Semmes, Kinetics and mechanisms of OH reactions with organic sulfides, *J. Phys. Chem., 90*, 4148-4156, 1986.

Legrand, M., and C. Feniet-Saigne, Methanesulfonic acid in South Pole snow layers: A record of strong El Nino?, *Geophys. Res. Lett., 18*, 187-190, 1991.

Legrand, M., C. Feniet-Saigne, E. S. Saltzman, C. Germain, N. I. Barkov, and V. N. Petrov, Ice core record of oceanic emissions of dimethylsulphide during the last climatic cycle, *Science, 350*, 144-146, 1991.

Li, S.-M., L. A. Barrie, R. W. Talbot, R. C. Harriss, C. I. Davidson, and J.-L. Jaffrezo, Seasonal and geographic variations of methanesulfonic acid in the Arctic troposphere, *Atmos. Environ., Part A, 27*, 3011-3024, 1993.

Minikin, A., D. Wagenbach, W. Graf, and J. Kipfstuhl, Spatial and seasonal variations of the snow chemistry at the central Filchner-Ronne Ice Shelf, *Ann. Glaciol., 20*, 283-290, 1994.

Mulvaney, R., E. C. Pasteur, and D. A. Peel, The ratio of MSA to non-sea-salt sulfate in Antarctic Peninsula ice cores, *Tellus, Ser. B, 44*, 295-303, 1992.

Porter, J. N., A. D. Clarke, G. Ferry, and R. F. Pueschel, Aircraft studies of size-dependent aerosol sampling through inlets, *J. Geophys. Res., 97*, 3815-3824, 1992.

Pszenny, A. A. P., A. J. Castelle, J. N. Galloway, and R. A. Duce, A study of the sulfur cycle in the Antarctic marine boundary layer, *J. Geophys. Res., 94*, 9818-9830, 1989.

Putaud, J.-P., S. Belviso, B. C. Nguyen, and N. Mihalopoulos, Dimethylsulfide, aerosols, and condensation nuclei over the tropical northeastern Atlantic Ocean, *J. Geophys. Res., 98*, 14,863-14,871, 1993.

Quinn, P. K., T. S. Bates, J. E. Johnson, D. S. Covert, and R. J. Charlson, Interactions between the sulfur and reduced nitrogen cycles over the central Pacific Ocean, *J. Geophys. Res., 95*, 16,405-16,416, 1990.

Quinn, P. K., D. S. Covert, T. S. Bates, V. N. Kapustin, D. C. Ramsey-Bell, and L. M. McInnes, Dimethylsulfide/cloud condensation nuclei/climate system: Relevant size-resolved measurements of the chemical and physical properties of atmospheric aerosol particles, *J. Geophys. Res., 98*, 10,411-10,427, 1993.

Raemdonck, H., W. Maenhaut, and M. O. Andreae, Chemistry of marine aerosol over the tropical and equatorial Pacific, *J. Geophys. Res., 91*, 8623-8636, 1986.

Saltzman, E. S., D. L. Savoie, R. G. Zika, and J. M. Prospero, Methane sulfonic acid in the marine atmosphere, *J. Geophys. Res., 88*, 10,897-10,902, 1983.

Saltzman, E. S., D. L. Savoie, J. M. Prospero, and R. G. Zika, Methanesulfonic acid and non-sea-salt sulfate in Pacific air: Regional and seasonal variations, *J. Atmos. Chem., 4*, 227-240, 1986a.

Saltzman, E. S., D. L. Savoie, J. M. Prospero, and R. G. Zika, Elevated atmospheric sulfur levels off the Peruvian coast, *J. Geophys. Res., 91*, 7913-7918, 1986b.

Savoie, D. L., and J. M. Prospero, Comparison of oceanic and continental sources of non-seasalt sulfate over the Pacific Ocean, *Nature, 339*, 685-687, 1989.

Singh, H. B., L. J. Salas, and R. E. Stiles, Methyl halides in and over the eastern Pacific (40°N-32°S), *J. Geophys. Res., 88*, 3684-3690, 1983.

Spiro, P. A., D. J. Jacob, and J. A. Logan, Global inventory of sulfur emissions with a 1° x 1° resolution, *J. Geophys. Res., 97*, 6023-6036, 1992.

Talbot, R. W., J. E. Dibb, E. M. Scheuer, D. R. Blake, N. J. Blake, G. L. Gregory, G. W. Sachse, J. D. Bradshaw, S. T. Sandholm, and H. B. Singh, Influence of biomass combustion emissions on the distribution of acidic trace gases over the southern Pacific basin during austral springtime, *J. Geophys. Res.*, this issue.

Wagenbach, D., U. Görlach, K. Moser, and K.O. Münnich, Coastal Antarctic aerosol: The seasonal pattern of its chemical composition and abundance, *Tellus, Ser. B, 40*, 426-436, 1988.

Whung, P.-Y., E. S. Saltzman, M. J. Spencer, P. A. Mayewski, and N. Gundestrup, Two-hundred-year record of biogenic sulfur in a south Greenland ice core (20D), *J. Geophys. Res., 99*, 1147-1156, 1994.

Yamato, M., and H. Tanaka, Aircraft observations of aerosols in the free marine troposphere over the North Pacific Ocean: Particle chemistry in relation to air mass origin, *J. Geophys. Res., 99*, 5353-5377, 1994.

Yamato, M., Y. Iwasaka, G.-W. Qian, A. Ono, T. Yamanouchi, and A. Sumi, Sulfuric acid particles and their neutralization by ammonia in the marine atmosphere: Measurements during cruise from Japan to Antarctica, *Proc. NIPR Symp. Polar Meteorol. Glaciol., 2*, 29-40, 1989.

Yin, F., D. Grosjean, and J. H. Seinfeld, Photooxidation of dimethyl sulfide and dimethyl disulfide, I, Mechanism development, *J. Atmos. Chem., 11*, 309-364, 1990.

D. R. Blake and N. J. Blake, Department of Chemistry, University of California, Irvine, CA 92717.

J. E. Dibb (corresponding author), E. M. Scheuer, and R. W. Talbot, Institute for the Study of Earth, Oceans, and Space, University of New Hampshire, Durham, NH 03824. (e-mail: jack.dibb@unh.edu)

G. L. Gregory and G. W. Sachse, NASA Langley Research Center, Hampton, VA 23681.

D. C. Thornton, Department of Chemistry, Drexel University, Philadelphia, PA 19104.

(Received January 12, 1998; revised August 28, 1998; accepted August 31, 1998.)

JOURNAL OF GEOPHYSICAL RESEARCH, VOL. 104, NO. D13, PAGES 16,233–16,241, JULY 20, 1999

Constraints on the age and dilution of Pacific Exploratory Mission-Tropics biomass burning plumes from the natural radionuclide tracer ^{210}Pb

Jack E. Dibb, Robert W. Talbot, L. David Meeker, and Eric M. Scheuer
Institute for the Study of Earth, Oceans, and Space, University of New Hampshire, Durham

Nicola J. Blake and Donald R. Blake
Department of Chemistry, University of California, Irvine

Gerald L. Gregory and Glen W. Sachse
NASA Langley Research Center, Hampton, Virginia

Abstract. During the NASA Global Troposphere Experiment Pacific Exploratory Mission-Tropics (PEM-Tropics) airborne sampling campaign we found unexpectedly high concentrations of aerosol-associated ^{210}Pb throughout the free troposphere over the South Pacific. Because of the remoteness of the study region, we expected specific activities to be generally less than 35 μBq m^{-3} but found an average in the free troposphere of 107 μBq m^{-3}. This average was elevated by a large number of very active (up to 405 μBq m^{-3}) samples that were associated with biomass burning plumes encountered on nearly every PEM-Tropics flight in the southern hemisphere. We use a simple aging and dilution model, which assumes that ^{222}Rn and primary combustion products are pumped into the free troposphere in wet convective systems over fire regions (most likely in Africa), to explain the elevated ^{210}Pb activities. This model reproduces the observed ^{210}Pb activities very well, and predicts the ratios of four hydrocarbon species (emitted by combustion) to CO to better than 20% in most cases. Plume ages calculated by the model depend strongly on the assumed ^{222}Rn activities in the initial plume, but using values plausible for continental boundary layer air yields ages that are consistent with travel times from Africa to the South Pacific calculated with a back trajectory model. The model also shows that despite being easily recognized through the large enhancements of biomass burning tracers, these plumes must have entrained large fractions of the surrounding ambient air during transport.

1. Introduction

The pervasive influence of long-traveled biomass burning plumes that were advected over the South Pacific from the west was an unexpected finding of the NASA Global Tropospheric Experiment (GTE) Pacific Exploratory Mission-Tropics (PEM-Tropics) airborne sampling campaign conducted in September - October 1996 [*Fuelberg et al.*, 1999; *Talbot et al.*, 1999; *Blake et al.*, this issue; *Fenn et al.*, this issue; J. Logan et al., unpublished manuscript, 1999; R. Lusher et al., unpublished manuscript, 1999; H. Singh et al., unpublished manuscript, 1999]. These plumes were manifested as layers up to several kilometers thick with elevated mixing ratios of O_3, CO, PAN, several NMHC combustion tracers, and the soluble acidic gases HNO_3, CH_3COOH, and HCOOH that could be hundreds of kilometers wide in the north-south direction and apparently extended thousands of kilometers to the west. *Dibb et al.* [1999] showed that the mixing ratios of aerosol-associated soluble ions, including NH_4^+ and K^+ which are typically enhanced in biomass burning plumes, were quite low in all of the plumes encountered during PEM-Tropics except for one on the transit between Tahiti and New Zealand. We hypothesized that the absence of strong signals in these aerosol-associated tracers of biomass burning indicated that the air masses must have been efficiently scavenged by precipitation during transit from the source region to the PEM-Tropics study area. Elevated concentrations of ^{7}Be throughout the South Pacific troposphere [*Dibb et al.*, 1999] and very high mixing ratios of HNO_3, CH_3COOH, and HCOOH in many of the plumes [*Talbot et al.*, 1999] indicate that such scavenging could not have occurred in the few days immediately prior to interception of the plumes. We therefore suggested that the soluble ions and their precursors were removed from these air masses in wet convective events, most likely over Africa but perhaps even as far upwind as South America, that provided the vertical lifting that transported the biomass burning emissions into the free troposphere.

Dibb et al. [1999] noted that ^{210}Pb activities in the initial aerosol samples (first 12 flights) analyzed from the PEM-Tropics campaign seemed to be enhanced in the plume-impacted air masses, making this natural radionuclide tracer the only aerosol-associated species to show a plume signal. All PEM-Tropics aerosol samples have now been analyzed for ^{210}Pb, and the enhancement in plume-impacted air masses persisted throughout the campaign. This paper focuses on the distribution of ^{210}Pb over the South Pacific during PEM-Tropics and examines whether the observed ^{210}Pb enhancements provide useful constraints on the age of the biomass burning plumes and the extent to which they have mixed with ambient, or background, air during transport to the South Pacific.

Paper number 1999JD900066.
0148-0227/99/1999JD900066$09.00

2. Methods

Details of our filter sampling for aerosols from the NASA DC-8 airborne laboratory are provided by *Dibb et al.* [1999]. Specific activities of ^{210}Pb were determined in 280 samples (which had first been analyzed for ^{7}Be by direct gamma counting) by alpha spectrometric determination of ^{210}Po after allowing 10-15 months for in-growth of this ^{210}Pb daughter. Samples were counted in groups of four until the uncertainty due to counting statistics for the least active sample in each group was ≤20%. In most cases this required counting times of 3-4 days.

All of the ^{210}Pb data is presented below, but much of the discussion will focus on those samples that were impacted by biomass burning plumes. We use the compilation of plume encounters based on CO and O_3 enhancements presented by J. Logan et al. (unpublished manuscript, 1999) to filter our data set. In some cases we collected two or three filter samples during a single plume encounter, but more often our samples integrate over intervals that include time within a plume and also in the surrounding ambient air. If an aerosol sample overlapped at all with a defined plume encounter, it was considered to be plume-impacted. As a result, our sampling can result in artifact dilution of the plumes, with some 10-15 min long plume-impacted samples including as little as 15 s within an identified plume.

Our ^{210}Pb activities are compared to the mixing ratios of various trace gases measured by other investigators on the DC-8. In all cases the integration period for these analyses is shorter than our sample collection intervals. A merged data product created at Harvard University, wherein all other measurements are averaged over the aerosol sample collection interval, is used exclusively in this paper. Details of the other instruments and higher-resolution versions of the resulting data sets are presented in companion papers in this issue and in the first special issue of *Journal of Geophysical Research* on the PEM-Tropics campaign (in press). All original data and several different merged products are archived, and available, at the Langley Distributed Active Archive Centre (DAAC).

Table 1. Activity of ^{210}Pb in Aerosol Samples Collected During PEM-Tropics

Altitude, km	n*	Mean	Standard Deviation	Median
		(μBq m^{-3} STP)		
>15 °N, 120 °-170 °W				
0-2	6	56	53	38
2-8	7	154	128	119
>8	12	144	54	152
0 °-15 °N, 120 °-170 °W				
0-2	2	128	36	128
2-8	0			
>8	1	80		80
0 °-15 °N, 120 °-170 °W				
0-2	8	49	56	18
2-8	12	99	44	107
>8	10	81	33	70
0 °-35 °S, E of 120 °W				
0-2	18	67	44	67
2-8	45	129	88	104
>8	40	90	58	72
0 °-35 °S, 120 °-170 °W				
0-2	12	74	50	61
2-8	31	96	61	80
>8	19	126	73	87
>35 °S, W of 120 °W				
0-2	3	32	6	36
2-8	3	69	11	75
>8	4	112	55	93
>35 °S, 120 °-170 °W				
0-2	15	48	26	45
2-8	23	121	100	91
>8	9	98	60	85

Geographic and altitude bins correspond to those used by *Dibb et al.* [1999] to summarize the distribution of aerosol-associated soluble ions and ^{7}Be during this mission.

* n is number of samples collected; ^{210}Pb was above detection limit in all samples.

3. Results

Activities of ^{210}Pb above 2 km averaged 70 to 130 μBq m^{-3} in all of the South Pacific regions sampled during PEM-Tropics (Table 1), with an overall mean of 107 μBq m^{-3}. Considering the distances to major land masses, we expected to encounter levels generally < 35 μBq m^{-3}. Such low values were frequently measured, but the averages were elevated by the numerous samples with activities between 75 and 405 μBq m^{-3} (Figure 1). The geographical and altitudinal distribution of these samples with high ^{210}Pb activities mirrors those of plume encounters, being most frequent between about 3 and 10 km and increasing toward the west [*Fuelberg et al.*, 1999; *Talbot et al.*, 1999; *Blake et al.*, this issue; *Fenn et al.*, this issue; J. Logan et al., unpublished manuscript, 1999; R. Lusher, unpublished manuscript, 1999; H. Singh et al., unpublished manuscript, 1999].

Scatterplots of ^{210}Pb in plume-impacted samples versus several trace gases enhanced in the plumes reinforce the impression that high ^{210}Pb activities were associated with the transport of biomass burning emissions, and photochemical products of these emissions, from the west (Figure 2). Correlations between ^{210}Pb and the combustion tracers in Figure 2 (r^2 = 0.5, 0.7, and 0.4 for C_3H_8, C_2H_6, and CH_3Cl, respectively) were not very tight, but they were comparable to or higher than those found between the soluble acidic gases apparently produced in the plumes and several plume tracers. (*Talbot et al.* [1999] reported r^2 values near 0.4 for correlations of HNO_3, CH_3COOH, and HCOOH versus CH_3Cl, PAN, and O_3.) Relatively strong relationships were also found for ^{210}Pb versus O_3, CO, and PAN in plume-impacted samples (r^2 = 0.5, 0.5, and 0.6, respectively). The correlation between ^{210}Pb and C_2H_2 in plume-impacted samples (not shown) was also quite strong (r^2 = 0.5), in contrast to the case for HNO_3 and C_2H_2 where any relationship was restricted to just a few of the plumes [*Talbot et al.*, 1999].

4. Discussion

The associations between ^{210}Pb and various biomass burning tracers in plumes over the South Pacific do not necessarily imply that ^{210}Pb is a product of combustion. It has been shown that very young fire plumes can be greatly enriched in Rn daughters including ^{210}Po and ^{210}Pb, reflecting volatilization of these tracers both within the plants and dry deposited onto their surfaces [*Lambert et al.*, 1991; *Le Cloarec et al.*, 1995]. However, these researchers have shown that the Po and Pb rapidly recondense when temperatures drop, returning them to the aerosol phase. In general, a large fraction is scavenged onto other particulates in the plume and does not travel far, though submicron aerosols formed in the free troposphere could be transported long distances. In the case of PEM-Tropics plumes transported to the South Pacific it is unlikely that this process is a significant source of aerosol ^{210}Pb (or ^{210}Po)

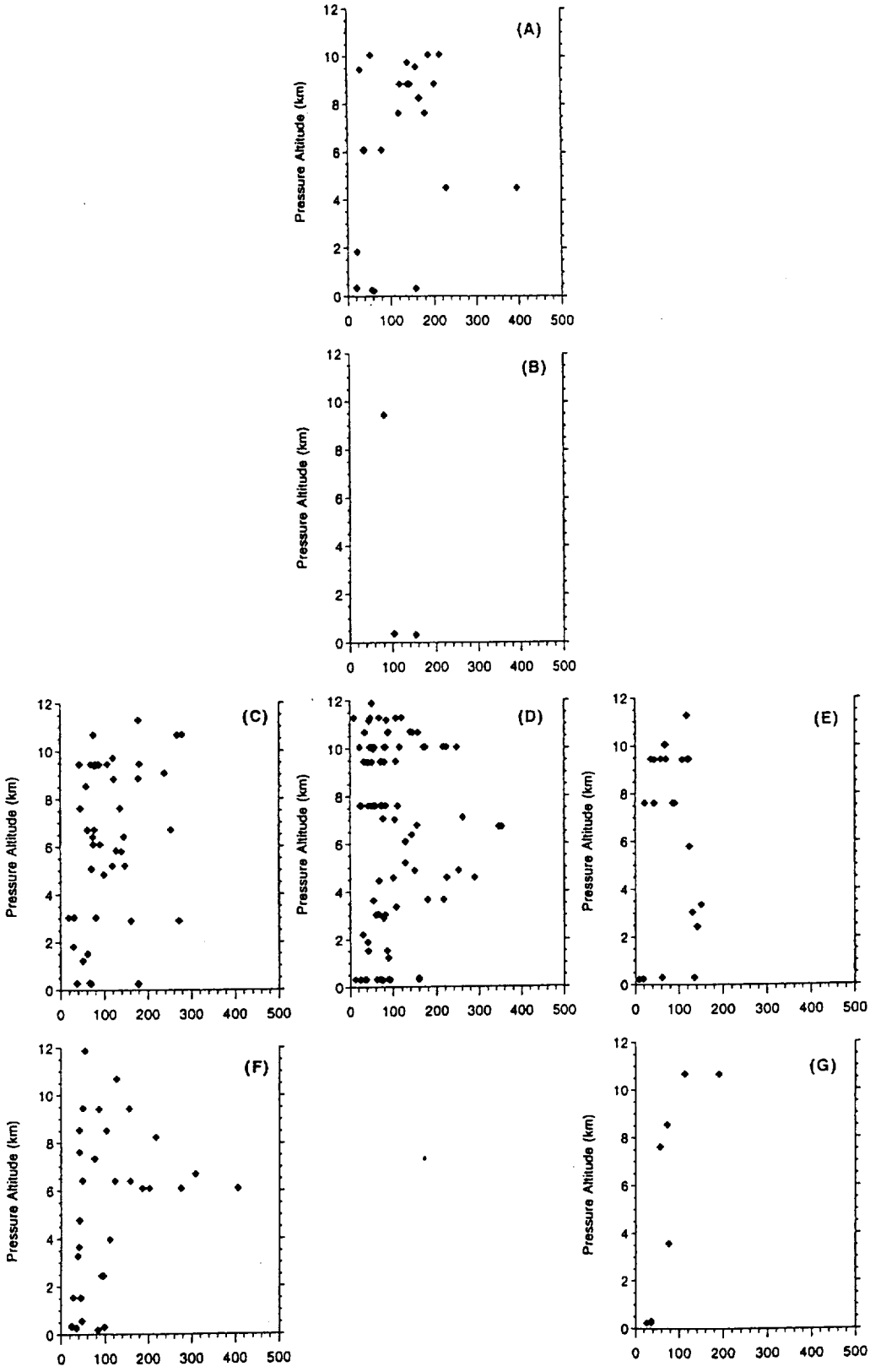

Figure 1. Vertical profiles of ^{210}Pb activity ($\mu Bq\ m^{-3}$) in seven regions sampled during PEM-Tropics. The regions are the same as those used by *Dibb et al.* [1999] and for Table 1. The geographic boundaries are: (a) >15°N, 120°-170°W, (b) 0°-15°N, 120°-170°W, (c) 0°-35°S, W of 170°W, (d) 0°-35°S, 120°-170°W, (e) 0°-35°S, E of 120°W, (f) >35°S, W of 170°W, and (g) >35°S, E of 120°W.

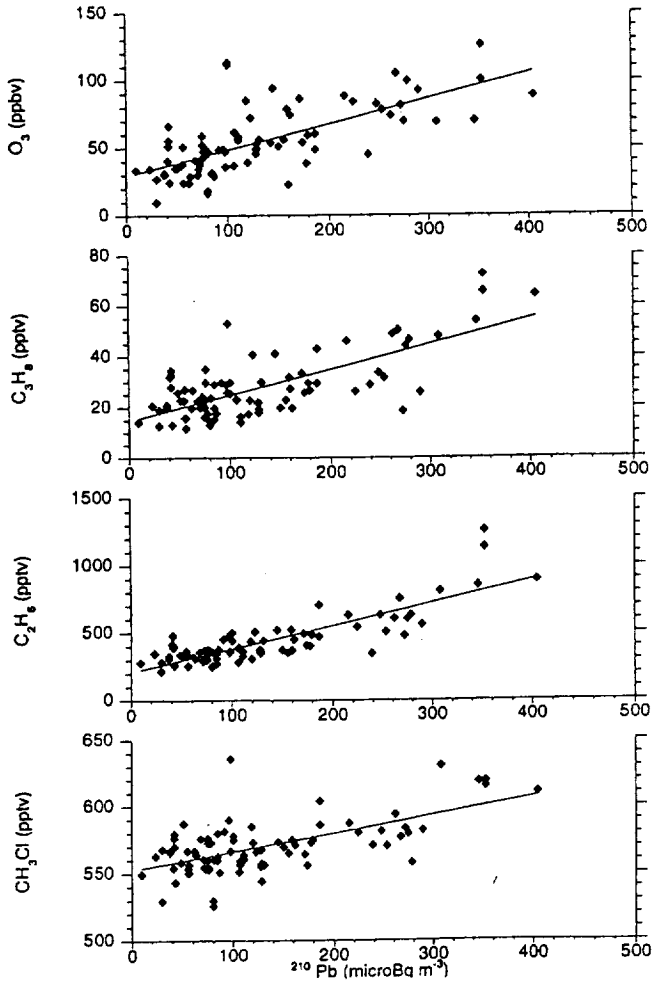

Figure 2. Scatterplots of O_3, C_3H_8, C_2H_6, and CH_3Cl as a function of ^{210}Pb activity in all plume-impacted samples collected during PEM-Tropics. The lines are least squares fits.

because we do not see any enhancements of other aerosol-associated species that should also be greatly enriched in the plumes. *Dibb et al.* [1999] suggested that effective scavenging in wet convective systems removed the other aerosol tracers of biomass combustion, and this process would also depress the concentrations of ^{210}Pb in recently uplifted boundary layer air (we will term such air masses "fresh plumes" in the following sections).

We suspect that the observed correlations result from pumping boundary layer air enriched in ^{222}Rn (the precursor of ^{210}Pb), and sparingly soluble trace gases emitted by biomass burning, into the free troposphere. Strong westerlies then advected this lifted boundary layer air into the PEM-Tropics study region [*Fuelberg et al.*, 1999]. Because Rn is a noble gas, it would not be depleted by the precipitation scavenging associated with wet convective uplift that we invoked to explain the low mixing ratios of aerosol-associated soluble ions in the plumes over the South Pacific [*Dibb et al.*, 1999; *Talbot et al.*, 1999].

Consider a hypothetical tropospheric air mass with very low levels of ^{210}Pb, but high levels of ^{222}Rn and biomass burning emissions, that experiences no loss of aerosols by scavenging and does not mix at all with surrounding air. Over timescales of hours to weeks, concentrations of ^{210}Pb would increase due to ^{222}Rn decay, while mixing ratios of primary combustion products would decrease, largely due to attack by OH. Given different OH reactivities, the various primary combustion products will be depleted at different rates, and the ratio of shorter/longer lived tracers (S/L) should decrease, while ratios of longer/shorter lived tracers (L/S) should increase.

We examined two S/L ratios (C_3H_8/CO and C_2H_2/CO) and two L/S ratios (C_2H_6/CO and CH_3Cl/CO) as a function of ^{210}Pb activity in all plume-impacted samples. Three of the four cases show trends opposite to those expected in an idealized, isolated, air mass. Both S/L ratios increase (rather than decrease) as ^{210}Pb increases, with a tighter trend for C_2H_2/CO ($r^2 = 0.4$) than that for C_3H_8/CO ($r^2 = 0.1$) (Figure 3). Given the much longer lifetime of CH_3Cl than CO, their ratio should increase as ^{210}Pb grows in over time, yet the ratio in plume-impacted samples sharply decreases with increasing ^{210}Pb ($r^2 = 0.4$) (Figure 3). In our data set, C_2H_6/CO is the only ratio to show the expected trend, increasing with ^{210}Pb activity ($r^2 = 0.3$). These relationships indicate that we cannot consider the plumes to be isolated air masses, but must consider dilution of the plumes with ambient air during transport.

4.1. A Simple Aging and Dilution Model

It has been shown that mixing between two different air masses generally does not result in linear mixing lines when one considers ratios of species (usually ratios of hydrocarbons (HC) or HC/CO or

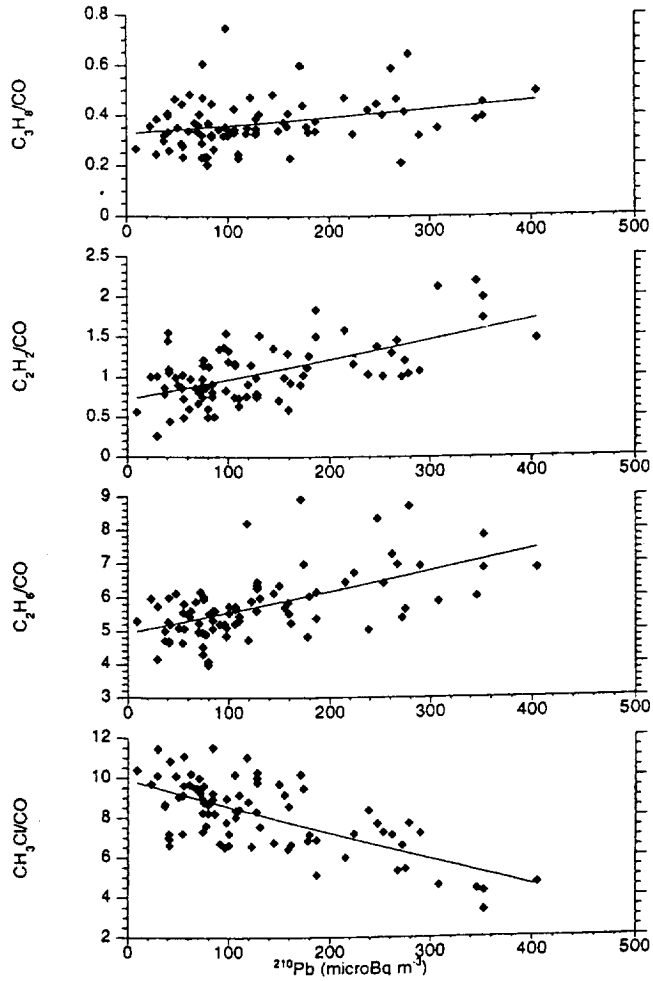

Figure 3. Scatterplots of C_3H_8/CO, C_2H_2/CO, C_2H_6/CO, and CH_3Cl/CO as a function of ^{210}Pb activity in all plume-impacted samples. The lines are least squares fits.

HC/CO_2) [*McKeen and Liu*, 1993; *Mckeen et al.*, 1990, 1996; *Mauzerall et al.*, 1998]. In addition, variations in OH levels over short time scales complicate the use of HC ratios to estimate the age of an air mass. However, the decay of ^{222}Rn to ^{210}Pb is not impacted by the composition of an air mass, and mixing of two air masses with different ^{210}Pb activities should be a simple dilution process. Therefore we used a very simple model to explore the relationships between ^{210}Pb and several primary emission products of biomass burning in plume-impacted samples from PEM-Tropics.

We consider ^{210}Pb and ^{222}Rn activities and the mixing ratios of four HC tracers of biomass burning (C_3H_8, C_2H_2, C_2H_6, and CH_3Cl) plus CO. The evolution of ^{210}Pb concentration in a plume impacted air mass is given by

$$dN_{Pb}/dt = \lambda_{Rn} N_{Rn} - S N_{Pb} - Dpb \quad (1)$$

where λ_{Rn} is the radioactive decay constant (0.18 d^{-1}), S denotes removal by scavenging, and D is dilution by ambient air. Loss of ^{210}Pb by radioactive decay (half-life equal to 22.3 years) is assumed to be insignificant. For ^{222}Rn the expression is similar though loss by scavenging is not a factor;

$$dN_{Rn}/dt = -\lambda_{Rn} N_{Rn} - Drn \quad (2)$$

For the five trace gases we use the simple model for the i^{th} species;

$$dC_i/dt = -k_i(OH)C_i - D_i \quad (3)$$

with the low solubilities of the trace gases again indicating that scavenging can be neglected.

In the atmosphere the details of mixing, and the impact of mixing on the various tracers, are very complex. In our model this complexity is entirely ignored by assuming that each sample represents a linear combination of plume air (which changes composition over time in a manner described shortly) and surrounding ambient air (of fixed composition).

Our aging plume is assumed identical to the hypothetical isolated air mass described in the second paragraph of the discussion. Within the plume we assume that loss of ^{210}Pb by scavenging must be very small on the basis of the high ^{7}Be activities and mixing ratios of soluble acidic gases measured in the South Pacific study area [*Dibb et al.*, 1999; *Talbot et al.*,1999]. Neglecting scavenging and mixing within the plume leads to a very simple solution to equation (1):

$$N_{Pb}(t) = N_{Pb}(0) + N_{Rn}(0)\,(1 - \exp(-\lambda_{Rn}\, t)) \quad (4)$$

For the hydrocarbons and CO an even simpler first-order loss expression results for the mixing ratio of the i^{th} species:

$$C_i(t) = C_i(0)\exp(-K_i\, t) \quad (5)$$

where $K_i = k_i(OH)$. Estimates for the constant loss rate (equivalent to 1/lifetime) were derived from the Harvard photochemical point model [*Schultz et al.*, 1999]. We binned our samples into four latitude/altitude bins based on where each sample was collected and use averages of all point calculations within these large bins for the model (Table 2). The model calculates the mixing ratios of all five gases in the mixture of aging plume and background air and then finds the HC/CO ratios.

We specify a constant initial composition for the fresh plumes that is based on low-altitude sampling over Africa during GTE TRACE- A [*Blake et al.*, 1996; *Mauzerall et al.*, 1998], since back trajectory calculations point to this region as a likely source of the PEM-Tropics plumes [*Fuelberg et al.*, 1999; R. Lusher et al., unpublished manuscript, 1999]. The mixing ratios of C_3H_8, C_2H_2, C_2H_6, and CH_3Cl are set at 700, 2000, 3600, and 860 ppt, respectively, with 600 ppb of CO. We must also specify initial activities of ^{222}Rn and ^{210}Pb. We are not aware of any airborne measurements of these tracers over Africa during austral spring, but *Ramonet et al.* [1996] report ^{222}Rn results for 10 samples collected on three flights in late January 1991. These ranged from below detection limit to 1.7 Bq m^{-3} with 3/10 samples > 1 Bq m^{-3} and half > 0.3 Bq m^{-3}. All of these elevated samples were clearly traced to strong wet convective uplift. The output of a global 3-D model suggests values of 3.7-7.4 Bq ^{222}Rn m^{-3} (100-200 pCi m^{-3}) in the boundary layer and 1.1-1.9 Bq m^{-3} (30-50 pCi m^{-3}) in convective outflow over Africa during spring (Y. Balkanski, personal communication, February 1998), so we tested the range 1.1-7.4 Bq m^{-3} (30-200 pCi m^{-3}). If wet convection is the process pumping boundary layer air into the free troposphere, ^{210}Pb activities should be quite low. However, this is an unproven hypothesis, so we tested sensitivity to initial ^{210}Pb activities over the range 0-93 μBq m^{-3} (0-2.5 fCi m^{-3}).

It is also necessary to assume a fixed composition of background air to mix into the aging plume. We use PEM-Tropics measurements outside of plumes to define the composition of this air: 15, 19, 230, and 540 ppt of C_3H_8, C_2H_2, C_2H_6, and CH_3Cl, respectively, 50 ppb of CO and 19 μBq ^{210}Pb m^{-3}. Each sample is then considered to be a mixture of aged plume and ambient air. With plume fraction f and plume age a this expresses the concentration of species i in the sample, $C_{i,S}$, in terms of the aged plume concentration and the ambient concentration of the species, $C_{i,A}$, as an estimated "theoretical" quantity, $C_{i,T}(f, a)$, depending on the estimated age and plume fraction,

$$C_{i,S} = f\, C_i(a) + (1 - f)\, C_{i,A} = C_{i,T}(f, a) \quad (6a)$$

Similarly, for ^{210}Pb (from equation (4)),

$$N_{Pb,S} = f\, N_{Pb}(a) + (1 - f)\, N_{Pb,A} = N_{Pb,T}((f, a) \quad (6b)$$

The observed ratio of hydrocarbon species i to CO, denoted by species 0, for a sample with theoretical plume fraction f and age a is

Table 2. Lifetimes in Days of the Hydrocarbons and CO Used in the Aging/Mixing Model

Sample Bin	C_3H_8	C_2H_2	C_2H_6	CH_3Cl	CO
0°-30°S, <6 km	8.6	12.4	42.8	302.9	38.1
0°- 30°S, >6 km	16.0	21.6	101.6	874.0	57.6
>30°S, <6 km	23.0	32.4	122.1	911.7	92.3
>30°S, >6 km	22.4	30.5	135.4	1121.6	82.0

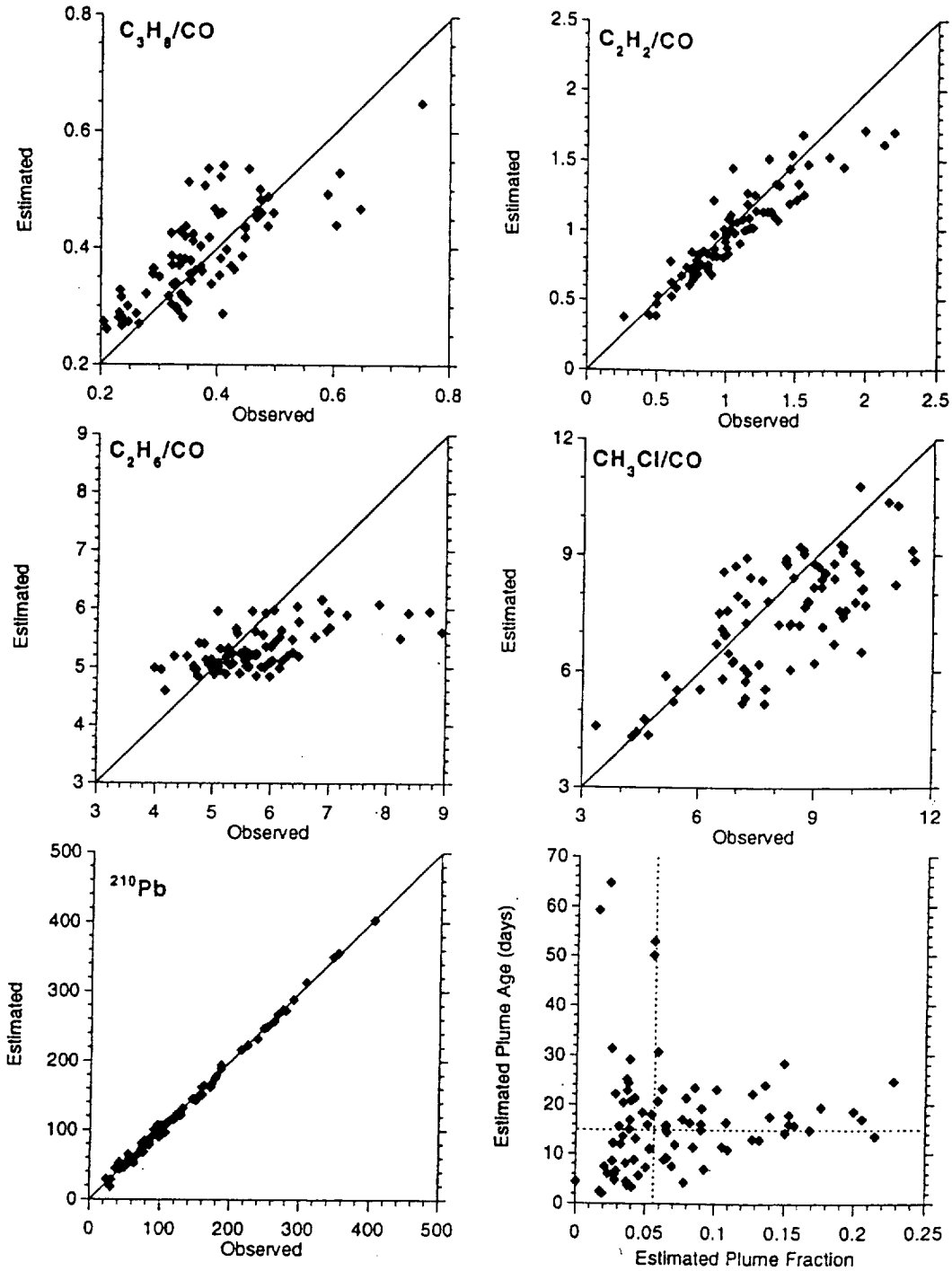

Figure 4. Comparison between model-predicted and observed values of four HC/CO ratios and ^{210}Pb activities in all plume-impacted samples. Activities of the radionuclide tracers in the fresh plume for this run were set at 3.7 Bq ^{222}Rn m^{-3} and 19 μBq ^{210}Pb m^{-3}. The model estimate of plume age and fraction of aged plume in each sample is also shown, with the median values for each shown as dashed lines.

$$R_{i,S} = C_{i,S}/C_{0,S} \text{ Å } C_{i,T}(f, a) / C_{0,T}(f, a) = R(f, a) \quad (7)$$

Equation (7) provides an approach to estimating the plume fraction and age of a sample. We define the "residual error" for the i^{th} species ratio as

$$E_i(f, a) = R_{i,S} - R_{i,T}(f, a) \quad (8)$$

and for ^{210}Pb,

$$E_{Pb}(f, a) = N_{Pb,S} - N_{Pb,T}(f, a) \quad (9)$$

and form the "sample error sum of squares,"

$$Q_S(f, a) = E_1(f, a)^2 + E_2(f, a)^2 + E_3(f, a)^2 + E_4(f, a)^2 + E_{Pb}(f, a)^2 \quad (10)$$

Our estimates of the plume fraction and age of the plume are determined for each sample independently by minimizing $Q_S(f, a)$ under the constraints, $0 \le f \le 1$ and $0 \le a$.

4.2. Model Results

4.2.1. A selected run. Since we use low-altitude measurements of CO and the HC to initialize the fresh plume, we suspect that

using estimates for ^{222}Rn activity in the boundary layer may be more internally consistent. The agreement between model results and observations when initial ^{222}Rn and ^{210}Pb activities are set at 3.7 Bq m^{-3} and 19 μBq m^{-3}, respectively, are shown in Figure 4. These results are typical in that the model does extremely well predicting ^{210}Pb activities and not as well with the reactive trace gases. However, the model-predicted HC/CO ratios are generally within 20% of the measured values (Figure 5), a finding which also applies to all of the other runs. Given the drastic simplifications made in the treatment of CO and the HC, we are quite pleased with the model performance. In particular, recall that a constant initial plume composition, based on a few samples from a single flight over Africa 4 years earlier, was assumed to be a valid representation of the composition of all of the plumes advected to the South Pacific during PEM-Tropics.

4.2.2. Sensitivity to initial Rn and Pb. The model is much more sensitive to the value of initial ^{222}Rn than to that of ^{210}Pb over the ranges of these parameters that we explored (Figure 6). Increasing initial ^{222}Rn from 1.1-3.7 Bq m^{-3} reduces the median estimated plume age by about a week, with the higher HC mixing

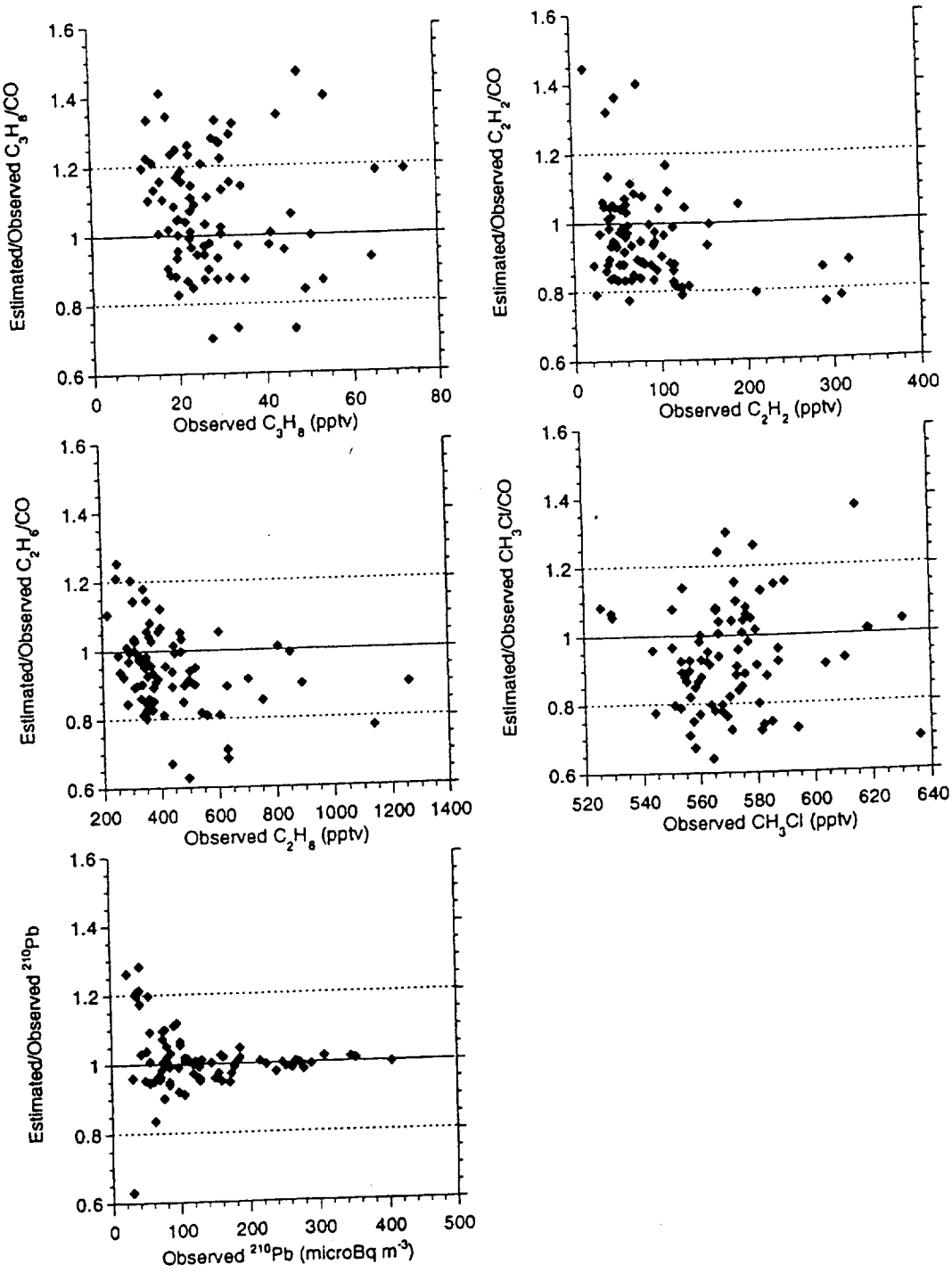

Figure 5. Ratios of model-predicted HC/CO and ^{210}Pb activities over observations, plotted against the observed mixing ratios of the tracer species.

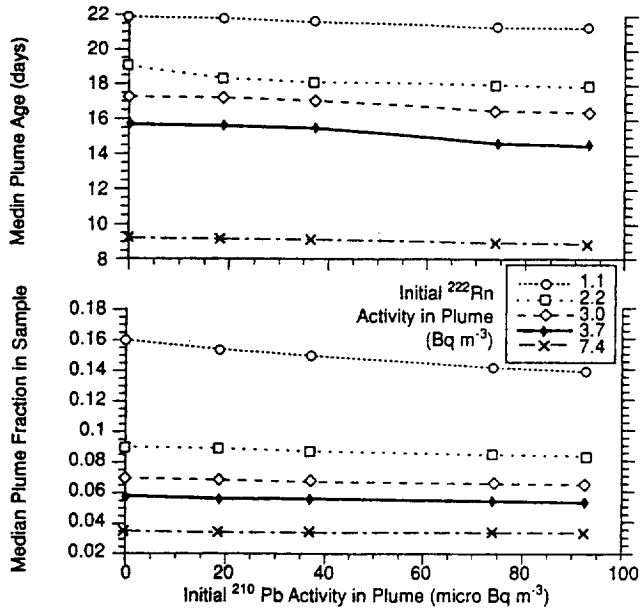

Figure 6. Median values of model-estimated plume ages and fractions of aged plume in each sample plotted as a function of prescribed initial ^{210}Pb activity. Each line/symbol combination corresponds to a different prescribed initial ^{222}Rn activity.

ratios in the younger plume compensated for by increased "entrainment" of background air (about 95% background with the younger plumes compared to roughly 85%). At 7.4 Bq ^{222}Rn m^{-3} in the fresh plume the median age when encountered over the South Pacific drops to about 9 days, and the samples are estimated to be 97% background air. In contrast, the age and dilution estimates vary only a few percent for a given value of initial ^{222}Rn as initial ^{210}Pb is allowed to vary from 0-93 μBq m^{-3} (Figure 6). This reflects the fact that production of ^{210}Pb from ^{222}Rn decay quickly overwhelms the initial value, with 1 Bq ^{222}Rn m^{-3} ultimately yielding 470 μBq ^{210}Pb m^{-3} within the aging plume (with 72% of this produced in 7 days and 92% by the end of the second week).

It should be noted that the model is also quite sensitive to the prescribed activity of ^{210}Pb in background air. The median-estimated plume age decreases from 16.6 to 4.5 days when background ^{210}Pb is increased from 0 to 93 μBq m^{-3} (assuming 3.7 Bq ^{222}Rn m^{-3} and no ^{210}Pb in the fresh plume). However, measured ^{210}Pb activities over the South Pacific outside of the plumes constrain the background to values less than 35 μBq m^{-3}, which yields median-estimated ages in the range of 13.7-16.6 days for the same initial conditions.

4.3. Implications of the Simple Model Results

The complete lack of observational constraints on the initial composition of the plumes that were advected to the South Pacific (from Africa or possibly even South America) during the PEM-Tropics campaign precludes quantitative assessment of the utility of such a simple modeling exercise. It is clear that the HC and CO mixing ratios are likely to vary considerably as a function of fuel and fire type, and the local meteorological conditions [e.g., *Lobert et al.*, 1991; *McKenzie et al.*, 1997].

Nevertheless, the model estimates of plume ages are in reasonable agreement with transport times from south Africa derived from back trajectory calculations. R. Lusher et al. (unpublished manuscript, 1999) report a mean transit time of roughly 8 days from South Africa to interception during PEM-Tropics for plumes that came in from the west. This is half the median age estimated for an initial ^{222}Rn activity of 3.7 Bq m^{-3} (Figure 6), but essentially the same as our estimate if initial ^{222}Rn is 7.4 Bq m^{-3} (Figures 4 and 6). Both analyses suggest that a significant fraction of the intercepted plumes were in the 5-14 day old range.

The model clearly demonstrates that all of the plumes entrained significant amounts of background air during transport. This finding is in agreement with more elaborate advective/photochemical models that cannot create air masses resembling the PEM-Tropics plumes out of any of the air masses sampled during GTE/TRACE- A without entraining large fractions of South Pacific background air (B. Heikes and F. Flocke, personal communication, April 1998). However, our estimates of dilution must be regarded as upper limits in most cases because of the mixture of "in plume" and "out of plume" time reflected in many of our sample collection intervals. In theory, it would be possible to account for this "sampling artifact" dilution and calculate better estimates of "transport" dilution, but the large uncertainties in our knowledge of the initial conditions imposed on the model suggest that such an exercise would have little merit.

5. Conclusions

Observed enhancements of ^{210}Pb in biomass burning impacted air masses over the South Pacific lend support to a conceptual model linking these plumes to fires in Africa. Wet convective uplift over or near Africa appears to have lofted boundary layer air with elevated ^{222}Rn activities, primary combustion products, and precursors of O_3, PAN, HNO_3, HCOOH, and CH_3COOH well into the free troposphere. Precipitation scavenging in the wet convective systems depleted the mixing ratios of aerosol-associated soluble ions and their soluble gaseous precursors in the lifted boundary layer air. The prevailing westerlies then advected these air masses to the PEM-Tropics study region where they were intercepted by the DC-8.

A simple aging and dilution model, initialized with plausible, but very poorly constrained, estimates of the composition of such lifted boundary layer air, reproduced ^{210}Pb activities over the South Pacific very well. The ratios of four HC tracers of biomass burning over CO were also reasonably captured by the model (generally to better than 20%).

Model-calculated ages of the plumes are one of the principal results. These were highly dependent on the prescribed activity of ^{222}Rn in the fresh plumes (which is not known), but using values which should bound typical boundary layer activities produced ages that agreed with independent ages based on back trajectories to within better than a factor of 2. This exercise demonstrates the potential power of ^{222}Rn and ^{210}Pb as transport tracers, but also points out the need for a greatly expanded observational data base on their distribution in the free troposphere.

Acknowledgments. We would like to thank M. Schultz for sharing the results of his calculations with the Harvard photochemical model, and B. Heikes and F. Flocke for sharing preliminary output from their attempts to model the evolution of PEM-Tropics plumes. The efforts of the Ames DC-8 flight and ground crews that made PEM-Tropics a success are greatly appreciated. This research was supported by the NASA Global Tropospheric Chemistry Program.

References

Blake, N. J., D. R. Blake, J. E. Collins Jr., G. W. Sachse, B. E. Anderson, J. A. Brass, P. J. Riggan, and F. S. Rowland, Biomass burning

emissions of atmospheric methyl halide and hydrocarbon gases in the South Atlantic region, in *Biomass Burning and Global Change*, vol. 2, *Biomass Burning in South America, Southeast Asia and Temperate and Boreal Ecosystems, and the Oil Fires of Kuwait*, edited by J. S. Levine, pp. 575-594, MIT Press, Cambridge, Mass., 1996.

Blake, N. J., et al., Influence of southern hemispheric biomass burning on midtropospheric distributions of nonmethane hydrocarbons and selected halocarbons over the remote South Pacific, *J. Geophys. Res.*, this issue.

Dibb, J. E., R. W. Talbot, E. M. Scheuer, D. R. Blake, N. J. Blake, G. L. Gregory, G. W. Sachse, and D. C. Thornton, Aerosol chemical composition and distribution during the Pacific Exploratory Mission (PEM) Tropics, *J. Geophys. Res.*, *104*, 5785-5800, 1999.

Fenn, M. A., et al., Ozone and aerosol distributions and air mass characteristics over the South Pacific during the burning season, *J. Geophys. Res.*, this issue.

Fuelberg, H. et al., A meteorological overview of the PEM-Tropics period, *J. Geophys. Res.*, *104*, 5585-5622, 1999.

Lambert, G., M. F. Le Cloarec, B. Ardouin, and B. Bonsang, Long-lived radon daughters signature of savanna fires, *Global Biomass Burning*, edited by J. S. Levine, pp. 181-184, MIT Press, Cambridge, Mass., 1991.

Le Cloarec, M. F., B. Ardouin, H. Cachier, C. Liousse, S. Neveu, and E.-Y. Nho, ^{210}Po in savanna burning plumes, *J. Atmos. Chem.*, *22*, 111-122, 1995.

Lobert, J. M., D. H. Scharffe, W.-M. Hao, T. A. Kuhlbusch, R. Seuwen, P. Warneck, and P. J. Crutzen, Experimental evaluation of biomass burning emissions: Nitrogen and carbon containing compounds, in *Global Biomass Burning - Atmospheric, Climatic, and Biospheric Implications*, edited by J. S. Levine, pp. 289-304MIT Press, Cambridge, Mass., 1991.

Mauzerall, D. L., et. al., Photochemistry in biomass burning plumes and implications for tropospheric ozone over the tropical South Atlantic, *J. Geophys. Res.*, *103*, 8401-8423, 1998.

McKeen, S. A., and S. C. Liu, Hydrocarbon ratios and photochemical history of air masses, *Geophys. Res. Lett.*, *20*, 2363-2366, 1993.

McKeen, S. A., M. Trainer, E. Y. Hsie, R. K. Tallamaraju, and S. C. Liu, On the indirect determination of atmospheric OH radical concentrations from reactive hydrocarbon measurements, *J. Geophys. Res.*, *95*, 7493-7500, 1990.

McKeen, S. A., S. C. Liu, E.-Y. Hsie, X. Lin, J. D. Bradshaw, S. Smyth, G. L. Gregory, and D. R. Blake, Hydrocarbon ratios during PEM-West A: A model perspective, *J. Geophys. Res.*, *101*, 2087-2109, 1996.

McKenzie, L. M., D. E. Ward, and W. M. Hao, Chlorine and bromine in the biomass of tropical and temperate ecosystems, in *Biomass Burning and Global Change*, vol. 1, edited by J. S. Levine, pp. 421-428, MIT Press, Cambridge, Mass., 1997.

Ramonet, M., J. C. Le Roulley, P. Bousquet, and P. Monfray, Radon-222 measurements during the Tropoz II campaign and comparison with a global atmospheric transport model, *J. Atmos. Chem.*, *23*, 107-136, 1996.

Schultz, M. G., et al., On the origin of tropospheric ozone and NO_x over the tropical South Pacific, *J. Geophys. Res.*, *104*, 5829-5843, 1999.

Talbot, R. W., J. E. Dibb, E. M. Scheuer, D. R. Blake, N. J. Blake, G. L. Gregory, G. W. Sachse, J. D. Bradshaw, S. T. Sandholm, and H. B. Singh, Influence of biomass combustion emissions on the distribution of acidic trace gases over the southern Pacific basin during austral springtime, *J. Geophys. Res.*, *104*, 5623-5634, 1999.

D. R. Blake and N. J. Blake, Department of Chemistry, University of California, Irvine, CA 92717.

J. E. Dibb (corresponding author), L. D. Meeker, E. M. Scheuer, and R. W. Talbot, Institute for the Study of Earth, Oceans, and Space, University of New Hampshire, Durham, NH 03824. (jack.dibb@unh.edu)

G. L. Gregory and G. W. Sachse, NASA Langley Research Center, Hampton, VA 23665.

(Received August 3, 1998; revised January 20, 1999; accepted February 3, 1999.)

Tropospheric Reactive Odd-Nitrogen over the South Pacific in Austral Springtime

R. W. Talbot[1], J. E. Dibb[1], E. M. Scheuer[1], J. D. Bradshaw[2*], S. T. Sandholm[2], H. B. Singh[3], D. R. Blake[4], N. J. Blake[4], E. Atlas[5], and F. Flocke[5]

[1]Institute for the Study of Earth, Oceans and Space
University of New Hampshire
Durham, NH 03824

[2]Department of Earth and Atmospheric Sciences
Georgia Institute of Technology
Atlanta, GA 30332

[3]NASA Ames Research Center
Moffett Field, CA 94035

[4]Department of Chemistry
University of California-Irvine
Irvine, CA 92697

[5]Atmospheric Chemistry Division
National Center for Atmospheric Research
Boulder, CO 80303

*Deceased

[Corresponding author: rwt@christa.unh.edu]

Submitted to *Journal of Geophysical Research - Atmospheres*
Special Section on NASA/GTE PEM-Tropics A

July 1999

ABSTRACT

The distribution of reactive nitrogen species over the South Pacific during austral springtime appears to be dominated by biomass burning emissions, and possibly lightning and stratospheric inputs. Absence of robust correlations of reactive nitrogen species with source-specific tracers (e.g., C_2H_2 [combustion], CH_3Cl (biomass burning], C_2Cl_4 [industrial], ^{210}Pb [continental], and ^{7}Be [stratospheric]) suggest significant aging and processing of the sampled air parcels due to losses by surface deposition, OH attack plus dilution processes. Classification of the air parcels based on CO enhancements indicates that the greatest influence was found in plumes at 3-8 km altitude in the distributions of HNO_3 and PAN. Here mixing ratios of these species reached 600 pptv, values surprisingly large for a location several thousand km removed from the nearest continental areas. The mixing ratio of total reactive nitrogen (NO_y sum), defined here as measured (NO + HNO_3 + PAN + CH_3ONO_2 +$C_2H_5ONO_2$) + modeled (NO_2), had a median value of 285 parts per trillion by volume (pptv) within these plumes compared to 120 pptv in non-plume air parcels. Comparison of these air parcels classifications for NO_x and alkyl nitrate distributions showed no perceivable plume influence, but recycling of reactive nitrogen may have masked this direct effect. In the marine boundary layer NO_y sum averaged 50 pptv in both air parcel classifications, being somewhat isolated from the polluted conditions above it by the trade wind inversion. In this region, however, alkyl nitrates appear to have an important marine source where they comprise 20-80% of NO_y sum in equatorial and high latitude regions over the South Pacific.

1. INTRODUCTION

Reactive odd-nitrogen species play central roles in tropospheric photochemistry. The concentration of NO_x ($NO + NO_2$) controls photochemical production or destruction of O_3 and it also influences the concentration of HO_x ($OH + HO_2$). Ozone and HO_x are important since they largely determine the oxidizing capacity of the troposphere. Due to the high chemical reactivity of NO_x, it is often converted photochemically to HNO_3 and the reservoir species peroxyacetyl nitrate (PAN). These conversions take place in a matter of hours during the summertime [*Logan*, 1983; *Kasting and Singh*, 1986]. Reactive nitrogen can be transported over long distances as HNO_3 and PAN, and they may eventually react to regenerate NO_x in remote areas. Removal of reactive nitrogen from the troposphere is primarily by wet and dry deposition of HNO_3 and particle-NO_3^- [*Logan*, 1983].

Total reactive odd-nitrogen (NO_y) has been defined as the sum of the individual species which are reactive in the troposphere. These species include NO, NO_2, NO_3, N_2O_5, HNO_3, HONO, PAN, $RONO_2$ (R= alkyl), and particle-NO_3^-. Together this suite of compounds has also been estimated by measurement of NO_y as NO using a gold catalytic converter and a reductant such as CO [*Bradshaw et al.*, 1998]. In air parcels without recent emission inputs, these two measures of NO_y often disagree [*Fahey et al.*, 1986; *Atlas et al.*, 1992a; *Sandholm et al.*, 1994 ; *Bradshaw et al.*, 1998]. Some of these differences may be due to certain species, such as organic nitrates, not being measured on an individual basis but they are still included in the more general NO_y measurement [e.g., *Atlas et al.*, 1992a]. In addition, some NO_y converters appear to convert non-NO_y compounds (e.g., NH_3 and HCN) with varying efficiency [*Kliner et al.*, 1997; *Bradshaw et al.*, 1998]. However, surprisingly good agreement in measured NO_y and NO_y sum was found recently for the upper troposphere over the North Atlantic [*Talbot et al.*, 1999a]. The reasons for varying degrees of

agreement are unclear and it may be more meaningful to measure the individual species and use their sum as representative of NO_y (NO_y sum). This approach has been adopted by the NASA Global Tropospheric Experiment (GTE) program and it is the one used in this paper.

The distribution of reactive odd-nitrogen species and the mechanisms that control their concentrations are not well understood for large areas of the global troposphere. This is particularly true for the South Pacific, and as such these measurements were an integral component of the NASA PEM-Tropics A airborne expedition over this region during September/October 1996. This paper presents the distributions and inter-relations of NO, NO_2, HNO_3, PAN, CH_3ONO_2, and $C_2H_5ONO_2$ over the South Pacific during PEM-Tropics A.

2. EXPERIMENTAL METHODS

2.1 *Study Area*

The PEM-Tropics A airborne expedition was conducted using the NASA Ames DC-8 research aircraft. Transit and intensive site science missions composed 18 flights, averaging 8-10 hours in duration and covering the altitude range of 0.3 to 12.5 km. The base of operations progressed as follows: (1) Tahiti (3 missions), (2) Easter Island (2 missions), (3) Tahiti (1 mission), (4) New Zealand (1 mission), and (5) Fiji (3 missions). The overall scientific rationale and description of individual aircraft missions are described in the PEM-Tropics A overview paper [*Hoell et al.*, 1999]. The features of the large-scale meteorological regime and associated air mass trajectory analyses for the September-October 1996 period are presented in *Fuelberg et al.* [1999]. The data used in this paper were obtained in the geographic grid approximately bounded by 60° N - 75° S latitude and 165° E - 105° W longitude. A geographic map with the flight location details is shown in several prior papers [e.g., *Hoell et al.*, 1999]. The measured and model calculated

parameters utilized in this paper are available from the NASA Langley Distributed Data Archive Center (DDAC) or the GTE project archive (ftp-gte.larc.nasa.gov).

2.2 *Sampling and Analytical Methodology*

NO:

Nitric oxide was measured with the Georgia Tech two-photon/laser induced fluorescence instrument [*Bradshaw et al.*, 1985; *Sandholm et al.*, 1990]. This technique is spectroscopically selective for NO. The system incorporated recent advancements in laser detection hardware as well as improvements in the airborne sampling manifold [*Bradshaw et al.*, 1999]. The inlet consisted of a 100 mm ID glass coated stainless flow system which skimmed and dumped to exhaust the air flow nearest the walls. The inlet was mounted in a 45°orientation to the fuselage and utilized a ram air flow rate of 40,000 liter per minute. This high flow rate created a "pseudo wall-less" sampling environment in that nearly all NO_y species that may have interacted with the walls would not have time to make it back to the volume element being sampled in the central core of the manifold before being exhausted overboard. Thus, NO was measured in the center core flow only, minimizing potential wall artifacts [*Bradshaw et al.*, 1999]. Wall effects were also greatly reduced by steering the two probe beams (sampling an area of < 1 cm^2) through the center of the sampling manifold which itself had a cross sectional area of ~ 80 cm^2. Given a 10 Hz probe frequency, this high flow rate also permitted adequate time for a complete turnover of the sampling region between laser shots, thus insuring that measurements of NO were being made under true ambient conditions. The measurements were reported using an integration time of one second. Accuracy of the instrument calibration is estimated to be ±16% for NO at the 95% confidence limit.

NO_2:

Model calculated NO_2 was used here instead of the Georgia Tech measured NO_2 due to better time overlap with the other NO_y sum measurements. It should be noted that the measured and modeled NO_2 data were highly correlated giving a $(NO_2)_{meas.}/(NO_2)_{calc.}$ ratio of 0.93 [*Bradshaw et al.*, 1999). The Harvard photochemical point model was used to calculate NO_2 along the DC-8 flight path from diurnal steady-state concentrations of radicals and chemical intermediates estimated using the ensemble of observations from the aircraft [*Schultz et al.*, 1999].

HNO_3:

Acidic gases were subsampled from a high-volume (500 - 1500 standard liters per minute, SLPM) flow of ambient air using the mist chamber technique [*Talbot et al.*, 1997a; *Talbot et al.*, 1999b]. The subsample flow rate was always <10% of the primary manifold total flow. Sample collection intervals were typically 4 minutes in the boundary layer, 6 minutes at 2-9 km altitude, and 8 minutes above 9 km altitude, reflecting decreased pumping rates in the middle and upper troposphere. The inlet manifold consisted of a 0.9 m length of 41 mm ID glass coated stainless steel pipe. The pipe extended from the DC-8 fuselage to provide a 90° orientation to the ambient air streamline flow. To facilitate pumping of the high-volume manifold flow on both the HNO_3 and Georgia Tech systems, a diffuser was mounted over the end of the inlet pipe parallel to the DC-8 fuselage. This device provided a "shroud" effect, slowing the flow of ambient air through it slightly below the true air speed of the DC-8 and adding 50-100 hPa of pressurization to the sampling manifold. This effectively eliminated the reverse venturi effect (≈40 hPa) on the sampling manifold. An additional feature of the diffuse was a curved step around the manifold pipe which provided the streamline effects of a backward facing inlet. Its function was to facilitate exclusion of aerosol

particles greater than ≈2 μm in diameter from the sampling manifold. Aerosols smaller than this were removed from the sampled air stream using a 1 μm pore-sized Zefluor teflon filter that was readily changeable every 5 - 10 minutes to minimize aerosol loading on the filter and gas/aerosol phase partitioning from ambient conditions. The accuracy of the HNO_3 measurements is estimated to be ±20% with a precision ranging from ±10-35% depending on the ambient mixing ratio.

PAN:

The NASA Ames PAN instrument provided measurements of this species using electron capture gas chromatography detection from a cryogenically enriched sample of ambient air [*Singh and Salas*, 1983; *Gregory et al.*, 1990]. The system uses an aft facing teflon inlet with the instrument operated at a constant pressure of 1050 mbar isolated from aircraft cabin pressure fluctuations. The sampling time of 2 minutes was followed by a 5 minute analysis time. In-flight calibration was accomplished using PAN synthesized in liquid n-tridecane. The PAN measurements have an estimated accuracy of about ±20% and a precision of ±10%. The detection limit for PAN was a 2-3 pptv.

Alkyl Nitrates:

C_1-C_4 alkyl nitrates were collected in stainless steel canisters and then separated analytically on a Restek-1701 column and quantified by electron capture detection [*Atlas et al.*, 1992b]. Oxygen doping enhanced the sensitivity of the electron capture detection for the alkyl nitrates. The precision is ±5% at mixing ratios above 5 pptv and ±10% below this value.

3. Results

3.1 Data Base

The data in this paper used the time scale defined by the HNO_3 measurements, with all other

species (including calculated NO_2) averaged to this time base. The data set was further refined by using only time periods where there was a measurement reported for all the reactive nitrogen species. This reduced the size of the merged product by about 50%, but it still allowed meaningful comparisons for NO_y sum with other parameters as data from each mission and a wide altitude span was included. Again, for the purposes of this paper NO_y is defined as the sum (NO_y sum) of the individual species NO, HNO_3, PAN, CH_3ONO_2, $C_2H_5ONO_2$ plus model calculated NO_2. The higher alkyl nitrate species were <1 pptv and present inconsistently, so they are not included in this analysis of NO_y sum.

Due to the significant impact of aged biomass burning emissions over the South Pacific in austral springtime [*Gregory et al.*, 1999; *Schultz et al.*, 1999; *Talbot et al.*, 1999b], the data were divided into two groups: (1) within biomass combustion plumes and (2) non-plume air parcels. The combustion data set corresponds to sampling times where CO was enhanced >10 ppbv in plumes well-defined by CO, O_3, C_2H_2, and C_2H_6 [*J. A. Logan et al.*, manuscript in preparation, 1999].

Although not discussed in detail this paper, particle-NO_3- mixing ratios were generally <50 pptv [*Dibb et al.*, 1999a]. The time resolution of these measurements was typically 10-15 minutes, so their inclusion in the NO_y discussion in this paper is difficult. In only a few cases in the combustion plume data set was particle-NO_3^- greater than 10% of NO_y sum. It appears that wet scavenging of particle-NO_3^- occurred early in the life of the biomass burning emissions, with only an occasional plume containing >50 pptv of particle-NO_3^- [*Dibb et al.*, 1999b].

3.2 Vertical Distributions

Figure 1 illustrates the vertical distribution encountered commonly over the South Pacific for species associated with combustion emissions. This plume was encountered west of Tahiti on

a spiral ascent during mission 6, and was particularly well defined by C_2H_2, a unique tracer of combustion emissions [*Blake et al.*, 1996a]. Note that C_2Cl_4, an industrial emissions tracer, was not elevated between 3 and 6 km altitude with the other trace gases. The biomass burning tracer CH_3Cl [*Blake et al.*, 1996b], fluctuated between 550-575 pptv over the entire spiral altitude, but did not show a pronounced plume like the other combustion associated species. In other cases, CH_3Cl exhibited a higher correlation with these species in plumes. The large-scale distribution of nonmethane hydrocarbons and selected halocarbons over the South Pacific during PEM-Tropics A is presented elsewhere [*Blake et al.*, 1999], where multiple spiral data illustrates the apparent impact of biomass burning emissions in the middle and upper troposphere.

It is important to recognize that the plumes sampled during PEM-Tropics A were aged from 1 to 2.5 weeks since they last passed over land based on model calculations of air parcel trajectories [*Fuelberg et al.*, 1999] and independent estimates using a combination of radioactive ingrowth of ^{210}Pb and OH decomposition of selected hydrocarbons [*Dibb et al.*, 1999b]. The air parcels sampled over the South Pacific last passed over land in Africa, Australia, or Indonesia, all regions of active biomass burning during austral springtime [*Fuelberg et al.*, 1999]. In addition, lightning associated with convection in these areas was very abundant [*Fuelberg et al.*, 1999], and it could have contributed reactive nitrogen to the plumes that we encountered over the South Pacific. It was rare to find elevated NO_x mixing ratios in these plumes due to the potentially long time periods from its injection from combustion or lightning over continental areas. During transport of this duration it should of been converted to HNO_3, PAN, and possibly other reactive nitrogen forms. Indeed, the absence of significant aerosols in these plumes but elevated mixing ratios of HNO_3 (e.g., Figure 1) indicates photochemical production of HNO_3 during long-range transport after being scavenged

initially by convection over continental areas [*Talbot et al.*, 1999b].

The vertical distributions of NO_x, HNO_3, PAN, CH_3ONO_2 and $C_2H_5ONO_2$ over the South Pacific are presented in Figures 2a (non-plume) and b (within plumes). In general, the mixing ratio of NO_x in non-plume air parcels was <50 pptv, with much of the data <20 pptv. Mixing ratios were <5 pptv in the marine boundary layer increasing to an average of 25 pptv in the upper troposphere. It was not uncommon to have areas in the marine boundary layer where the mixing ratio of NO was <1 pptv, and as low as 0.2 pptv [*Bradshaw et al.*, 1999].

The mixing ratios of HNO_3 and PAN were usually <100 pptv, but larger departures from this value are evident in the non-plume air parcels. Notice that in the middle troposphere (3 - 10 km), HNO_3 and PAN are both present at several hundred pptv. In the marine boundary layer PAN was <5 pptv and HNO_3 <20 pptv. Thermal decomposition of PAN occurs on the order of hours in this warm (25-30°) moist region which should lead to HNO_3 production from the NO_2 + OH mechanism. The mixing ratio of HNO_3 is, however, kept <20 pptv due to its deposition to the ocean and uptake onto salt aerosol in the boundary layer [*Talbot et al.*, 1999b]. Below 4 km altitude the NO_x responsible for O_3 production is largely explained by the decomposition of PAN [*Schultz et al.*, 1999].

The mixing ratios of NO_x, HNO_3 and PAN in the non-plume air parcels over the South Pacific in the middle and upper troposphere were comparable to those typically found at remote locations. NO_x, HNO_3, and PAN are typically 50-100 pptv at Mauna Loa [*Atlas et al.*, 1992a] and over the North Pacific in aged marine air [*Talbot et al.*, 1996a, 1997]. The principal difference in the reactive nitrogen distributions over these Pacific regions is for NO_x in the marine boundary layer. With the South Pacific being by far the most remote of these locations, NO_x mixing ratios are 2- to

5-fold lower.

The alkyl nitrate distribution over the South Pacific was dominated by CH_3ONO_2, which averaged 15 pptv in the marine boundary layer to around 10 pptv from 2-12 km altitude. The only other significant alkyl nitrate was $C_2H_5ONO_2$, with it distribution mainly <5 pptv at all altitudes.

Looking at the vertical distributions of reactive nitrogen species in the combustion plume air parcels (Figure 2b) shows that NO_x was very similar to the non-plume group. The difference in the two groups altitude bin means is <10 pptv above 2 km, with the plume data exhibiting the slightly higher values. The differences are even less for the two alkyl nitrates but in the opposite direction, with about 3 pptv less on average in the plume data vertical distribution of CH_3ONO_2.

The largest differences in the vertical distributions between the two groups is in the middle troposphere where HNO_3 and PAN were enhanced in the plume data set. The greatest mixing ratios of HNO_3 and PAN were observed in the 2-8 km altitude region. We found average mixing ratios of HNO_3 of 175 pptv and 165 pptv for PAN compared to 100 and 50 pptv respectively in the non-plume air parcels. Mixing ratios of HNO_3 and PAN around 500 pptv over the South Pacific are among the largest ever observed in the remote middle troposphere (Figure 2b). This is quite remarkable considering that the South Pacific is one of the most isolated locations on Earth. Here the large-scale flow pattern dominated by westerlies [*Fuelberg et al.*, 1999] apparently brings quite aged continentally derived combustion emissions to the South Pacific during the austral springtime period. This source influence is barely perceivable in NO_x and alkyl nitrates, but easily noticeable in HNO_3 and PAN.

The vertical distributions of NO_y sum in the non-plume and plume air parcel classifications are shown in Figure 3. In the marine boundary, which is somewhat isolated from the polluted

conditions above it by the trade wind inversion, NO_y sum averaged ≈50 pptv in both air parcel types. The impact of the combustion plumes was significant from 2 to 12 km altitude. In this region NO_y sum averaged 285 pptv in the plumes compared to 120 pptv in non-plume air parcels. Values of NO_y sum of 100-150 pptv are typical of air parcels over remote regions not recently influenced by emission sources [*Atlas et al.*, 1992a; *Ridley*, 1991; *Talbot et al.*, 1996a, 1997b, 1999a].

3.3 NO_y Partitioning

To examine the relationship of various species to NO_y, the vertical distribution of their ratio to NO_y sum are shown in Figures 4a (non-plume) and b (within plumes). In both air mass types the ratio NO_x/NO_y sum is 10-15% from the boundary layer to 7 km altitude, then increases to 25% at 12 km. The opposite trend is seen for the alkyl nitrates, decreasing from ≈30% in the boundary layer to 5-10% at 12 km. In the non-plume data the ratio was higher at all altitudes by about 5%, presumably driven by a stronger marine source for these species compared to combustion plumes over the South Pacific.

The ratio HNO_3/NO_y sum in the non-plume air parcels has a value of ≈50% in the boundary layer, increases to 70% in the 2-4 km region and then decreases linearly to ≈25% at 12 km altitude. The sharp increase in the value of this ratio near 3 km may reflect the influence of cloud processes in this layer. Small cumulus with bases at the top of the marine boundary layer (1-1.5 km) may be releasing soluble gases to the gas phase as cloud tops in this transition layer dissipate at 3-4 km. Chemical and dynamical processes in this cloudy region are known to produce aerosols [*Clarke et al.*, 1999], and it seems likely that soluble gases would also be released by these same mechanisms. In the plume air parcels this effect is less noticeable due to elevated mixing ratios in and above this region. The ratio HNO_3/NO_y sum is still ≈50% in the boundary layer, but this value is maintained

up to 6 km before decreasing to ≈40% at 12 km altitude. Thus, there is a major impact on the NO_y partitioning above the marine boundary layer attributed to combustion/lightning inputs of reactive nitrogen.

The impact of the same inputs on PAN/NO_y sum is less, even in the middle troposphere. This ratio is 5-10% in the boundary layer increasing to 30-40% in the middle troposphere before decreasing to ≈ 20% at 12 km altitude. In the middle troposphere, long-range transport appears to increase the ratio PAN/NO_y sum by about 10% in the plume air parcels compared to the non-plume cases.

4. Species Inter-Relationships

Comparisons between the non-plume and plume data sets shows that a very similar combustion influence is present in both air parcel classifications. Various species inter-relationships demonstrate this point in Figure 5. In each of the correlations shown in Figure 5 the non-plume and plume distributions overlap fairly tightly, with the highest mixing ratios of C_2H_2, and the other parameters associated with the plume air parcels. The correlation of CH_3Cl and C_2H_2 indicates a that biomass burning source is responsible for at least some portion of the chemical signatures. The lack of similar correlation of C_2H_2 with industrial tracers (e.g., Figure 1) suggests that the combustion influence is mainly derived from biomass burning.

As can be seen in Figure 5, there was a substantial amount of O_3 associated with these plumes, a chemical characteristic of biomass burning emissions from South American and Africa [*Fishman and Brackett,* 1997]. In fact, about half of the O_3 in the tropospheric column over the South Pacific appears to have been advected eastward in biomass burning emissions from South America and Africa [*Schultz et al.*, 1999]. The apparent dispersion of these emissions throughout

the most of the tropospheric column over the South Pacific is likely due to mixing and dilution of combustion plumes with background air. The non-plume data chemical signature reflects this combustion influence. This is particularly pronounced for NO_y sum, where data from both data classifications overlap significantly. The wide scatter in the C_2H_2/NO_y sum relationship is probably driven to a large degree by varying loss or production of HNO_3 and PAN. Plots of these two species against C_2H_2 (not shown) show scatter similar to that for NO_y sum.

The relationships of CH_3Cl with PAN and NO_y sum are presented in Figure 6. The extensive scatter in the relationship for NO_y sum is similar to that with C_2H_2 (Figure 5). Slightly better correlation is found for PAN ($r^2 = 0.35$), but its driven mainly by the highest values in both species. The GTE program investigated the chemical environment over the South Atlantic during the 1992 austral spring. Biomass burning pollution was evident throughout the tropospheric column, with CH_3Cl mixing ratios in the 600-700 pptv range [*Talbot et al.*, 1996b]. If we take a value of 650 pptv over the biomass burning source areas and 560 pptv over the South Pacific, this represents a 14% decrease in CH_3Cl over about a two week period. Attack by OH (at say, 1×10^6 cm^{-3}) can account for maybe half of this drop, with the rest attributed to dilution. These rough estimates are consistent with other air mass history analyses, where OH attack and dilution were found to be equally responsible for decreases in hydrocarbon species [e.g., *McKeen and Liu*, 1993]. Thus, the mixing ratios of CH_3Cl over the South Pacific are in the range expected for a South American/African biomass burning source.

These same air parcels could of had inputs of reactive nitrogen besides that from biomass burning. In some cases lightning may have provided an additional source of reactive nitrogen. Additionally, we can not rule out the stratosphere as a source of reactive nitrogen. ^7Be, a reasonably

good stratospheric tracer in the troposphere, frequently exceeded 400 fCi (10^{-15} Ci) m^{-3} throughout much of the tropospheric column (Figure 7). Such concentrations of ^{7}Be are quite elevated, being 2-3 times higher than we have observed previously over the North Pacific [*Talbot et al.*, 1996a, 1997b]. Even though the correlation of NO_y sum with ^{7}Be is not very robust (Figure 7), it still leaves open the possibility that the stratosphere could of been a source of reactive nitrogen. A somewhat better correlation (a 2nd order fit gives $r^2 = 0.41$) is found between NO_y sum and ^{210}Pb, a tracer of continental emissions [*Dibb et al.*, 1996]. Both data classifications support this relationship, endorsing the idea that the chemistry of the non-plume air parcels was strongly influenced by plume dissipation. This correlation indicates that continental combustion emissions were probably an important source of NO_y sum, but the distinction between combustion and lightning inputs can not be uniquely resolved. With possible multiple sources of NO_y sum without concomitant CH_3Cl inputs, its not surprising that the correlation in these two species is weak over the South Pacific (Figure 6).

Relationships of NO_y sum with other selected parameters are depicted in Figure 8. As with CH_3Cl, the relationships exhibit significant scatter except for that with O_3. Again, we attribute this scatter to multiple possible sources for NO_y sum and the aged nature of the air parcels from dilution and OH decomposition of CO and hydrocarbons. Despite the fact that well-defined relationships are not present, its clear that the most aged air parcels with C_2H_2/CO ratios <0.5 contain the lowest mixing ratios of NO_y sum. The majority of the non-plume data fall into this category, where most of the reactive nitrogen has probably been converted to HNO_3 and subsequently lost from the atmosphere by wet and dry deposition processes.

Quite a different picture appears to be plausible for the alkyl nitrate species. In this case they

appear to be comprise the largest fraction of NO_y sum coincident with the smallest mixing ratios of O_3 and values of the ratio C_2H_2/CO (Figure 9). This, of course, corresponds to air parcels in the marine boundary layer which contain direct marine emissions of alkyl nitrates and are somewhat isolated from the air above (by temperature inversions), photochemically aged (low C_2H_2/CO) and contain low O_3 due to chemical and surface deposition losses. It should be noted that aerosol NO_3^- mixing ratios were very similar to those for the alkyl nitrates in the marine boundary layer, generally ranging from 20-50 pptv [*Dibb et al.*, 1999a]. Thus, these nitrate compounds together comprise nearly all the NO_y sum in this lower tropospheric region.

In the most aged air masses sampled with C_2H_2/CO<0.5, alkyl nitrates often composed >20% of NO_y sum. The majority of the alkyl nitrate plume data contained low mixing ratios and ratios values to NO_y sum. The majority of the data with the greatest alkyl nitrate/NO_y sum ratios were in the non-plume air parcel classification. There appears to be two different distributions, one with C_2H_2/CO ratio values <0.5 and the second around a ratio value of 1.0 (Figure 9). Most of the data associated with ratio values around 1.0 were collected at high latitude (50-70°S) during a flight south of New Zealand to Antarctica where NO_y sum was <70 pptv. The other distribution at lower C_2H_2/CO ratio values are from flights in the tropical South Pacific region. Thus, it appears that alkyl nitrates are important reactive nitrogen species in the marine boundary layer in equatorial and high latitude regions of the Pacific Ocean. Although this point has been speculated on previously [*Atlas*, 1988], the PEM-Tropics A data is a first definitive demonstration of it.

5. CONCLUSION

This paper presents the distribution of reactive odd-nitrogen species over the South Pacific Ocean during austral springtime. Mixing ratios of NO_x were generally low (<20 pptv) throughout

the tropospheric column (0-12.5 km), with little evidence for a dominant source. The absence of clear chemical signatures correlated with the NO_x distribution is attributed to the 1-2.5 week old age of the sampled air parcels. The distributions of HNO_3 and PAN indicate an important biomass burning source for reactive nitrogen in the free troposphere, although contributions from lightning and the stratosphere can not be ruled out. In the marine boundary layer alkyl nitrate species are a major component of NO_y sum, with this natural oceanic source especially important in equatorial and high latitude regions.

Acknowledgments: This research was sponsored by the NASA Tropospheric Chemistry Program. We appreciate the excellent support provided by the NASA Ames DC-8 flight and ground crews.

REFERENCES

Atlas, E., Evidence for ≥C3 alkyl nitrates in rural and remote atmospheres, *Nature*, *331*, 426-428, 1988.

Atlas, E. L., B. A. Ridley, G. Hübler, J. G. Walega, M. A. Carroll, D. D. Montzka, B. J. Huebert, R. B. Norton, F. E. Grahek, and S. Schauffler, Partitioning and budget of NO_y species during the Mauna Loa Observatory Photochemistry Experiment, *J. Geophys. Res.*, *100*, 10,449-10,462, 1992a.

Atlas, E., S. M Schauffler, J. T. Merrill, C. J. Hahn, B. Ridley, J. Walega, J. Greenberg, L. Heidt, and P. Zimmerman, Alkyl nitrate and selected halocarbon measurements at Mauna Loa Observatory, Hawaii, *J. Geophys. Res.*, *97*, 10,331-10,348, 1992b.

Blake, N. J., et al., Influence of southern hemispheric biomass burning on midtropospheric distributions of nonmethane hydrocarbons and selected halocarbons over the remote South Pacific, *J. Geophys. Res.*, *104*, 16,213-16,232, 1999.

Blake, D. R., T.-Y. Chen, T. W. Smith, Jr., C J.-L. Wang, O. W. Wingenter, N. J. Blake, and F. S. Rowland, Three-dimensional distribution of nonmethane hydrocarbons and halocarbons over the northwestern Pacific during the 1991 Pacific Exploratory Mission (PEM-WestA), *J. Geophys. Res.*, *101*, 1763-1778, 1996a.

Blake, N. J., D. R. Blake, B. C. Sive, T.-Y. Chen, and F. S. Rowland, Biomass burning emissions and vertical distribution of atmospheric methyl halides and other reduced carbon gases in the South Atlantic region, *J. Geophys. Res.*, *101*, 24,151-24,164, 1996b.

Bradshaw, J. D., M. O. Rogers, S. T. Sandholm, S. Kesheng, and D. D. Davis, A two-photon laser-induced fluorescence field instrument for ground-based and airborne measurements of atmospheric NO, *J. Geophys. Res.*, *90*, 12,861-12,873, 1985.

Bradshaw, J. D., S. T. Sandholm, and R. W. Talbot, An update on reactive odd-nitrogen measurements made during NASA's GTE programs, *J. Geophys. Res.*, 103, 19,129-19,148, 1998.

Bradshaw, J. D., D. Davis, J. Crawford, G. Chen, R. Shetter, M. Muller, G. Gregory, G. Sachse, D. Blake, B. Heikes, J. Mastromarino, and S. Sandholm, *Geophys. Res. Lett.*, *26*, 471-474, 1999.

Clarke, A. D., F. Eisele, V. N. Kapustin, K. Moore, D. Tanner, L. Mauldin, M. Litchy, B. Lienert, M. A. Carroll, and G. Albercook, Nucleation in the free troposphere: Favorable environments during PEM-Tropics, *J. Geophys. Res.*, *104*, 5735-5744, 1999.

Dibb, J. E., R. W. Talbot, K. I. Klemm, G. L. Gregory, H. B. Singh, J. D. Bradshaw, and S. T. Sandholm, Asian influence over the western North Pacific during the fall season: Inferences from lead 210, soluble ionic species and ozone, *J. Geophys. Res.*, *101*, 1779-1792, 1996.

Dibb, J. E., R. W. Talbot, E. M. Scheuer, D. R. Blake, N. J. Blake, G. L. Gregory, G. W. Sachse, and D. C. Thornton, Aerosol chemical composition and distribution during the Pacific Exploratory Mission (PEM) Tropics, *J. Geophys. Res.*, *104*, 5785-5800, 1999a.

Dibb, J. E., R. W. Talbot, L. D. Meeker, E. M. Scheuer, N. J. Blake, D. R. Blake, G. L. Gregory, and G. W. Sachse, Constraints on the age and dilution of PEM-Tropics biomass burning plumes from the natural radionuclide tracer ^{210}Pb, *J. Geophys. Res.*, 104, 16,233-16,241, 1999b.

Fahey, D. W., G. Hübler, D. D. Parish, E. J. Williams, R. B. Norton, B. A. Ridley, H. B. Singh, S. C. Liu, and F. C. Fehsenfeld, Reactive nitrogen species in the troposphere: Measurements of NO, NO_2, HNO_3, particulate nitrate, peroxyacetyl nitrate (PAN), O_3, total reactive odd nitrogen (NO_y) at Niwot Ridge, Colorado, *J. Geophys. Res.*, *91*, 9781-9793, 1986.

Fishman, J., and V. G. Brackett, The climatological distribution of tropospheric ozone derived from satellite measurements using version 7 Total Ozone Mapping Spectrometer and Stratospheric Gas Experiments data sets, *J. Geophys. Res.*, *102*, 19,275-19,278, 1997.

Fuelberg, H. E., R. E. Newell, S. Longmore, Y. Zhu, and D. J. Westberg, A meteorological overview of the Pacific Exploratory Mission (PEM) Tropics period, *J. Geophys. Res.*, *104*, 5585-5622, 1999.

Gregory, G. L., J. M. Hoell, Jr., B. A Ridley, H. B. Singh, B. Gandrud, L. J. Salas, and J. Shetter, An intercomparison of airborne PAN measurements, *J. Geophys. Res.*, *95*, 10,077-10,087, 1990.

Gregory, G. L., et al., Chemical characteristics of Pacific tropospheric air in the region of the Intertropical Convergence Zone and South Pacific Convergence Zone, *J. Geophys. Res.*, *104*, 5677-5696, 1999.

Hoell, J. M., D. D. Davis, D. J. Jacob, M. O. Rogers, R. E. Newell, H. E. Fuelberg, R. J. McNeal, J. L. Raper, and R. J. Bendura, Pacific Exploratory Mission in the tropical Pacific: PEM-Tropics A, August-September 1996, *J. Geophys. Res.*, 104, 5567-5583, 1999.

Kasting, J. F., and H. B. Singh, Nonmethane hydrocarbons in the trospophere: Impact on odd hydrogen and odd nitrogen chemistry, *J. Geophys. Res.*, *91*, 13,239-13,256, 1986.

Kliner, D. A. V., B. C. Daube, J. D. Burley, and S. C. Wofsy, Laboratory investigation of the catalytic reduction technique for measurement of atmospheric NO_y, *J. Geophys. Res.*, *102*, 10,759-10,776, 1997.

Logan, J. A., Nitrogen oxides in the troposphere: Global and regional budgets, *J. Geophys. Res.*, *88*, 10,785-10,807, 1983.

McKeen, S. A., and S. C. Liu, Hydrocarbon ratios and photochemical history of air masses, *Geophys. Res. Lett.*, *20*, 2363-2366, 1993.

Sandholm, S. T., J. D. Bradshaw, K. S. Dorris, M. O. Rogers, and D. D. Davis, An airborne compatible photofragmentation two-photon laser-induced fluorescence instrument for measuring background tropospheric NO, NO_x, and NO_2, *J. Geophys. Res.*, *95*, 10,155-10,161, 1990.

Sandholm, S. T., et al., Summertime partitioning and budget of NO_y compounds in the troposphere over Alaska and Canada: ABLE 3B, *J. Geophys. Res.*, *99*, 1837-1861, 1994.

Schultz, M. G., et al., On the origin of tropospheric ozone and NO_x over the tropical South Pacific, *J. Geophys. Res.*, *104*, 5829-5843, 1999.

Singh, H. B., and L. J. Salas, Methodology for the analyses of peroxyacetyl nitrate (PAN) in the unpolluted atmosphere, *Atmos. Environ.*, *17*, 1507-1516, 1983.

Talbot, R. W., et al., Summertime distribution and relations of reactive odd nitrogen species and NO_y in the troposphere over Canada, *J. Geophys. Res.*, *99*, 1863-1885, 1994.

Talbot, R. W., et al., Chemical characterisitics of continental outflow from Asia to the troposphere over the western Pacific Ocean during September-October 1991: Results from PEM-West A, *J. Geophys. Res.*, *101*, 1713-1725, 1996a.

Talbot, R. W., et al., Chemical characteristics of continental outflow over the tropical South Atlantic Ocean from Brazil and Africa, *J. Geophys. Res.*, *101*, 24,187-24,202, 1996b.

Talbot, R. W., et al., Large-scale distribution of tropospheric nitric, formic, and acetic acids over the western Pacific basin during wintertime, *J. Geophys. Res.*, *102*, 28,303-28,313, 1997a.

Talbot, R. W., et al., Chemical characteristics of continental outflow from Asia to the troposphere over the western Pacific Ocean during February-March 1994: Results from PEM-West B, *J. Geophys. Res.*, *102*, 28,255-28,274, 1997b.

Talbot, R. W., et al., Reactive nitrogen budget during the NASA SONEX mission, *Geophys. Res. Lett.*, in press, 1999a.

Talbot, R. W., J. E. Dibb, E. M. Scheuer, D. R. Blake, N. J. Blake, G. L. Gregory, G. W. Sachse, J. D. Bradshaw, S. T. Sandholm, and H. B Singh, Influence of biomass combustion emissions on the distribution of acidic trace gases over the southern Pacific basin during austral springtime, *J. Geophys. Res.*, *104*, 5623-55634, 1999b.

Figure Captions

1. Vertical distribution of selected trace gases during a spiral ascent on mission 6 just west of Tahiti at 15° S and 155° W. Mixing ratios of O_3 and CO are in ppbv and the other species pptv.

2a. Vertical distribution of reactive odd-nitrogen species in non-plume air parcels over the South Pacific. The open symbols represent the average value ± one standard deviation for 2 km altitude bins.

2b. Vertical distribution of reactive odd-nitrogen species in combustion plumes over the South Pacific. The open symbols represent the average value ± one standard deviation for 2 km altitude bins.

3. Vertical distribution of NO_y sum in non-plume and plume air parcel classifications. Blue symbols are non-plume data and red are from within combustion plumes. The open symbols represent the average value ± one standard deviation for 2 km altitude bins.

4a. Ratio of reactive odd-nitrogen species to NO_y sum in non-plume air parcels over the South Pacific. The open symbols represent the average value ± one standard deviation for 2 km altitude bins.

4b. Ratio of reactive odd-nitrogen species to NO_y sum in combustion plumes over the South Pacific. The open symbols represent the average value ± one standard deviation for 2 km altitude bins.

5. Relationship between selected species and C_2H_2 over the South Pacific. Blue symbols are non-plume data and red are from within combustion plumes.

6. Relationship between PAN and NO_y sum with CH_3Cl over the South Pacific. Blue symbols are non-plume data and red are from within combustion plumes. Note that the plot has a semi-logarithmic scale.

7. Relationship between NO_y sum and ^{210}Pb, a continental tracer, and ^{7}Be, a tracer of stratospheric inputs to the troposphere. Blue symbols are non-plume data and red are from within combustion plumes. Note that the plot has a semi-logarithmic scale.

8. Relationship of NO_y sum with selected pollution-associated species over the South Pacific. Blue symbols are non-plume data and red are from within combustion plumes.

9. Ratio of alkyl nitrates ($CH_3ONO_2 + C_2H_5ONO_2$) to NO_y sum as a function of O_3 and C_2H_2/CO. Blue symbols are non-plume data and red are from within combustion plumes.

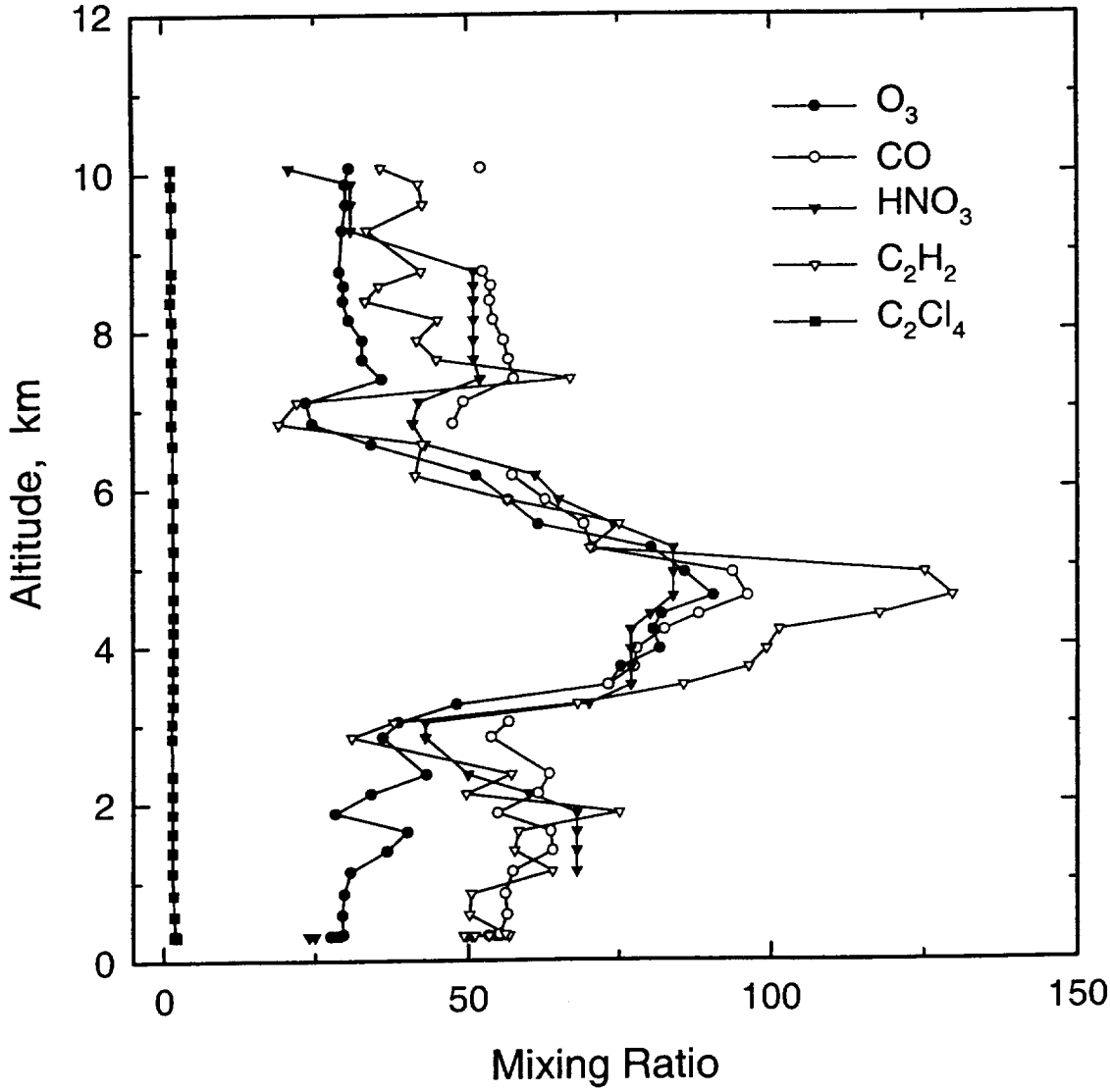
12
10
8
6
4
2
0
Altitude, km
0
50
100
150
Mixing Ratio
O_3
CO
HNO_3
C_2H_2
C_2Cl_4

Fig. 1

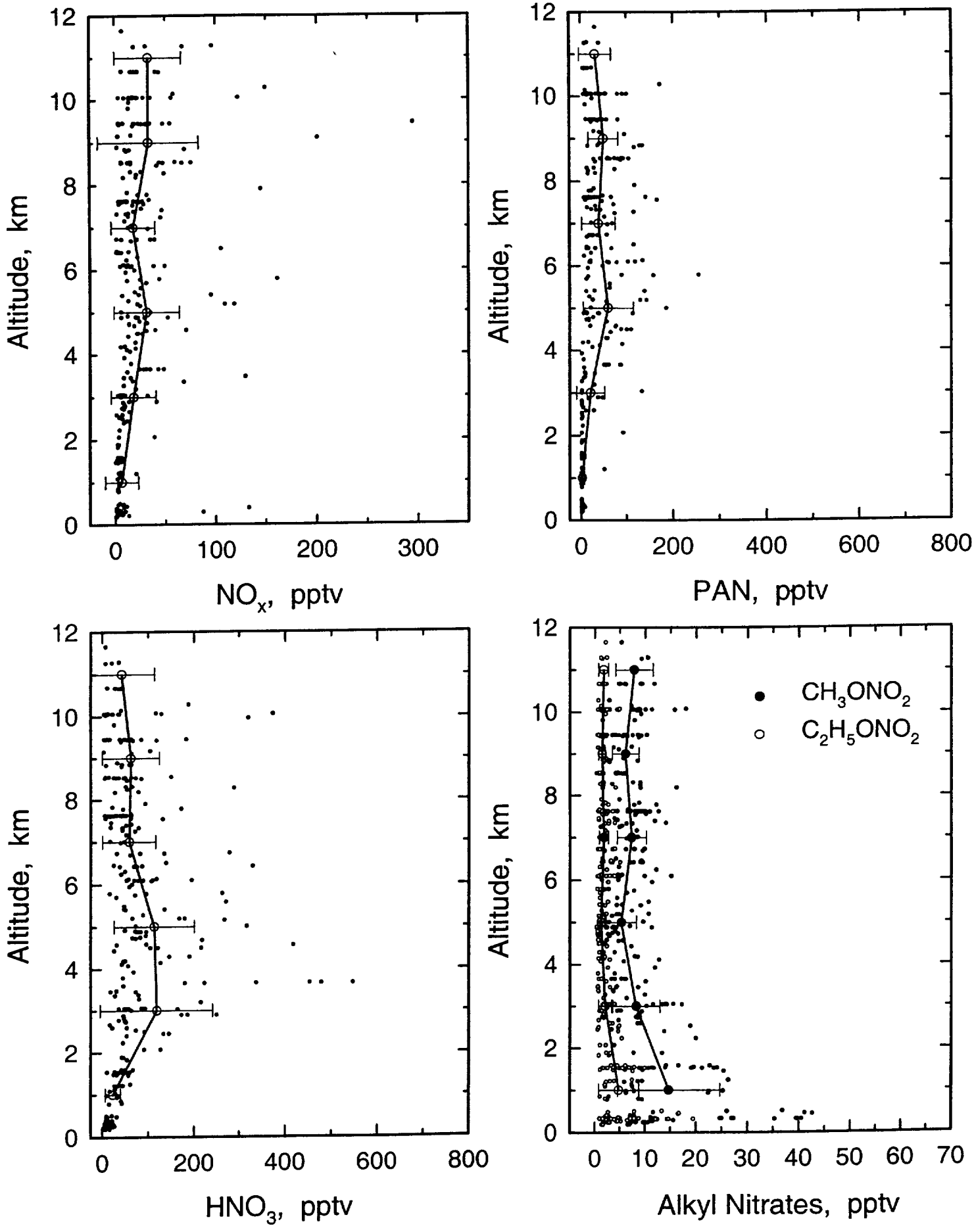
Altitude, km
NO_x, pptv
PAN, pptv
HNO_3, pptv
Alkyl Nitrates, pptv
CH_3ONO_2
$C_2H_5ONO_2$

Fig. 2a

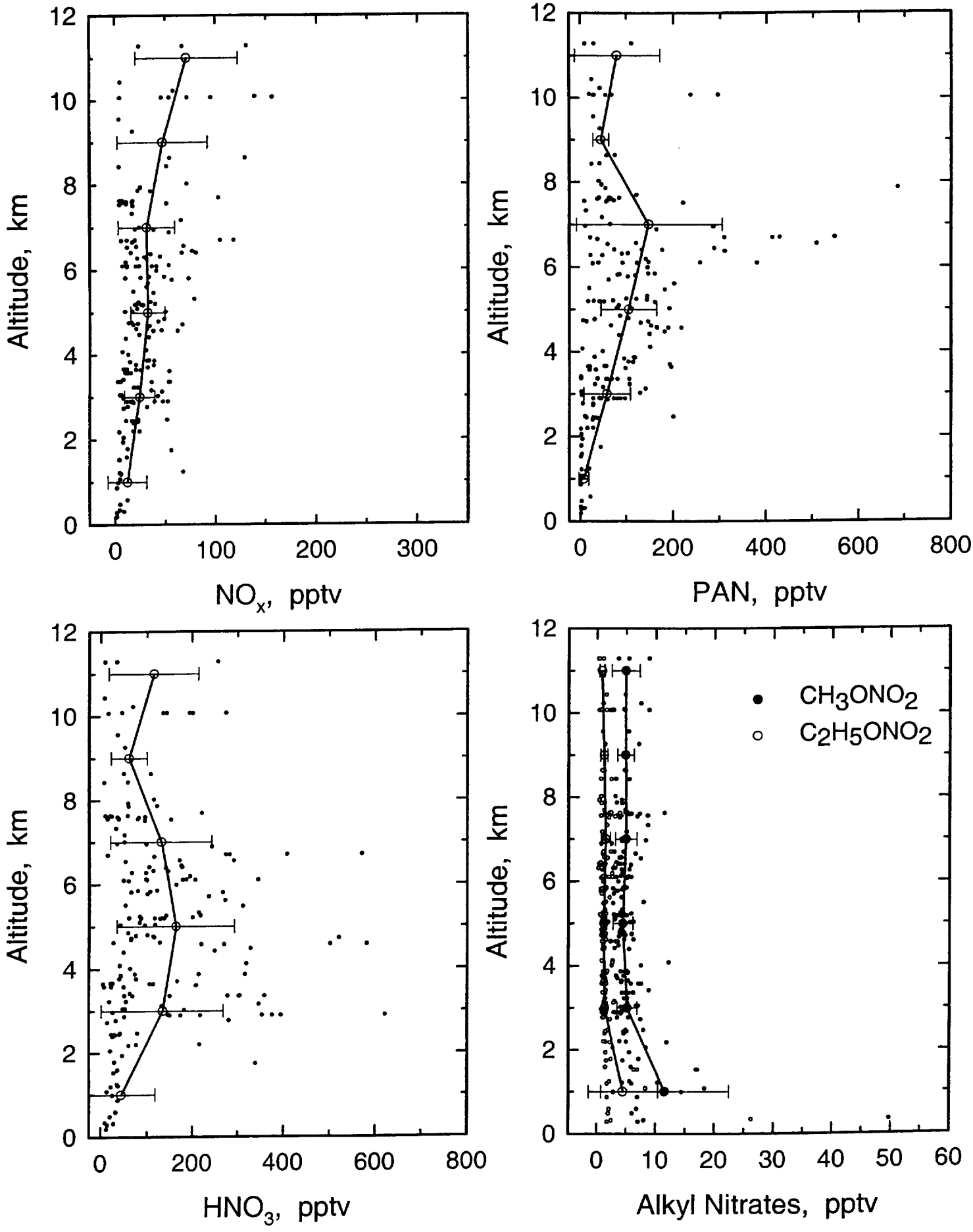
Altitude, km
NO_x, pptv
PAN, pptv
HNO_3, pptv
Alkyl Nitrates, pptv
CH_3ONO_2
$C_2H_5ONO_2$

Fig. 2b

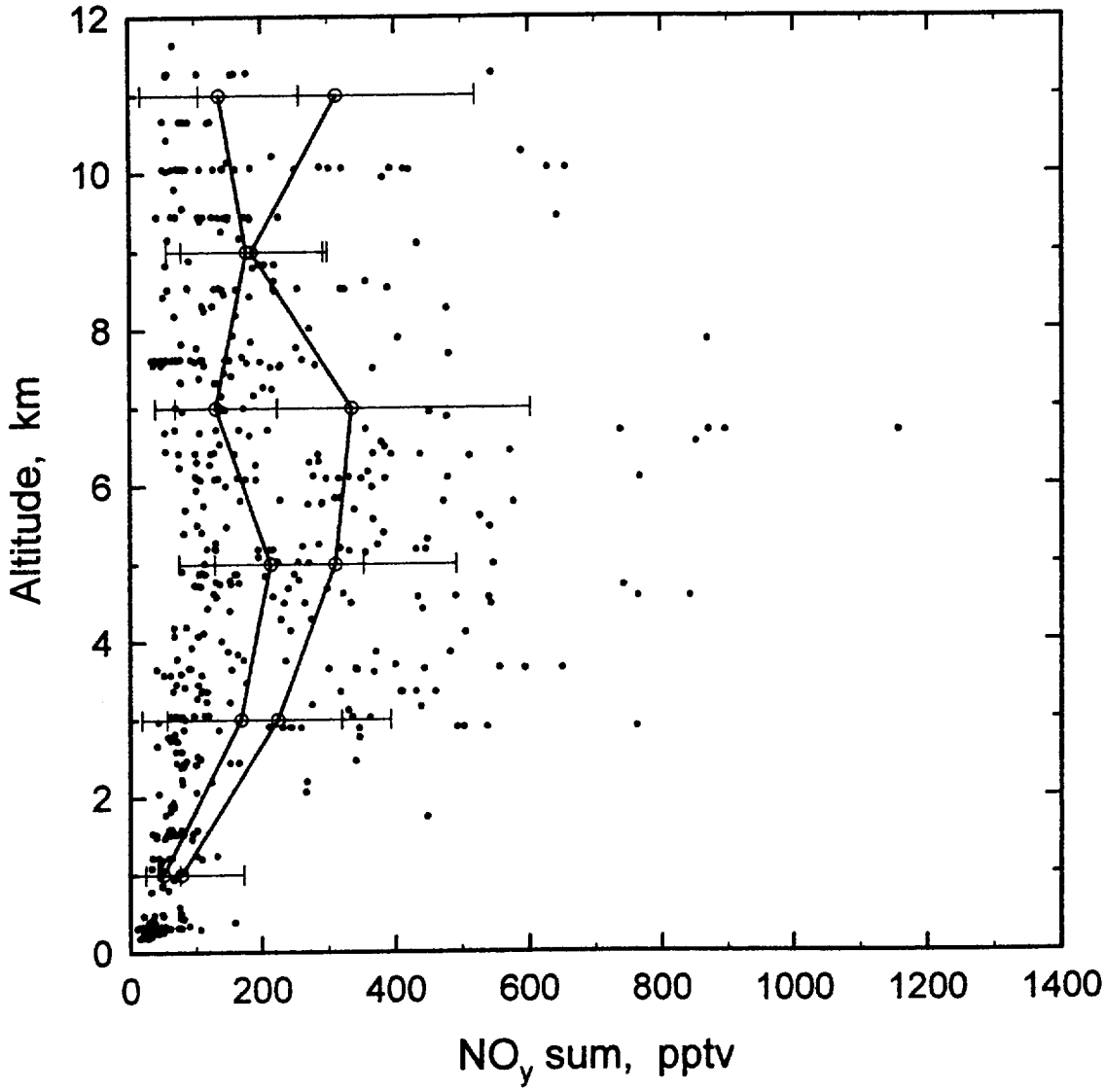
12
10
8
6
4
2
0
Altitude, km
0
200
400
600
800
1000
1200
1400
NOy sum, pptv

Fig. 3

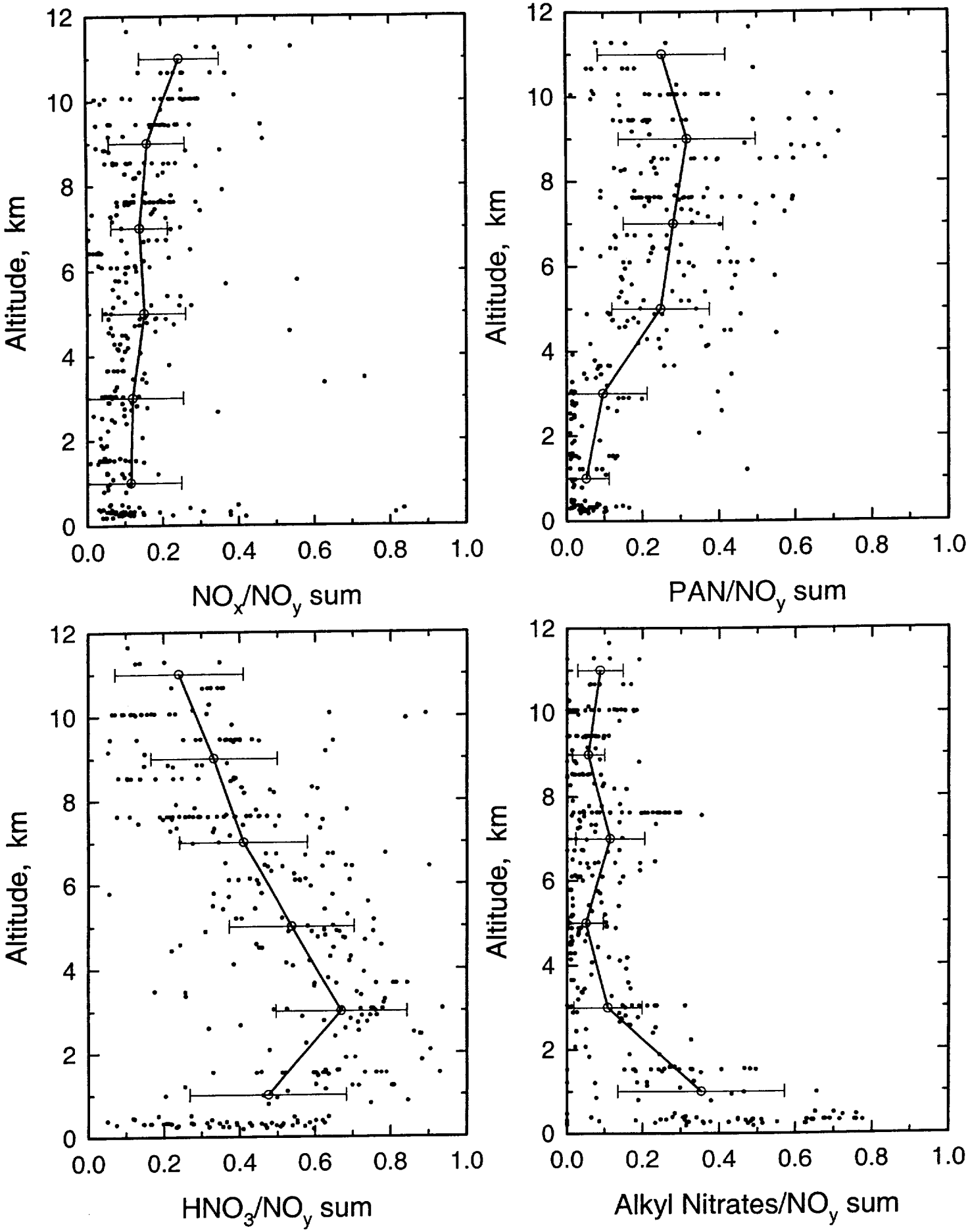
Altitude, km
0
2
4
6
8
10
12
0.0
0.2
0.4
0.6
0.8
1.0
NO_x/NO_y sum
PAN/NO_y sum
HNO_3/NO_y sum
Alkyl Nitrates/NO_y sum

Fig. 4a

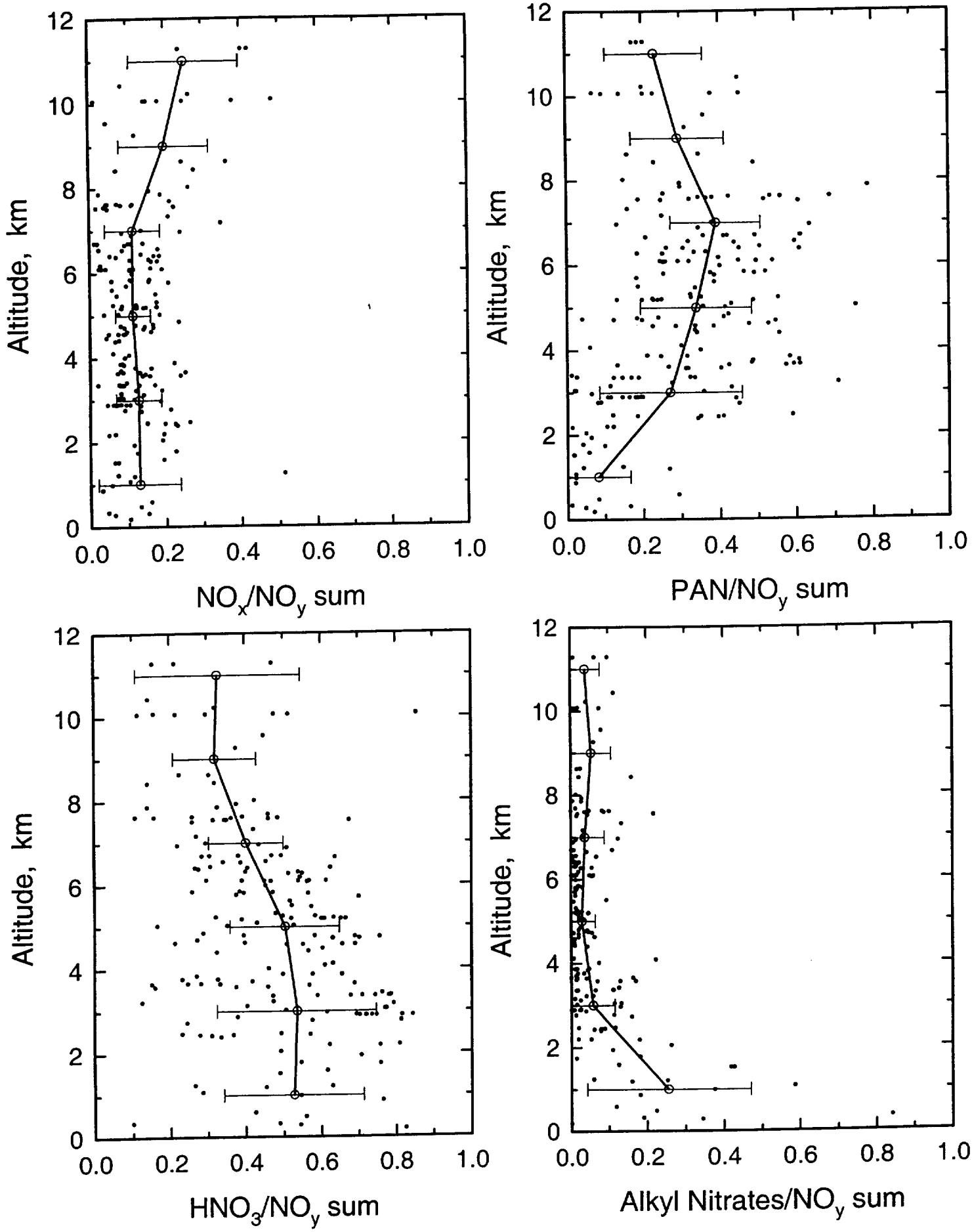
Altitude, km
NOx/NOy sum
PAN/NOy sum
HNO3/NOy sum
Alkyl Nitrates/NOy sum
0
2
4
6
8
10
12
0.0
0.2
0.4
0.6
0.8
1.0

Fig. 4b

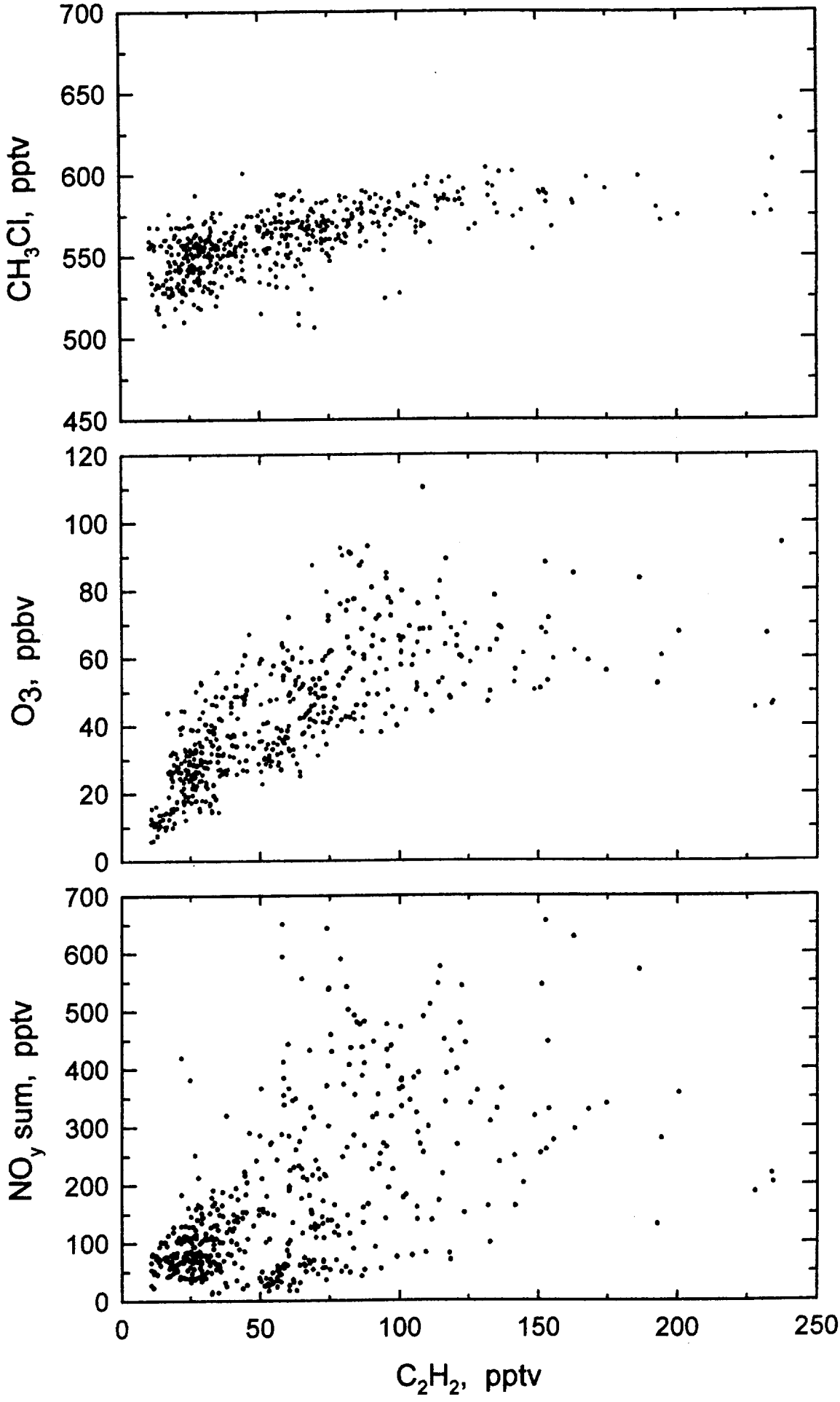
700
650
600
550
500
450
CH_3Cl, pptv
120
100
80
60
40
20
0
O_3, ppbv
700
600
500
400
300
200
100
0
NO_y sum, pptv
0
50
100
150
200
250
C_2H_2, pptv

Fig. 5

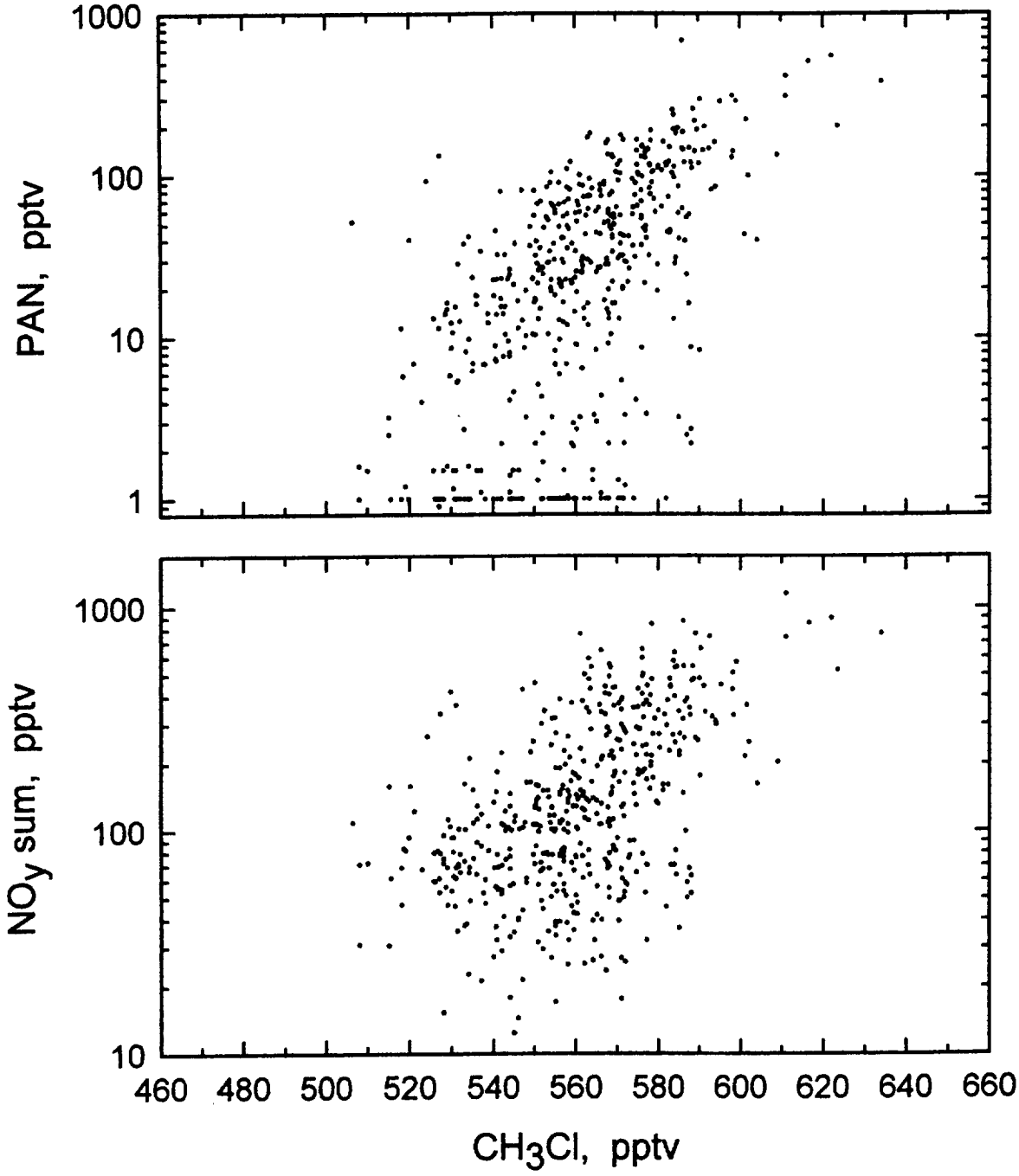
1000
100
10
1
PAN, pptv
1000
100
10
NOy sum, pptv
460
480
500
520
540
560
580
600
620
640
660
CH3Cl, pptv

Fig. 6

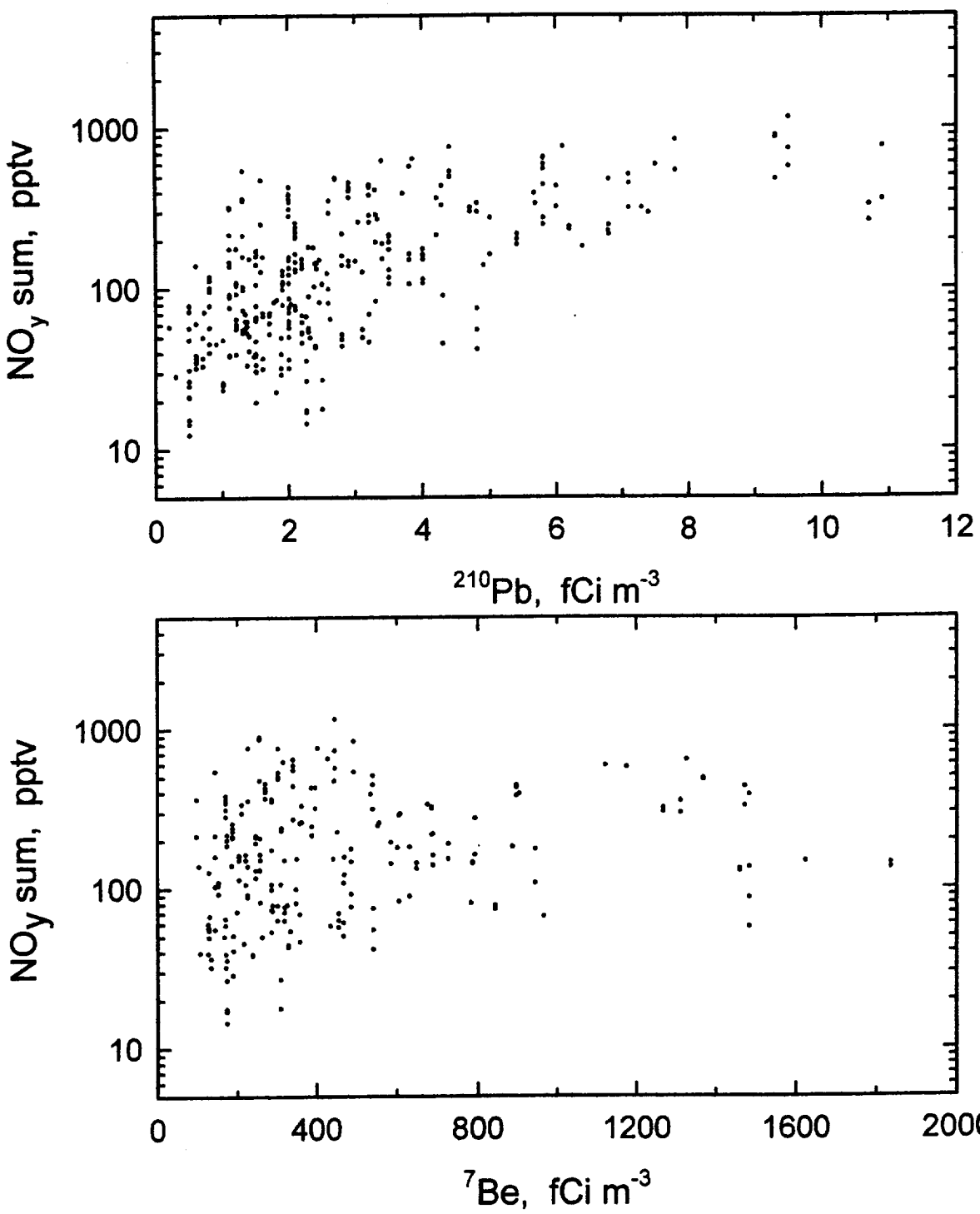
1000
100
10
NO_y sum, pptv
0
2
4
6
8
10
12
^{210}Pb, fCi m^{-3}
1000
100
10
NO_y sum, pptv
0
400
800
1200
1600
2000
^{7}Be, fCi m^{-3}

Fig. 7

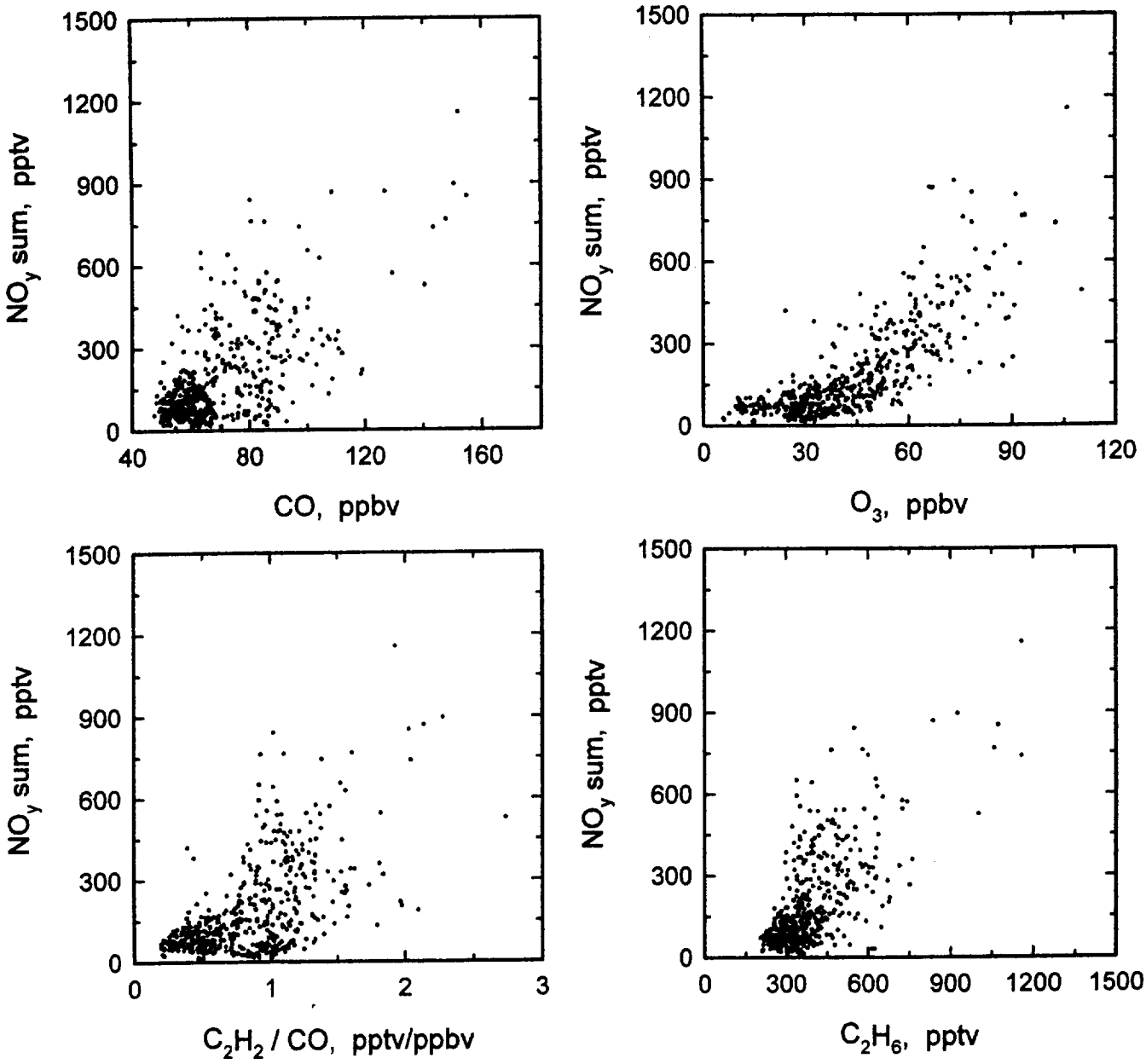
1500
1200
900
600
300
0
NO_y sum, pptv
40
80
120
160
CO, ppbv
0
30
60
90
120
O_3, ppbv
0
1
2
3
C_2H_2 / CO, pptv/ppbv
300
600
900
1200
1500
C_2H_6, pptv

Fig. 8

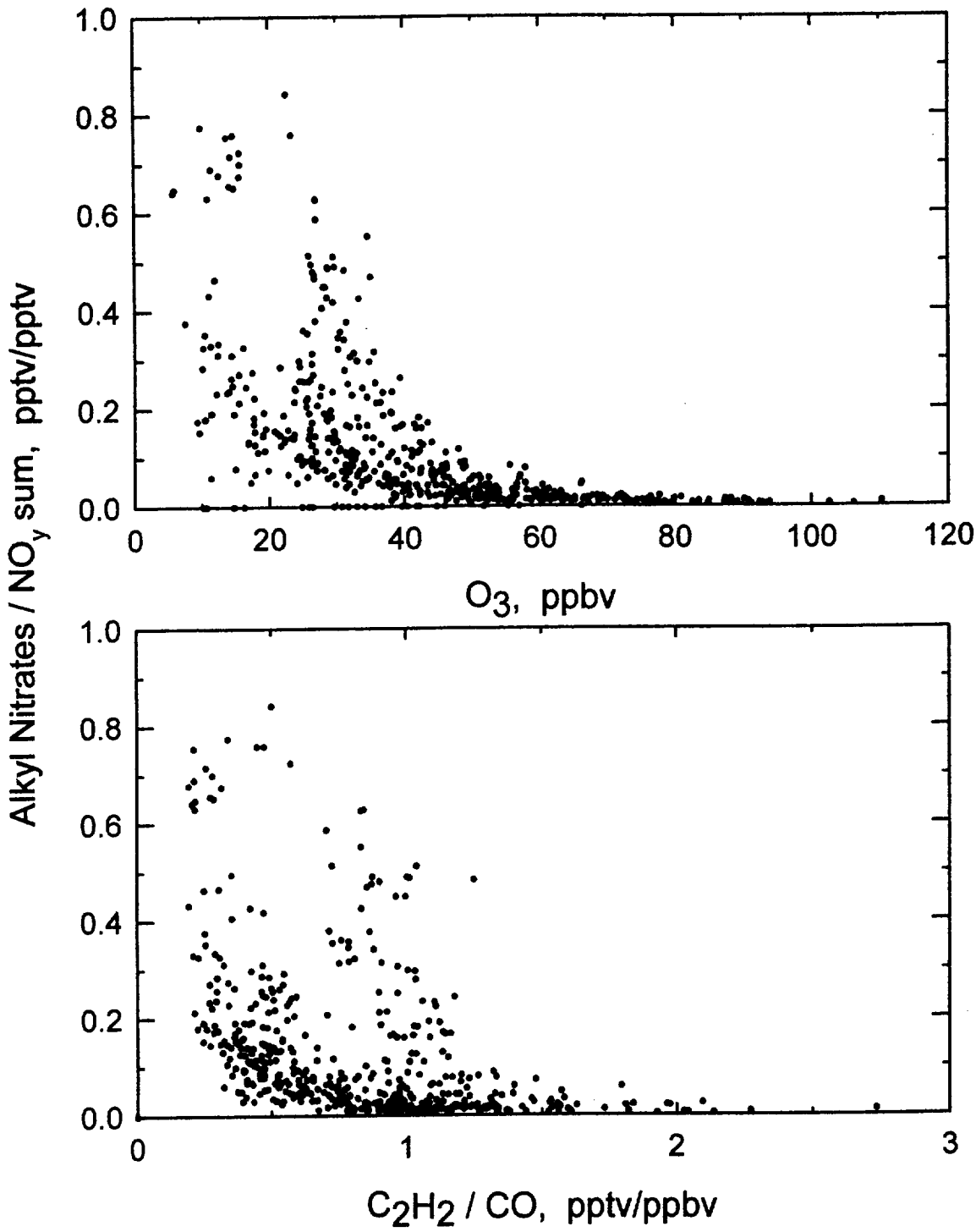
Alkyl Nitrates / NO_y sum, pptv/pptv
1.0
0.8
0.6
0.4
0.2
0.0
0
20
40
60
80
100
120
O_3, ppbv
1.0
0.8
0.6
0.4
0.2
0.0
0
1
2
3
C_2H_2 / CO, pptv/ppbv

Fig. 9